

# The International Spillover of Monetary Policy Shock: New Evidence from Nighttime Light\*

Kaiji Chen<sup>†</sup>    Qichao Wang<sup>‡</sup>    Juanyi Xu<sup>§</sup>    Jingbo Yao<sup>¶</sup>

25 January 2025

## Abstract

We revisit the spillover effects of US monetary policy shocks using a new data source, the daily nighttime light (NTL), as a high-frequency proxy for real economic activities. Taking China as an example, the unexpected US tightening dampens its output, and the peak comes about two months later. This is explained by a construction channel, with the NTL variation mainly driven by non-built-up areas instead of city centers and suburbs. Consistently, cities with lower urbanization rates and tighter financial conditions respond more negatively. Moreover, the US shock also drives output fluctuation in other economies, especially emerging countries or regions.

**Keywords:** Monetary Policy Spillover, Nighttime Light, Construction Channel

**JEL codes:** E52, F14, F42, F44

---

\*We are grateful to Zhang Chen, Sangyup Choi, Zhenyu Gao, Kaiji Robin Gong, Rustam Jamilov, Kohei Kawaguchi, Paymon Khorrami, Nobuhiro Kiyotaki, Byoungchan Lee, Yao Amber Li, Zhiyuan Li, Yan Liu, Yang Lu, Peter Maxted, Ryungha Oh, Luigi Paciello, Benjamin Pugsley, Wei Qiao, Deyu Rao, Harrison Shieh, Zheng (Michael) Song, Eric Swanson, Jieran Wu, Wei Xiong, Jianpo Xue, Haonan Zhou, Xiaodong Zhu, Yu Zhu, and other participants at 2025 China Accounting and Finance Conference, 2024 European Winter Meeting, IFABS 2024 Shanghai, The 14th Annual Meeting of China Trade Research Group cum International Conference on US-China Trade Disputes and Rearchitecture in Globalization, The 11th International Conference on The Chinese Economy: Past, Present and Future, 2024 Annual Conference of Economic Fluctuation and Growth Forum and the 4th National Macroeconomics PhD student academic forum, and the HKUST CEP brown bag seminar, for helpful comments and suggestions. We also thank Xiaoyu Zhang for sharing the land transaction data.

<sup>†</sup>Emory University, CQER Senior Research Fellow at Federal Reserve Bank of Atlanta.  
Email:kaiji.chen@emory.edu.

<sup>‡</sup>The Department of Economics at The Hong Kong University of Science and Technology. Email: qwangcq@connect.ust.hk.

<sup>§</sup>The Department of Economics at The Hong Kong University of Science and Technology. Email: jennyxu@ust.hk.

<sup>¶</sup>The Department of Economics at The Hong Kong University of Science and Technology. Email: jyaoam@connect.ust.hk.

# 1 Introduction

The cross-border spillover effect of monetary policy is an essential topic in both monetary and international economics, especially for the US monetary shock, which is a key driver of the global financial cycle (Miranda-Agrippino and Rey, 2020). Although the impact on the international financial market has been explored a lot in the literature (see Bhattarai and Neely, 2022 for a survey), the empirical evidence on the real economy responses is still deficient. Moreover, despite the fact that monetary tightening is agreed to dampen domestic economic activities, the effect is ambiguous in an international context. For example, on the one hand, the Fed tightening reduces the aggregate expenditure of the US households which then induces a lower import demand from Brazil. On the other hand, the US tightening may appreciate the US dollar thus increasing the purchasing power of dollar holders, which implies an increase in import demand. Apart from the trade side effects, the US monetary policy could also influence the economic activities of other countries through the financial side, which makes this answer even more unclear.

Compared with investigating the effects on asset prices and yields, studying the real effects is both more important and challenging (Swanson, 2021). It is more important because the ultimate focus of central banks is output and consumer welfare. It is also more difficult because omitted variables, reverse causality, measurement errors, and misspecification are much more serious problems for macro studies than for financial markets, which are amenable to using event studies (Bhattarai and Neely, 2022).

Specifically, traditional indicators, such as GDP or industrial production, are released at a monthly frequency or even lower, which means that many confounding factors instead of monetary shocks could also determine the real activities during the time window. This task is even more challenging if there is a lagged effect. Moreover, the performance of real activities will determine the implementation of monetary policy, which poses a reverse causality problem. Finally, the traditional output variables have measurement errors due to misreporting, aggregation and manipulation, etc. It is even more serious for emerging

markets (see Clark et al., 2020; Henderson et al., 2012; Martínez, 2022, etc. for more details). These variables also differ across countries by accounting standards and they are only available for administrative areas. In light of this, we try to employ a proxy of real activity that is at a higher frequency, internationally comparable, relatively objective, and available at any spatial level.

An ideal candidate is the geospatial data of nighttime light (NTL), which has been emerging in recent economics studies, and it has several advantages that suit our study. First, the data is released at a daily frequency and has been publicly available since early 2012 with an ongoing update. Second, the satellite-related measurement errors are orthogonal to economic activities (Pinkovskiy & Sala-i-Martin, 2016) and are also free of potential data manipulation (Chor & Li, 2024; Martínez, 2022). Third, the images captured by satellites at night measure the brightness of different places with a uniform lens, avoiding accounting standard differences across administration boundaries in traditional economic data. Fourth, spatial aggregation is also available at any level, enabling the identification of policy effects in any selected area. The GDP-NTL correlation holds when we change the unit of observation from the administrative city or county to arbitrarily chosen areas (Sherman et al., 2023).

The variations in NTL reflect changes in real activities. The association of GDP and NTL has been well-established in recent economic literature (Chor & Li, 2024; Henderson et al., 2012; J. Kim et al., 2022; Martínez, 2022). An increase in NTL indicates booming economic activities of different types, including service, manufacturing, and construction. In the city center, NTL mainly reflects service activities at night, such as the buzzing commercial streets with entertainment facilities that run up to the whole night. In more remote areas of the cities, some factories operate at night, as the night shift is a common practice in emerging markets (Chor & Li, 2024). The outskirts of the cities are characterized by the expanding urban boundary, especially in rapidly urbanizing emerging economies such as China in the 2010s. Construction activities at night can increase light. Working night shifts on construction sites is very common in emerging economies.

For example, during the boom of the real estate market, developers often arrange night construction in order to complete and sell as soon as possible. Moreover, when newly finished buildings are put into use, they also produce additional lighting at night.

With the NTL data and monetary shocks in hand, we could then study the international spillover effects of monetary policy shocks (MPS). In the main part, we take China, the largest emerging market, as an example, where we have detailed spatial level and micro level data to explore the channel.<sup>1</sup> The baseline results come from the Local Projection (henceforth “LP”, Jordà, 2005) regressions of China’s overall NTL on US MPS. The NTL data are from Visible Infrared Imaging Radiometer Suite (VIIRS) instruments operated by the National Aeronautics and Space Administration (NASA) with a daily frequency. The baseline MPS we use is the 30-minute high-frequency Federal Fund Rate change around FOMC announcements. We aggregate the daily series from 2012 to 2023 to weekly in the baseline to avoid unpleasant noises. Several main findings are shown as follows.

To begin with, China’s overall NTL negatively responds to the US MPS. The response appears right after the shock, and the peak is at 7 weeks later. It gradually declines then and turns insignificant since the 16th week after the shock. Besides, it is also surprising to know that this effect is much quicker than traditional expectations (e.g. one-quarter lag). Benefiting from the high-frequency data, our event-study approach could do a sharper identification of the policy effect and capture the dynamics more clearly. Our results are robust to many checks such as the subperiod analysis, using alternative bootstrap standard errors, adopting different specifications or measurements, applying daily frequency NTL, conducting a falsification test, and controlling more confounding variables like the US news shocks, China’s monetary stance, US-China tension, and weather conditions.

Consistent with the NTL effects, by applying the same specification with traditional output variables like quarterly GDP and monthly industrial production, we also observe negative responses but less significant which may be due to additional noises associated

---

<sup>1</sup>In the extension part, we also study the impacts of the US monetary policy on other countries.

with longer time windows. Furthermore, we find that, in the short run, the GDP decline is mainly driven by the drop in investment, while the effects on consumption and net exports are quite mild. In the longer run, the reduction in investment eventually causes the shrinking of consumption. Although the net export slightly increases, it can't overturn the overall pattern.

To account for those findings, we propose a construction channel. Firstly, We decompose a city into a city center, suburb, and non-built-up area, and then run the same LP regressions separately. It is found that the responses in non-built-up areas are quite significantly negative while the other two parts are relatively insignificant, which indicates that the overall spillover effect is mainly driven by construction-related activities in the non-built-up areas instead of service-associated activities in city centers or manufacturing activities in the suburbs. Secondly, using aggregate market indicators, we show that projects under construction and land investment drop immediately after a tightening US shock, then with an around 3-month lag, construction investment, real estate investment, and land building sales all drop. Moreover, it is verified that the decrease in number of ongoing projects is associated with NTL decline. Thirdly, consistent with this construction channel, we show that Chinese interest rates increase and equity prices fall in response to a tightening US shock, which worsens firms' financing conditions. Also, at the micro level, evidence shows that US monetary tightening leads to a decline in firms' revenue, profits, and trade credits, especially real estate firms.

To strengthen our construction channel, we also provide more cross-sectional evidence. We display that cities with lower urbanization rates suffer a bigger impact after a tightening US shock as construction activities are more pervasive in these cities. Consistently, we show that cities with more rapid land transaction records, higher fixed assets investment to GDP ratio, and more projects under construction, undergo a bigger decline in NTL. Besides, it is found that the shock has a more adverse impact on financially less developed cities. This is plausible as the financing conditions of these cities are more likely to be aggravated, thus causing a larger drop in construction activities. Moreover, we illustrate

that in a place, where the firms in the construction sector have worse financial conditions (such as higher financial-expense-to-revenue ratio, larger liability-to-asset ratio, and bigger accounts-receivable-to-revenue ratio), the NTL response is more negative.

Lastly, as a further extension, we first show that the adverse effects are weaker in a city with a higher net export over GDP ratio, which partially offsets the negative effects on investment and consumption. Secondly, we illustrate that conventional US monetary policy shocks are more effective in affecting foreign real activities than unconventional tools, like forward guidance. Thirdly, the spillover effects of the monetary shocks from the European Central Bank and the Bank of Japan are relatively insignificant, which suggests the special role of the Fed monetary policy in affecting the global business cycle. Finally, we find that the US monetary policy also affects the NTL in other economies, especially emerging market countries or regions.

## 1.1 Literature

Our study mainly contributes to three strands of literature. Firstly, our paper is related to the broad literature on the spillover effects of monetary shocks on the real economy and financial markets, especially those empirical works. Due to the low frequency of output data, people usually employ the VAR approach to study the impact on real activities (e.g. S. Kim, 2001, Maćkowiak, 2007, Bluedorn and Bowdler, 2011, and Georgiadis, 2016; see Bhattarai and Neely, 2022 for a survey)<sup>2</sup>. However, this method suffers from several criticisms, such as misspecification, improper identification restriction, instability, etc. (see Rudebusch, 1998 and Miranda-Agrippino and Ricco, 2021 for more discussion). Benefiting from a higher frequency proxy of real activities, we instead use an event-study-based approach, which is commonly used in the literature to study the responses of financial markets (e.g. Nakamura and Steinsson, 2018, Chari et al., 2021, Swanson, 2021, R. Gürkaynak et al., 2022). This method has less concern about the problem of reverse causality and omitted variables, and thus offers a sharper identification of the causal impacts of monetary policy shocks (R. S. Gürkaynak and Wright, 2013). Some papers

---

<sup>2</sup>As for theoretical work, please see Akinci and Queralto (2024) as an example.

also use the same approach to study the impacts on firms' balance sheet variables such as R. Gürkaynak et al., 2022 and Di Giovanni and Rogers, 2024, however, these variables are usually at the quarterly or annual frequency. To our knowledge, we are the first to study the international monetary policy spillover effects using nighttime light (NTL) as a high-frequency proxy of real activities. Also, we reveal a new channel where the US tightening affects emerging markets' output through construction-related activities in non-built-up areas.

Moreover, our approach has several other appealing advantages. (1) Previous papers usually study the spillover impact at the country level. By contrast, the observation unit of the NTL data is as small as a square cell with about 464 meters on one side, which allows us to explore a finer heterogeneity. For instance, we identify the NTL changes in areas with different functions within a city, namely the city center, the industrial parks, and the construction fields. The data can also be flexibly aggregated at any level (e.g. county, city, province) and can be easily extended to other countries. (2) Unlike traditional national accounts, such as GDP, which have different accounting standards across jurisdictions and countries, the NTL data expose all administrative units under the same measurement standard. (3) The NTL is quite objective and irrelevant to the measurement error of traditional economic indicators, originating from reasons such as statistical capacity and potential data manipulations.

Secondly, our paper relates to the literature on how monetary policy shapes the real estate markets. For example, Jordà et al. (2015) finds that loose monetary conditions lead to booms in real estate lending and house price bubbles and Aastveit and Anundsen (2022) reveals the asymmetric effects of monetary policy in regional housing markets. Drechsler et al. (2022) studies how monetary policy affects the funding structure of the mortgage market. Consistent with most of the papers in this strand, we also find that monetary tightening deteriorates the real estate market and the difference lies in that we focus on the international spillover effects rather than domestic impact. In this regard, our paper is closer to Ho et al. (2018) who find that the deduction of the US policy rate

since the Great Recession has led to a significant increase in Chinese housing investment using a FVAR model. Unlike these papers, we stretch a further step and show that the decline in real estate investment and sales caused by US monetary tightening is preceded by a slump in construction activities.

Finally, our paper is also part of the emerging studies utilizing the nighttime light (NTL) data. The geospatial NTL data associate nighttime luminosity with economic activities, therefore they are used to improve the data quality of regions without sufficiently accurate traditional economic data in cross-country comparisons (Henderson et al., 2012; Martínez, 2022; Pinkovskiy & Sala-i-Martin, 2016). Besides, they also enable regional studies, such as measuring regional inequality (D. Kim, 2022) and the UN sanction impact in North Korea (J. Kim et al., 2022), which does not publish any official economic data. Chor and Li (2024) uses the data to proxy registered firms' activities in China and assesses the impact of the US-China trade war. More recently, the data is used in measuring the COVID-19 lockdown impact (Bustamante-Calabria et al., 2021; L. Jiang & Liu, 2023; Xu et al., 2021), which requires an identification frequency higher than quarterly and a unit of measurement beyond administrative boundaries. The highest frequency of the data is daily, and Cohen and Gonzalez (2024) uses the daily NTL time series to associate a higher temperature with more activities at night. Unlike these papers, we use this data to study the spillover effects of monetary policy shocks.

The following sections of the paper are as follows. Section 2 presents the data sources and measurements. Section 3 reveals the relation of NTL and other output variables. Section 4 shows the baseline results of China's overall NTL responses to US MPS. Section 5 and 6 illustrate the construction investment mechanism with both time-series and cross-sectional evidence. Section 7 is a further extension. Section 8 concludes.



## 2 Data and Measurements

This section describes the datasets used in our study. Firstly, we introduce the exogenous monetary policy shocks (MPS). Secondly, we present the nighttime luminosity (NTL) data captured by NASA’s VIIRS-based satellites and the way of aggregation. Thirdly, we explain official national accounts used to associate NTL with economic output. Lastly, we display supplementary data, such as weather data and financial market indicators used to support our main findings.

### 2.1 Monetary Policy Shock

The baseline monetary policy shock (MPS) used in the study is extracted from 30-minute high-frequency changes in federal fund rates around the Federal Open Market Committee (FOMC) meetings, which captures the unexpected part of interest rate changes.<sup>3</sup> FOMC meetings are usually held on average 8 times each year. We focus on the meetings from 2012 to 2023, as the NTL data starts from 2012. 96 FOMC meetings were held during the period, and the extracted baseline MPS (MP1) is shown in Figure 1.

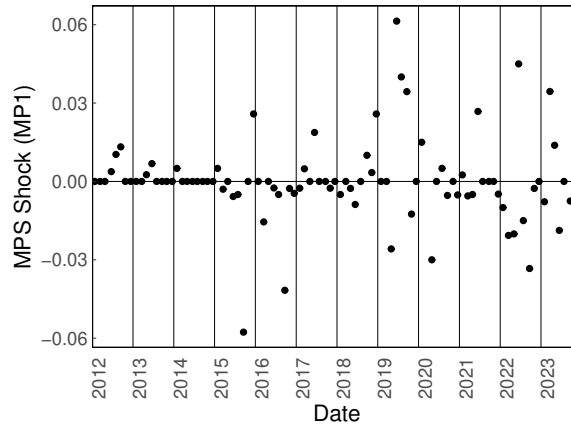


Figure 1: Proxies of Monetary Policy Shock: Baseline

Notes: For each MPS event, the corresponding date is the day when the FOMC is held.

---

<sup>3</sup>This data is from the personal website of Marek Jarocinski.

## 2.2 Nighttime Light

The daily NTL data is from NASA’s Black Marble with public access dating back to 19 January 2012. We use the period until the end of 2023. The data are captured by satellites with the VIIRS (Visible Infrared Imaging Radiometer Suite) instrument, which is the latest and the most accurate version of Suomi Polar-orbiting Partnership jointly by NASA and NOAA.<sup>4</sup> A pixel in the digitalized image corresponds to 15 arc seconds out of 360 degrees in both latitude and longitude, converting to 464m on the equator. The cells are small enough to identify economic activities in regional event studies. Unlike the previous generation of satellite images for NTL, the DMSP, the VIIRS is time consistent (Gibson et al., 2021), which enables the intertemporal comparison required in the study. It also has no top-coding problems (Bluhm & Krause, 2022), a vital issue when measuring in bright places, such as the city center. The neighboring cells are not autocorrelated (Michalopoulos & Papaioannou, 2018), which enables precisely distinguishing light sources at the cell level.

We use the Black Marble VIIRS product VNP46A2, which applies the Bidirectional Reflectance Distribution Function (BRDF) on the raw satellite image. It removes distraction factors such as stray light and moonlight. It also adjusts the satellite angle, which varies daily when the satellite captures the image at the same place. Additionally, the product labels cells contaminated by cloud and snow covers, enabling our further processing to remove such noises. We use cloud computers to process the product at the cell level and generate aggregated daily NTL series for 345 out of 367 cities (prefectures) in mainland China.<sup>5</sup>

When aggregating the geospatial data at the city level, the shape files of the administrative boundaries of the cities we use are derived from the official source (National

---

<sup>4</sup>For details of the data sources, see subsection A.2.1. A web-based interface of the VIIRS light map is available at: <https://www.lightpollutionmap.info> (light pollution map).

<sup>5</sup>The remaining 22 cities are large in area but have relatively small populations and economic activities. The processing time on cloud computers positively correlates with the area processed. Therefore, we drop them off in the processing for budget and time considerations. The detailed process is in subsection A.2.2.

Bureau of Statistics of China, henceforth NBSC) with revisions to show the updated boundaries across cities in 2022.

We match the NTL with MPS data after aggregating them to weekly frequency. Every week is defined as from a Sunday to the closest upcoming Saturday (included). Aggregating NTL to weekly series substantially reduces the noise while keeping the frequency sufficiently high to identify the MPS impact on the real economy. Meanwhile, as FOMC is conducted every six weeks on average, converting the daily series to weekly does not have overlapping issues. We assign each MPS value to the week of the FOMC date and interpolate the weeks with no FOMC meetings as having zero shocks. The weekly series of logged NTL and the first-order differentiated log NTL are in Figure 2.

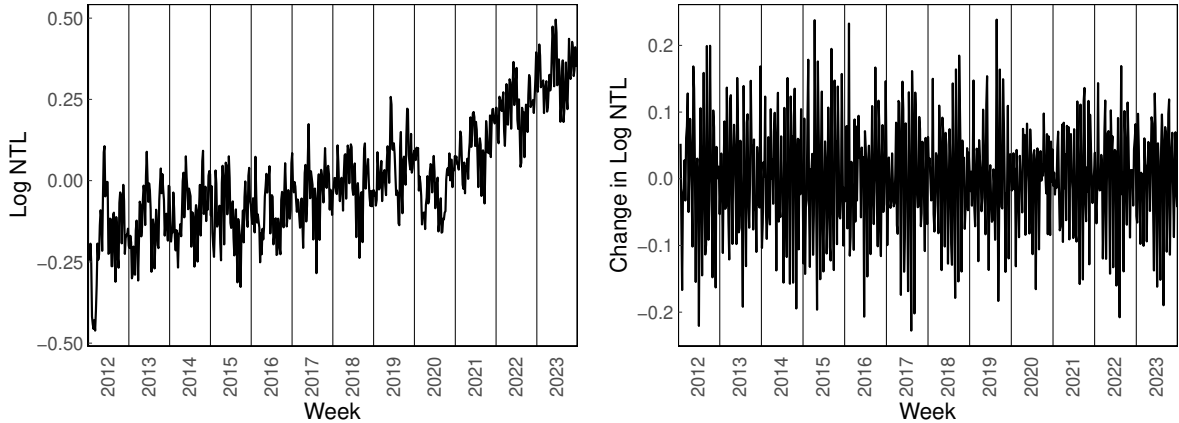


Figure 2: Nationwide Weekly Average Log NTL

Notes: For each week, the date chosen is the Monday of the week. Log NTL shown is the logged value of the average NTL across every day in the week. For each day, NTL is the average value of all cells nationwide.

The time series of the differentiated log NTL looks like a random walk, excluding potential unit roots. The summary statistics of the matched weekly data are in Table A.1.

## 2.3 Other Data

Apart from the data shown above, we also use the national account records from China and other countries, weather data, financial market data, real estate and construction

investment data, news shocks data, land transaction data, firm data, etc. For more details, please refer to Appendix subsection A.3.

### 3 NTL and Output

In this section, we illustrate NTL is a good proxy for real output. Intuitively, NTL should positively correlates with traditional economic activity indicators, such as GDP. Figure 3 shows such associations at the city level.

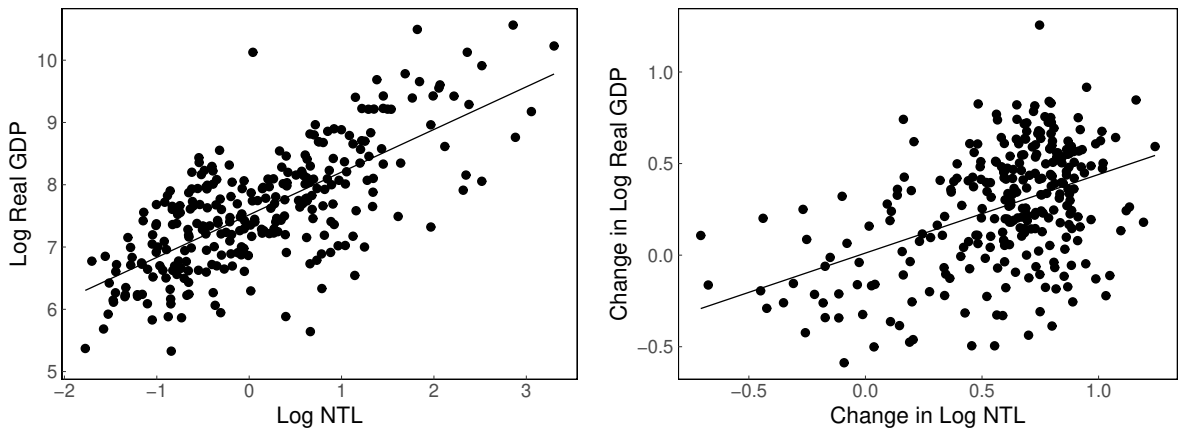


Figure 3: NTL and GDP by City

Notes: Log NTL is converted to the corresponding frequency of the national account indicators in each plot. Log NTL is the logged value of the average NTL across every day in the converted periods. For each day, NTL is the average value of all cells in each city. The left graph shows the data in 2020. The right graph shows the changes from 2012 to 2021.

Using the annual panel data with NTL and different indicators from the national accounts, we apply the following regression equation.

$$y_{i,t} = \beta_0 l_{i,t} + \gamma_i + \tau_t + u_{i,t} \quad (1)$$

Here  $y$  is an output indicator (e.g., log GDP), and  $l$  is the log NTL.  $i$  and  $t$  are identifiers for city and year, respectively. To address the endogeneity issue, we use NTL in the last year as the IV of the current NTL following J. Kim et al. (2022) and Chor and Li (2024). We also control for two-way fixed effects. When both  $y$  and  $l$  are in log

forms,  $\beta_0$  is the elasticity of output on NTL. The regression results of overall GDP and GDP by sector on NTL are in Table 1.

Table 1: Regression of GDP on NTL: Sector

Dependent Variable:		Log GDP			
Sector:	All	Primary	Secondary	Tertiary	
Model:	(1)	(2)	(3)	(4)	
<i>Variables (Second stage)</i>					
Log NTL	0.3958*** (0.0648)	-0.0122 (0.0541)	0.5819*** (0.0911)	0.3474*** (0.0710)	
<i>Fixed-effects</i>					
City	Yes	Yes	Yes	Yes	
Year	Yes	Yes	Yes	Yes	
<i>Fit statistics</i>					
N	2,569	2,569	2,569	2,569	
R <sup>2</sup>	0.9830	0.9814	0.9673	0.9846	
F-test	1,868.8	1,674.1	948.7	2,040.5	

Notes: The instrumental variable of the log nighttime light is the same indicator in the previous period. The first-stage regression coefficient is 0.8403 (s.e.: 0.0138). Significance levels are based on Clustered (Region) standard-errors. Significance Codes: \*\*\*: 0.01, \*\*: 0.05, \*: 0.1.

The elasticity for aggregate GDP is about 0.4, consistent with previous literature. Further looking at the elasticity by sector, the primary sector (agriculture) GDP does not correlate with NTL, as agriculture activities mainly occur during the days. Both secondary (manufacturing and construction) and tertiary (service) sectors' GDP significantly and substantially correlate with NTL. Table B.1 implies the significant elasticity

across periods. Therefore, the fluctuation in NTL reflects changes in economic output.

NTL partly comes from economic activities such as urbanization and trade. Table B.2 shows the significance of the two channels. First, urban expansion reflects the output in the construction sector. When the city’s boundary expands from more construction, NTL in the newly built-up area increases. Figure B.1 shows the positive correlation between urbanization rate growth and NTL growth from 2012 to 2021, a period characterized by rapid urbanization in China. Second, the export-oriented manufacturing sector has night shifts, and their activities at night positively correlate with export amount (Chor & Li, 2024).

Next, we run the same regression in Equation 1 at the country level using the cross-country national accounts, and the results are in Table B.3. In line with previous literature (Bickenbach et al., 2016; Henderson et al., 2012; Martínez, 2022), NTL better proxies GDP for emerging economies. Intuitively, several channels of GDP growth reflected on NTL mostly apply to emerging economies, including urbanization and night shifts in the manufacturing sector.

## 4 The Spillover Effects

Following the mainstream literature (e.g. Swanson, 2021, and Jarociński, 2024), we adopt the local projection (LP, Jordà, 2005) method to study the spillover effects. Specifically, we apply the following regression equation.

$$y_{t+h} - y_{t-1} = \alpha^{(h)} + \sum_{q=1}^Q \phi_q^{(h)} \Delta y_{t-q} + \sum_{m=0}^M \beta_m^{(h)} x_{t-m} + \sum_{r=1}^R \gamma_r^{(h)} W_{t-r} + \tau_t + u_{t+h|t} \quad (2)$$

where  $y_t$  is log NTL in week  $t$ ,  $\Delta y_t$  is the change in log NTL in week  $t$  relative to week  $t - 1$ ,  $x$  is the high-frequency federal fund rate shock around the FOMC announcement.<sup>6</sup> We use AIC criteria to choose the lags of the dependent variable and the shocks. In the extended specifications, we add controls as  $W$  and time fixed effects as  $\tau_t$ . The key

---

<sup>6</sup>We only study the effects of conventional monetary policy here. The comparison with unconventional monetary policy will be discussed later.

underlying assumption here is that the change of NTL is mainly affected by the US MPS in such a short window around the FOMC meetings.

Applying the equation for  $h = 0, \dots, H$ , the IRF is obtained from  $\{\beta_0^{(0)}, \dots, \beta_0^{(H)}\}$ . We look up to  $H = 20$  for the weekly series. The IRF of the baseline LP regressions is displayed in Figure 4.

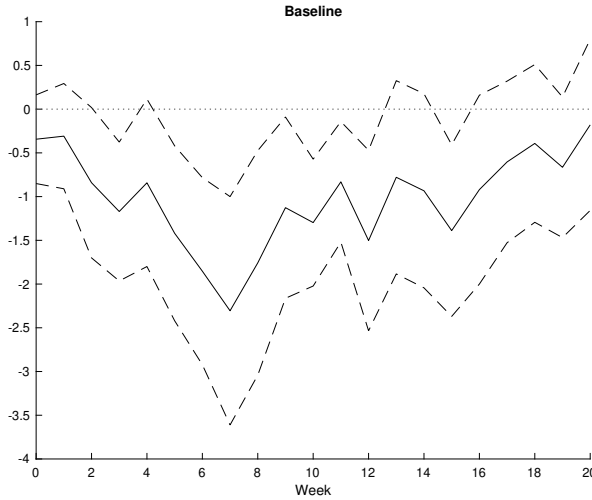


Figure 4: Local Projection of NTL on US MPS: Baseline

Notes: MPS is aggregated to the weekly frequencies consistent with the dependent variable. The number of lags of the dependent variable ( $Q$ ) and the shock ( $M$ ) are selected by the AIC criteria for up to 4 periods. The dashed ribbons are the 90 percent confidence intervals generated based on the Newey-West standard errors.

There are several takeaways from our baseline results: (1) Using a high-frequency specification, we confirm that the US monetary policy shocks negatively affect China’s real activities, which is consistent with previous literature (e.g. S. Kim, 2001, Maćkowiak, 2007, and Bluedorn and Bowdler, 2011, etc.). (2) People tend to believe that monetary transmission, especially cross-border spillover, is lagged. Usually, the foreign real activity is assumed to be affected by US interest rate shocks by a lag of one quarter (Uribe and Yue, 2006). However, we find that the spillover effect is much quicker than people’s traditional expectations. It peaks in the seventh week (about two months) after the shock and reaches half of the peak in the third week. It then gradually dies out and turns

insignificant after the 20th week. (3) The magnitude of the shock on the real economy is material. A unit of the US MPS shock declines China’s NTL by 2.3 log points at peak (7 weeks after the shock).<sup>7</sup> Using the correlation we obtain from the NTL-GDP (0.4), the estimated unit impact on the real economy is around one log point.

## 4.1 Robustness

A natural question is whether our findings are robust in subsamples. First, we check whether the responses to MPS differ when the zero lower bound (ZLB) is binding. Following the FRED database,<sup>8</sup> we define non-binding period as from December 16th, 2015 to March 16th, 2020 and since March 17th, 2022.<sup>9</sup> Correspondingly, the binding period is from early 2012 to December 16th, 2015, and from March 16th, 2020 to March 17th, 2022. We apply the baseline LP identification for the two subperiods and the results are in Figure 5. It shows that the effects are negative in both periods with a slightly higher statistical significance for the former. This indicates that the spillover effect of US MPS is not discounted by the ZLB constraint in the US.

---

<sup>7</sup>The standard deviation of the shock is 0.017 from 2012 to 2023 (our sample period), implying that one standard deviation shock would cause a peak of 1.56% drop in China’s weekly output.

<sup>8</sup>We use the indicator “EFFR” (Effective Federal Fund Rate) as the reference.

<sup>9</sup>We include a week in the subsample only if the Monday in the week is within the period. The starting date of the period is inclusive, and the ending date of the period is exclusive.



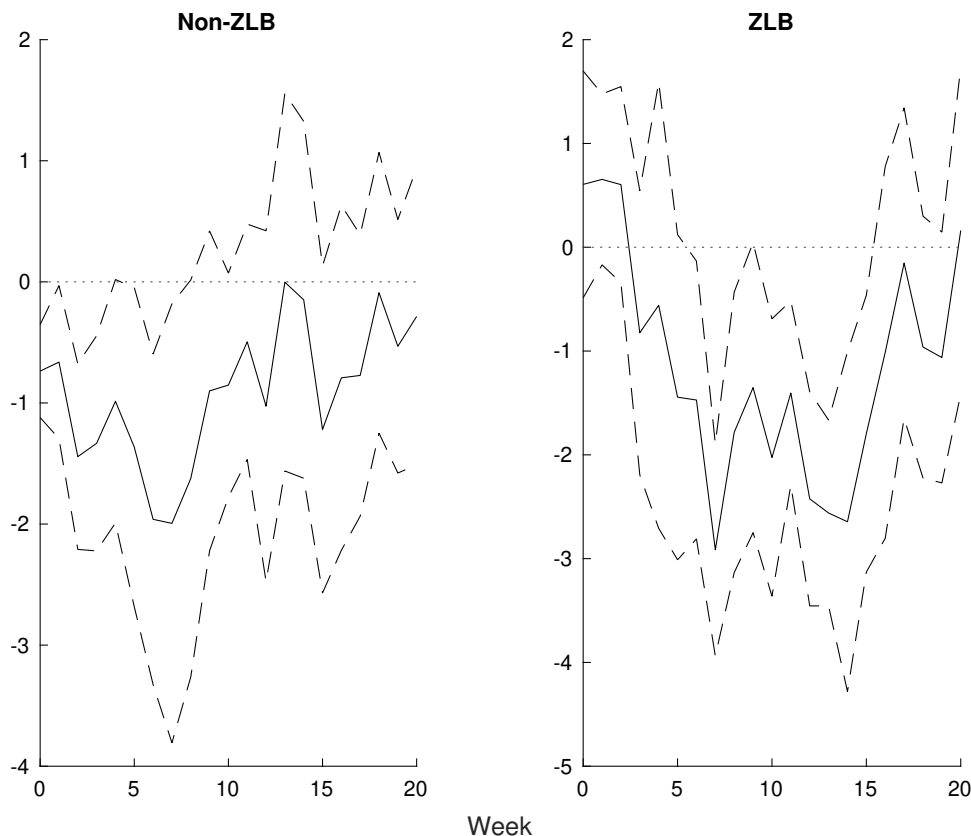


Figure 5: Local Projection of NTL on US MPS: ZLB

Notes: The non-ZLB period is from December 16th, 2015 to March 16th, 2020 and from March 17th, 2022 to late 2023. Correspondingly, the ZLB period is from early 2012 to December 16th, 2015 and from March 16th, 2020 to March 17th, 2022. MPS is aggregated to the weekly frequencies consistent with the dependent variable. The number of lags of the dependent variable ( $Q$ ) and the shock ( $M$ ) are selected by the AIC criteria for up to 4 periods. The dashed ribbons are the 90 percent confidence intervals generated based on the Newey-West standard errors.

Moreover, there has been a trade war between the US and China since January 2018, which potentially changed the transmission of the US shock to China. To verify this conjecture, we conduct the baseline analysis across two periods: Before the trade war (2012-2017) and Since the trade war (2018-2023). The results are in Figure 6, which shows that the US tightening could weak China's NTL in both periods with magnitudes before the trade war slightly bigger and more significant. This is plausible as the two economies are more connected before the intensification of trade conflicts.



Figure 6: Local Projection of NTL on US MPS: Before and Since the US-China Trade War

Notes: The Before Trade War period is from early 2012 to late 2017. Correspondingly, the Since Trade War period is from early 2018 to late 2023. MPS is aggregated to the weekly frequencies consistent with the dependent variable. The number of lags of the dependent variable ( $Q$ ) and the shock ( $M$ ) are selected by the AIC criteria for up to 4 periods. The dashed ribbons are the 90 percent confidence intervals generated based on the Newey-West standard errors.

Our results are robust to many other checks. (1) The response remains almost the same by replacing our baseline shock with the conventional MPS identified by Acosta (2022), as shown in Figure C.1. (2) The confidence band is qualitatively the same by bootstrapping the standard error instead of using the Newey-West in the baseline, as shown in Figure C.2. (3) We restrict the identification to exclude the lags of the shocks and use only one period lag of NTL change as a control. The results are in Figure C.3, which remain qualitatively unchanged, though the peaks of the negative responses are in the eighth week. (4) By changing the frequency of the series from weekly to daily, the

results are consistent as in Figure C.4. The peaks of the negative responses are at about the 50th day, close to the 7-week peaks in the weekly identification. (5) Concerning the measurement error induced by recorded light in the human-less areas, we remove the mountain and other inhabitable areas, and the overall NTL responses are in Figure C.5.

There might be some confounding factors other than MPS that affect the NTL in China. (1) The NTL may also be affected by the US news shock that happened in the same week as the monetary announcement. So, we add some concurrent macro news shocks (such as GDP, CPI, PPI, and Employment) or S&P 500 return to the identification and find robust results, as shown in Figure C.6.<sup>10</sup> As another way to control the US macro or financial news effect, we also add past cumulative news shocks or equity return to the baseline LP regression, and the result is qualitatively similar, see Figure C.7.<sup>11</sup> Moreover, controlling US GDP or Industrial Production as controls also yields a consistent conclusion, see Figure C.8. (2) The NTL possibly changes with the weather conditions irrelevant to economic performance. To address this concern, we add weather controls to the baseline, and the results are robust and are displayed in Figure C.9. We also perform a falsification test by replacing the baseline’s NTL with weather indicators. The results are in Figure C.10. As expected, we do not find any significant responses by these indicators. (3) China’s monetary policy may also change the output, so we control the concurrent SHIBOR interest rate in the baseline to absorb China’s monetary effects. These results are in Figure C.11 suggesting that adding the control does not change our baseline conclusion. Moreover, adding SHIBOR as another “shock” in the LP identification does not change the responses to the US MPS either, as shown in Figure C.12, and the interest increase in China also harms the domestic activities. (4) The trade relationship between China and the US may determine China’s real activities as we have illustrated above, thus we also try to control the US-China tension constructed by Rogers et al. (2024) in the baseline,

---

<sup>10</sup>The macro news shocks are the differences between the data release and the previous consensus expectations, which are obtained from the widely used survey by Action Economics, the successor to Money Market Services. We use the “advance” GDP release, headline CPI and PPI inflation, and non-farm payrolls from the employment report. The data are from Lakdawala et al. (2021).

<sup>11</sup>We use cumulative values for each macro news shock or equity return with a 60-day window before the FOMC meetings. Adjusting the window length does not qualitatively change the results.

and the results are almost unchanged. Please refer to Figure C.13.

## 4.2 Low-frequency Output Responses

Now, we compare our high-frequency results with those of low-frequency variables of output. For China's nationally aggregated time series, we look at two key indicators for real output: real GDP and Industrial Production (IP) at their highest frequency. We apply the LP method (Jordà, 2005) for quarterly GDP and monthly IP, and the impulse response functions (IRF) are in Figure 7. It was found that the spillover effects are negative overall for both series, which is consistent with our weekly and daily results.<sup>12</sup> Nevertheless, the results are not quite statistically significant. This highlights the benefits of employing higher-frequency measurements for a cleaner identification.

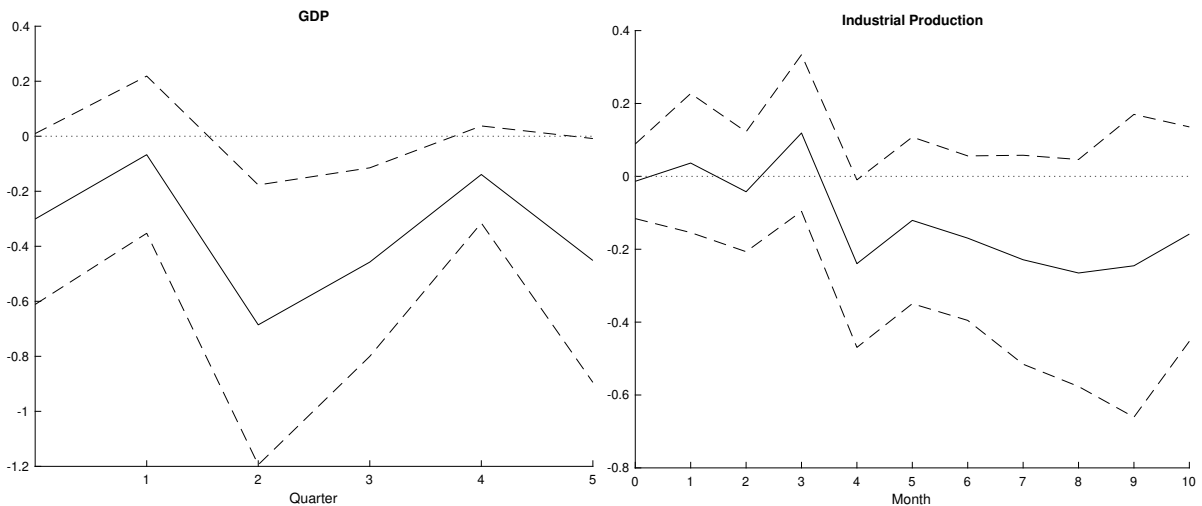


Figure 7: IRF of China's Quarterly GDP and Monthly Industrial Production on US MPS

Notes: MPS is aggregated to the frequencies consistent with the corresponding dependent variables. The number of lags of the dependent variable ( $Q$ ) and the shock ( $M$ ) are selected by the AIC criteria for up to 4 periods. The dashed ribbons are the 90 percent confidence intervals generated based on the Newey-West standard errors.

Then, we turn to the impacts on different parts of GDP including consumption,

<sup>12</sup>The responses of industrial production are relatively weak within the first 3 months. As we will explain later, the overall negative responses of NTL, especially in the short run, are driven by construction activities in non-build-up areas rather than manufacturing activities in suburbs.

investment, government spending, and net export.<sup>13</sup> The IRFs are in Figure 8. To begin with, at the aggregate level, we find that the CCAT (“China Cyclical Activity Tracker”) index declines. This is derived from a set of eight non-GDP economic indicators. The GDP responses here are also overall negative, consistent with the official GDP records and industrial production. Regarding the decomposition, it is seen that in the short run ( $t = 0$ , current quarter), consumption, government spending, and net exports are barely affected, the negative responses of GDP are mainly driven by investment reduction. Later, due to a decline in investment, which may cause a rise in the unemployment rate and a drop in household income and tax, consumption and government spending begin to shrink, with the magnitude even exceeding the investment reaction. Although net exports slightly increase, it can not offset the negative impacts on investment, consumption, and government spending. Recall our NTL analysis, we see that the peak of effects comes at around 7 weeks and the effects eventually die out at around 20 weeks, which suggests that the NTL variation may mainly reflect the changes of real activities on investment as consumption, government spending, and export responses have a longer time lag. The IRFs using official economic indicators are in Figure C.14, and the results are overall consistent.

---

<sup>13</sup>This data is from K. Chen et al., 2024, which provides internally more consistent decomposed series of GDP with a longer period than the official data.

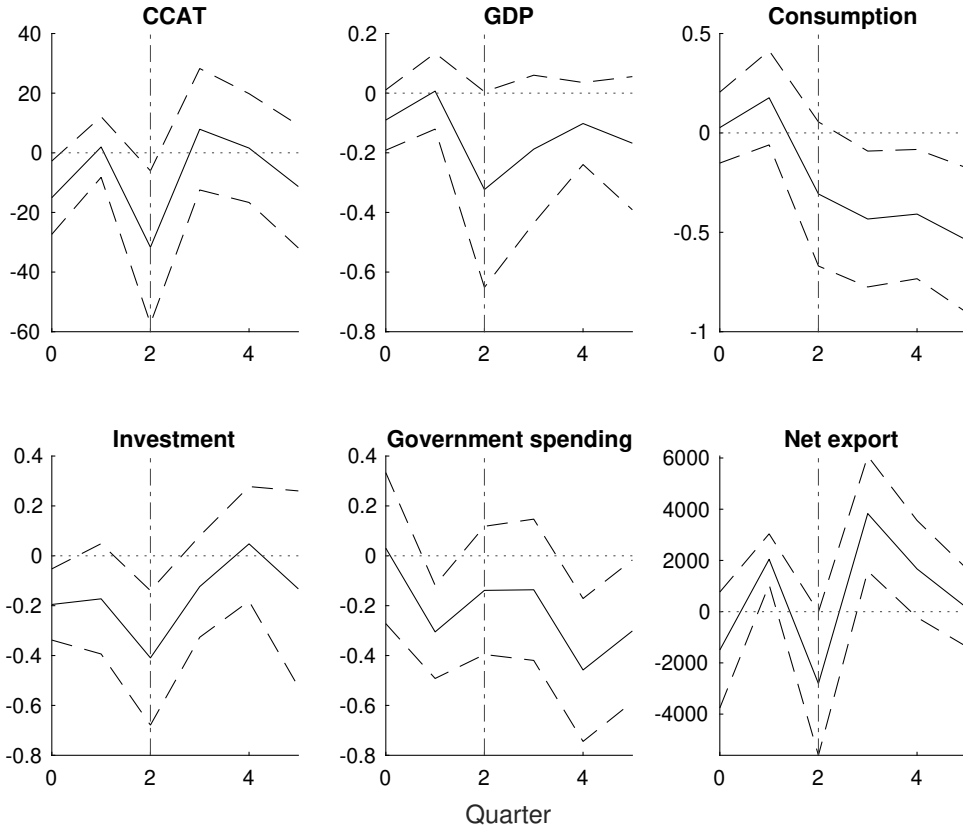


Figure 8: IRF of China's Quarterly Alternative Economic Indicators on US MPS

Notes: MPS is aggregated to the quarterly frequencies consistent with the dependent variable. The number of lags of the dependent variable ( $Q$ ) and the shock ( $M$ ) are selected by the AIC criteria for up to 4 periods. The dashed ribbons are the 90 percent confidence intervals generated based on the Newey-West standard errors.

## 5 Construction channel

In this section, we illustrate that our baseline finding is in line with a construction channel. We first decompose the NTL responses into three parts: city centers, suburbs, and non-built-up areas. It is seen that the overall negative responses of NTL are driven by the reaction in non-built-up areas that feature construction-related activities. We then directly verify this channel by showing that the real estate investment, construction investment, land investment, building sales, and land transactions all decrease after a US tightening shock. Finally, we find that the construction activity responses are consistent with a worsening in China's financial market, including the rise of interest rates and the

drop in equity prices, especially real state stocks.

## 5.1 Decomposition of Different City Sectors

To look at the heterogeneous responses by different sectors, we separately apply the baseline identification on the city center, the suburbs, and the non-built-up area as of 2010. Using the satellite image-based identification by H. Jiang et al. (2022), we define the city center as the built-up area as of 1990, and the suburb as the area built up in 2010 but not in 1990.<sup>14</sup> We choose 2010 as the threshold year because the NTL series starts from 2012, therefore excluding potential endogeneity issues. We illustrate the city center, the suburb, and the non-built-up area for selected cities as follows.

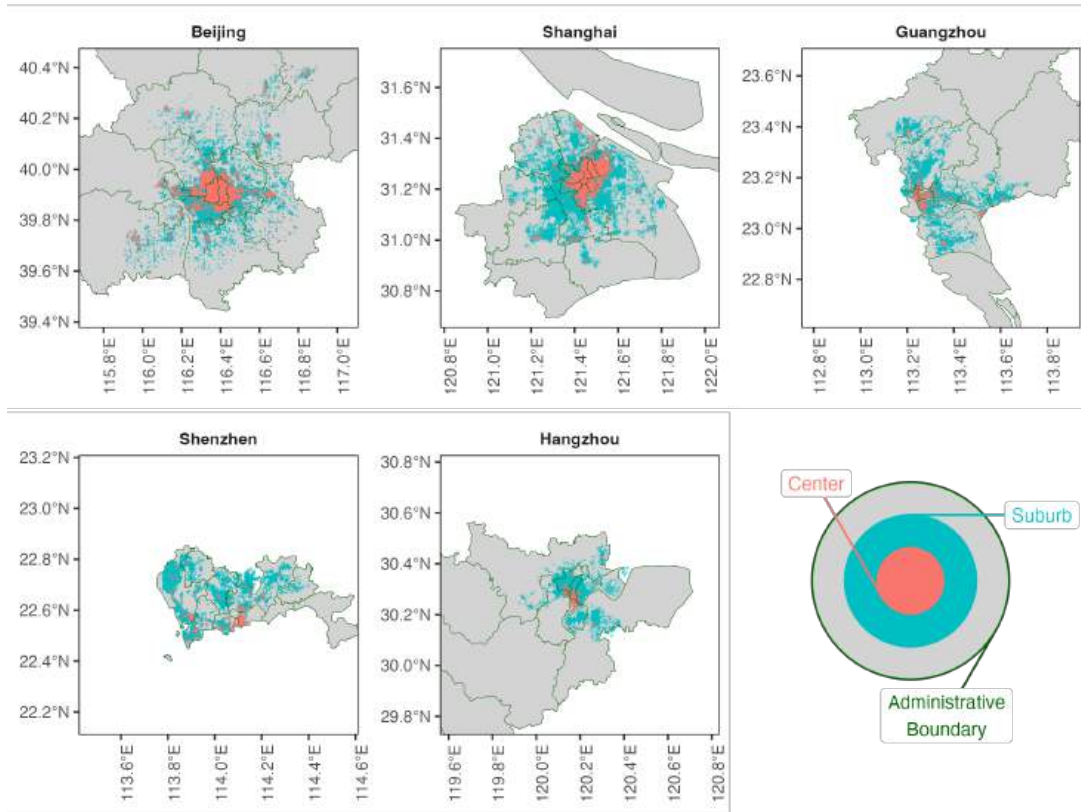


Figure 9: Built-up Areas of Selected Cities

Notes: The boundaries of the built-up areas are identified up to 2012.

<sup>14</sup>We confirm the validity of the identification after manually checking the identified centers and suburbs for major Chinese cities, including Beijing, Shanghai, Guangzhou, Shenzhen, and Hangzhou. The identification closely matches the conventional definition of centers and suburbs in these cities.

The heterogeneous responses by sectors are displayed in Figure 10. It shows that the effects on non-built-up areas are quite significantly negative, driving the overall responses. The NTL in non-built-up areas mainly reflects the real activities of construction, such as the light from construction sites at night and from new buildings. These are highly sensitive to concurrent changes in the economic and financial environment. Intuitively, the US tightening could quickly worsen China’s financial markets and harm people’s economic outlook, and later deteriorate firms’ operations<sup>15</sup>, which would lead to a delay, slowing, or even stagnation in the construction works. In a boom of the housing market, real estate developers may urge the construction firms to work more so that they can quickly sell houses and get more cash flows. In this case, more night working may be arranged and more houses will be put into use, thus generating more light. Instead, in a recession period after the US tightening, the pattern is the opposite.

By comparison, the impacts are insignificant for the center and suburbs, the NTL of which mainly implies service and manufacturing activities respectively. In the previous section, we display that the current quarter GDP change is mainly driven by investment. Based on the NTL responses of the different city sectors, we may further conclude that the investment reduction is more likely to be caused by construction-related activities, rather than manufacturing activities.

As a robustness check, we stack the NTL of the three areas together and identify MPS times city area dummies (MPS  $\times$  Center, MPS  $\times$  Suburb, and MPS  $\times$  Non-built-up Area) as three separate shocks so that we can estimate the response in different sectors simultaneously.<sup>16</sup> The results are similar, as shown in Figure D.1.

<sup>15</sup>Evidence will be provided in later sections.

<sup>16</sup>The specification is  $y_{i,t+h} - y_{i,t-1} = \alpha^{(h)} + \sum_{q=1}^Q \phi_q^{(h)} \Delta y_{i,t-q} + \sum_{m=0}^M \beta_{m1}^{(h)} \cdot x_{t-m} \cdot Center_i + \sum_{m=0}^M \beta_{m2}^{(h)} \cdot x_{t-m} \cdot Suburb_i + \sum_{m=0}^M \beta_{m3}^{(h)} \cdot x_{t-m} \cdot NBA_i + u_{i,t+h|t}$ , where  $y_{i,t}$  is the NTL of a sector (Center, Suburb, or Non-built-up area) in time  $t$ ,  $Center$ ,  $Suburb$ ,  $NBA$  are three dummies of city area, respectively. We choose  $M = 0$  and  $Q = 4$  for the number of lags in line with the specifications when we regress the three areas’ NTL separately. We plot the IRF of  $\beta_{01}$ ,  $\beta_{02}$ , and  $\beta_{03}$ .



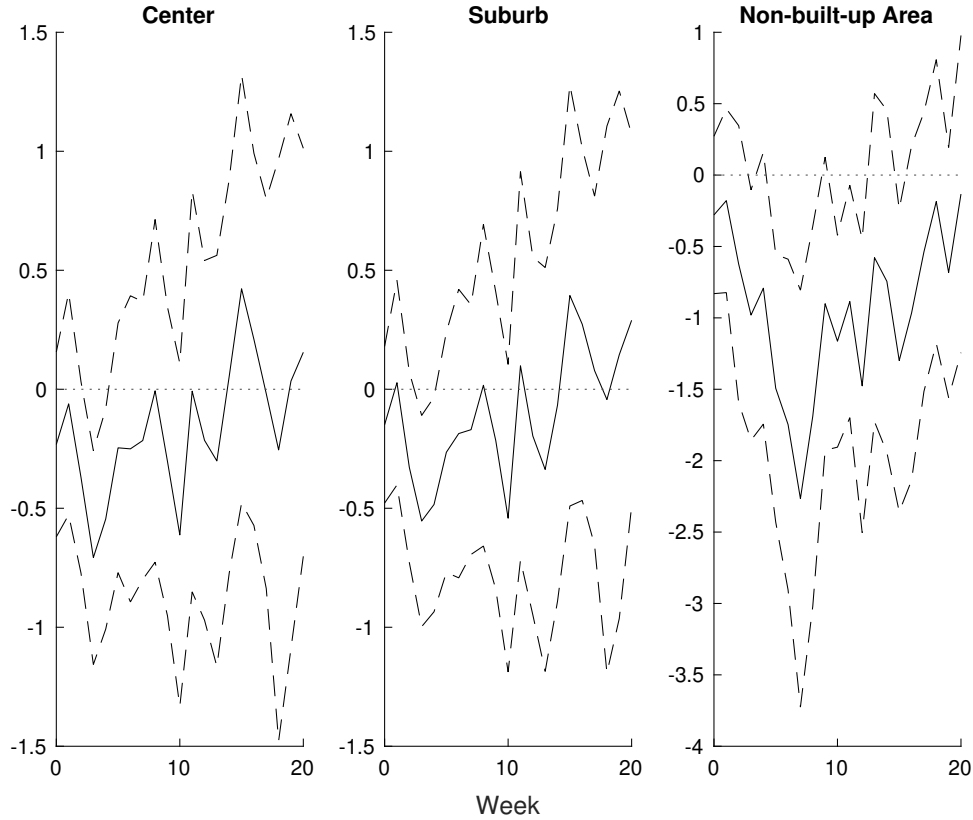


Figure 10: Local Projection of NTL on US MPS: City Areas

Notes: MPS is aggregated to the weekly frequencies consistent with the dependent variable. The number of lags of the dependent variable ( $Q$ ) and the shock ( $M$ ) are selected by the AIC criteria for up to 4 periods. The dashed ribbons are the 90 percent confidence intervals generated based on the Newey-West standard errors.

## 5.2 Responses of Construction-related activities

To verify this construction channel, apart from the NTL responses decomposition, we also directly display how construction-related activities are affected using monthly market indicators.<sup>17</sup> The specification is similar to our baseline. In Figure 11, it is seen that after a US monetary tightening, there is a significant decrease in projects under construction in the current month and it is even more pronounced later, which directly contributes to the NTL drop in non-build-up areas. Besides, we can also observe a decline trend for construction investment, the responses of which seem to have a three-month lag. This is

<sup>17</sup>The data on market indicators are obtained from the CEIC database.

plausible as an investment in a building may be pre-determined so that it is free from the impact of current factors. By comparison, construction works could be quickly delayed or slowed even in the current period in facing an adverse economic for financial shock.

Also, land investment, the activities in upstream of the construction industry, drop even more prominently and quickly.<sup>18</sup> Consistently, China's real estate investment and residential building investment, the activities in downstream of the construction sector, later significantly decline too.<sup>19</sup> Moreover, from the transaction data, we show that both building sales and land transactions (including cases, area, and value) go down when facing a contractionary US monetary policy.

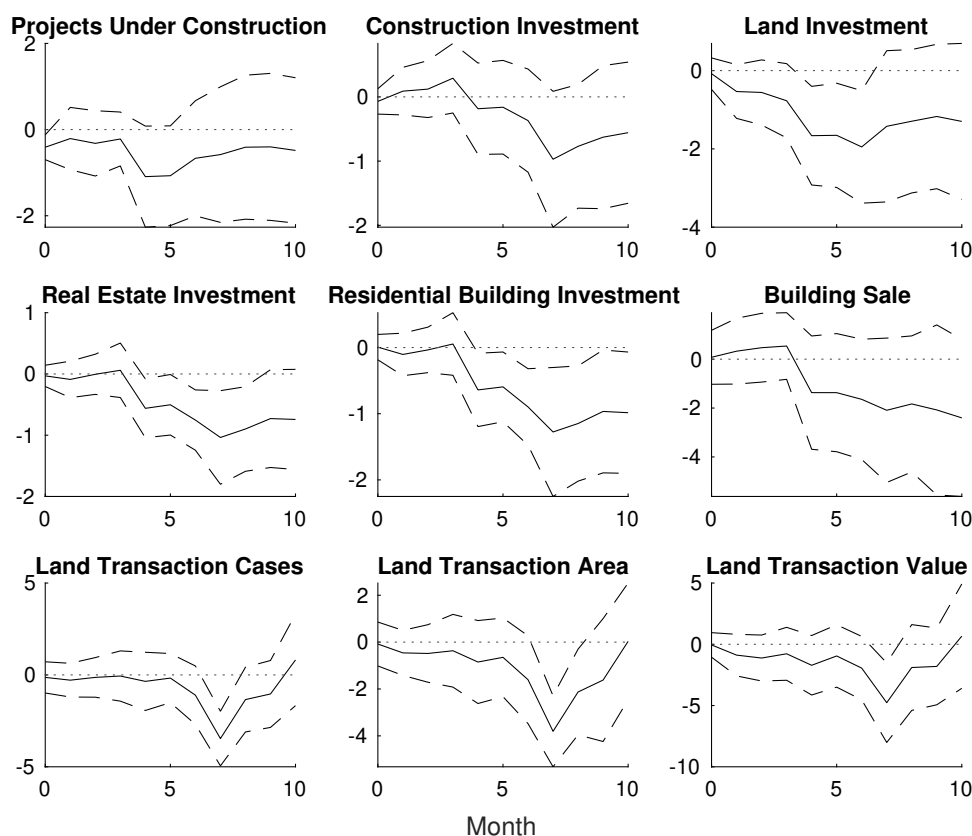


Figure 11: IRF of China's Monthly Real Estate Market Indicators on US MPS

Notes: MPS is aggregated to the monthly frequencies consistent with the dependent variable. The number of lags of the dependent variable ( $Q$ ) and the shock ( $M$ ) are selected by the AIC criteria for up to 4 periods. The dashed ribbons are the 90 percent confidence intervals generated based on the Newey-West standard errors.

<sup>18</sup>Land investment involves the money allocated in purchasing, holding, or developing a land.

<sup>19</sup>This is in line with the literature, such as Jordà et al. (2015) and Ho et al. (2018).

Then, we look at how the NTL is associated with projects under construction. Specifically, we regress NTL changes on the number of projects under construction using the US MPS as the IV.<sup>20</sup> The results are in Figure D.2. As expected, NTL increases with the number of ongoing construction projects.

### 5.3 High-frequency Financial Market Responses

Consistent with the effects on construction activities, we also find negative impacts of the US tightening on China's financial markets, which may justify why the construction and real estate sectors are adversely affected. Firstly, we show that the interest rates in China will increase after a US MPS tightening. This explains why there is a drop in construction activities as construction firms and real estate firms are usually quite financially constrained. Specifically, similar to previous literature, we use the 7-day Interbank Bond Collateral Repo Rate as a proxy for China's market interest rate. The result is displayed in Figure 12, where we document a generally positive co-movement between the US tightening and China's interest rate variations, especially within two months. This result is robust to using other market interest rates, such as the SHIBOR rates (see Figure D.3).

---

<sup>20</sup>We use lagged MPS values up to 10 months apart from the contemporary MPS in the first stage.

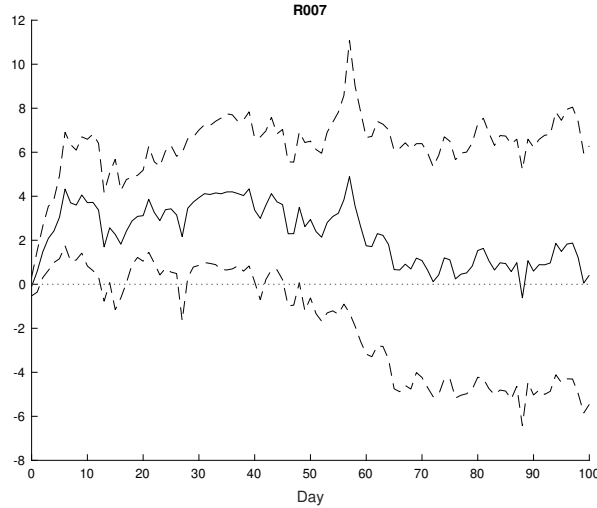


Figure 12: IRF of Interbank Bond Collateral Repo Rate on US MPS by Maturity

Notes: The number of lags of the dependent variable ( $Q$ ) and the shock ( $M$ ) are selected by the AIC criteria for up to 4 periods. The dashed ribbons are the 90 percent confidence intervals generated based on the Newey-West standard errors.

Secondly, the stock prices reflect the market expectation of economic performance. We use several daily Shanghai Stock Exchange (SSE) Indexes as examples and check their responses to the US MPS. These results are shown in Figure 13. It is seen that the overall stock indexes (SSE composite, SSE 50, and SSE180) negatively respond to the US tightening, peaking at around 7 weeks after the shock, which is quite close to the impacts on nighttime light. Looking at each sector, the movements align with the overall market, with real estate stocks reacting even more negatively and quickly than the aggregate market. The aggravation in the stock market will further deteriorate the financial tightness for real estate and construction firms and hence harm their investment and other real activities.

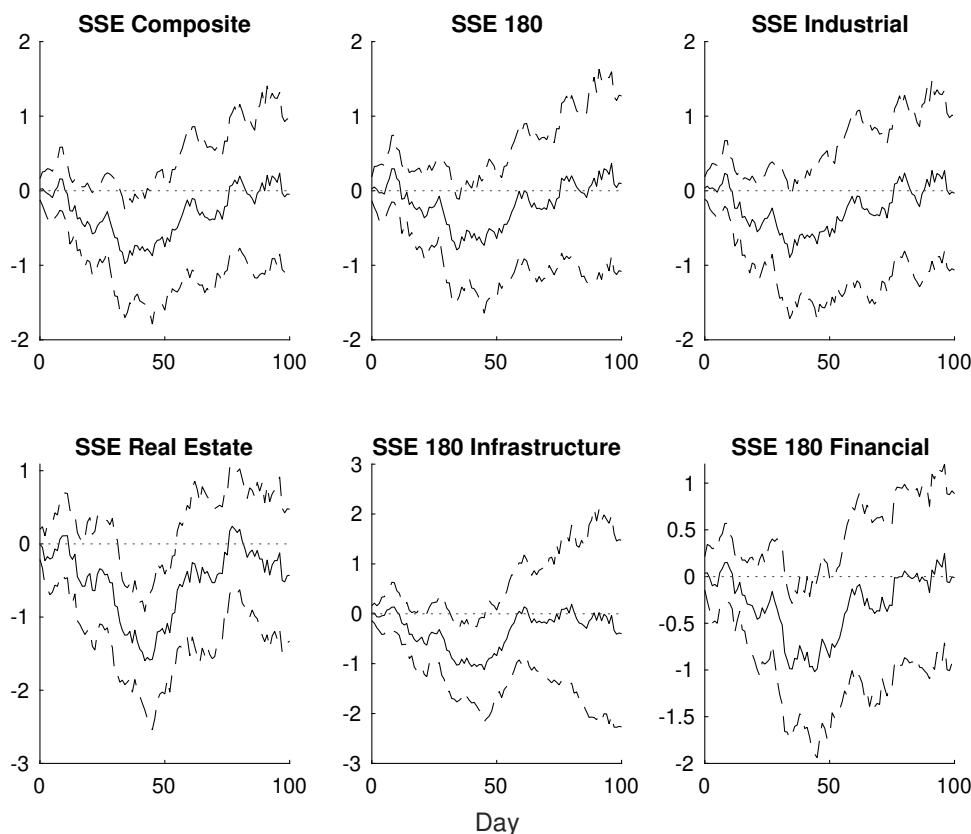


Figure 13: IRF of Shanghai Stock Index on US MPS by Maturity

Notes: The number of lags of the dependent variable ( $Q$ ) and the shock ( $M$ ) are selected by the AIC criteria for up to 4 periods. The dashed ribbons are the 90 percent confidence intervals generated based on the Newey-West standard errors.

As suggested by the evidence of the listed firms, we find that the firm operation indicators, including revenue, profit, and trade credit (accounts receivable and accounts payable) all decline in response to US tightening and this detrimental effect is more pronounced for real estate firms (see Table D.1 and Table D.2). Moreover, for real estate firms, those get more involved in land transactions are more sensitive to such shocks. Please see Table D.3 for more details.

## 6 Spatial Heterogeneity and Cross-Sectional Evidence

In this section, we first show that the heterogeneous responses across regions are quite dispersed. Then, we illustrate that this heterogeneity is consistent with our proposed

construction channel. In particular, we find that cities with lower urbanization rates and tighter financial conditions experience a larger drop in NTL after a US tightening shock.

In addition to the overall response of NTL in China, the next question is what are the heterogeneous effects in different places? By leveraging the advantage of the geospatial data, we compare each city's response in China. Applying the same identification specification as Equation 2 to each city, we obtain the corresponding IRF for each place. Then, we take the average responses from the shock period to 20 weeks later.<sup>21</sup> The map plot of the average response by city is in Figure 14.

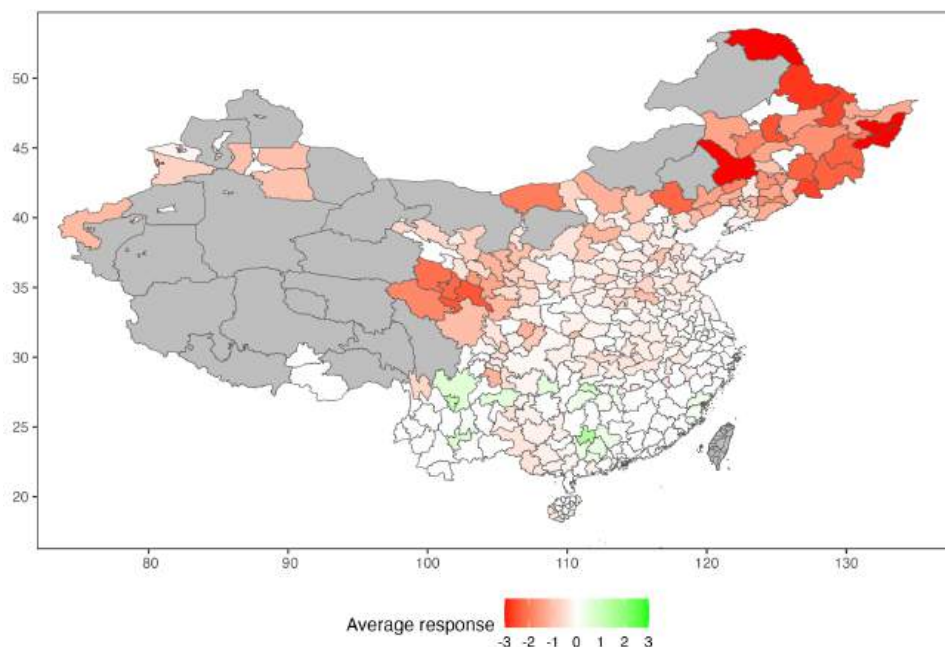


Figure 14: Average Response of NTL on US MPS by City

Notes: MPS is aggregated to the weekly frequencies consistent with the dependent variable. The number of lags of the dependent variable ( $Q$ ) and the shock ( $M$ ) are selected by the AIC criteria for up to 4 periods. When taking the average across the time horizon from the week the MPS is realized to 20 weeks later, insignificant values at a 90 percent confidence level are treated as zero. If the city has both significantly positive and significantly negative responses, the average response by the city is interpreted as zero. Extreme values with absolute values greater than 3 are winsorized on the map.

<sup>21</sup>Insignificant responses are treated as zero. For cities with significant responses of both signs along different horizons, which applies to a few cases, the average responses are also treated as zero.

The spatial heterogeneity is visible across Chinese cities. The negative responses are more substantial in the hinterland, notably the northeastern and the western areas. Cities in the eastern coastal area have the least negative responses, and some even have slightly positive reactions. Therefore, the overall negative NTL response to a US tightening shock is mainly driven by the inland areas.<sup>22</sup> We also look at the heterogeneity at the province level. The map plot is in Figure D.4. The results are consistent with the city-level version, with the negative responses most substantial in the inland provinces.

Then we look at the city-level responses across the three city areas. The results are in Figure D.6. The overall negative responses are driven by the non-built-up area for most cities, and the negative responses in the non-build-up area are mainly in inland cities.

## 6.1 Urbanization Rate

We conjecture that if the NTL responses reflect a construction channel, cities that have more construction activities should be more affected. To verify that, we use the urbanization rate to measure the intensity of construction. For each city, the urbanization rate is defined as the percentage of the population with urban household registration over the total population. Usually, cities with lower urbanization rates should be more engaged in construction-related activities. To quantitatively associate the urbanization rate with the responses to US MPS, we identify with a city-level panel of NTL, US MPS, and urbanization rate. The regression equation is as follows.

$$y_{i,t+h} - y_{i,t-1} = \beta_1^{(h)} s_{i,t-L} + \beta_2^{(h)} x_t s_{i,t-L} + \gamma^{(h)} W_{i,t-1} + \alpha_i^{(h)} + \tau_t^{(h)} + u_{i,t+h|t} \quad (3)$$

Here  $y_{i,t}$  is log NTL in city  $i$  in week  $t$ .  $x_t$  is MPS in week  $t$ .  $s_{i,t}$  is the urbanization rate in city  $i$  in week  $t$ .<sup>23</sup>  $W$  includes controls, such as weather.  $\alpha$  and  $\tau$  are city and week fixed effects, respectively. To exclude potential endogeneity, the urbanization rate

---

<sup>22</sup>Like the previous section, we also add weather control variables to the identification, and the map plot is in Figure D.5. The results are qualitatively the same as the baseline. The weather data is unavailable for a considerable proportion of cities in the eastern coastal area.

<sup>23</sup>In the baseline, the urbanization rate is updated on an annual basis. Therefore, the value used depends on the year in which the week  $t$  is located.

used in the regression is lagged by  $L$ . We choose the length of the lag as one year in the baseline. The key coefficient estimates are  $\beta_2^{(h)}$  and the IRF of each horizon  $h$  is displayed in the first panel of Figure 15. We find that the coefficients of interaction terms are overall significantly positive, which indicates that a city with a lower urbanization ratio is more negatively affected by the US tightening. The results are almost similar using the urbanization rate in 2008 (see the right upper panel). What's more, the results using alternative indicators of urbanization based on land classification, such as urban area rate and urban constructed rate,<sup>24</sup> are in Figure 15, which are qualitatively consistent with the urbanization rate based on population compositions.<sup>25</sup> The map plot of the urbanization rate and the urban area rate are in Figure D.7 and Figure D.8.

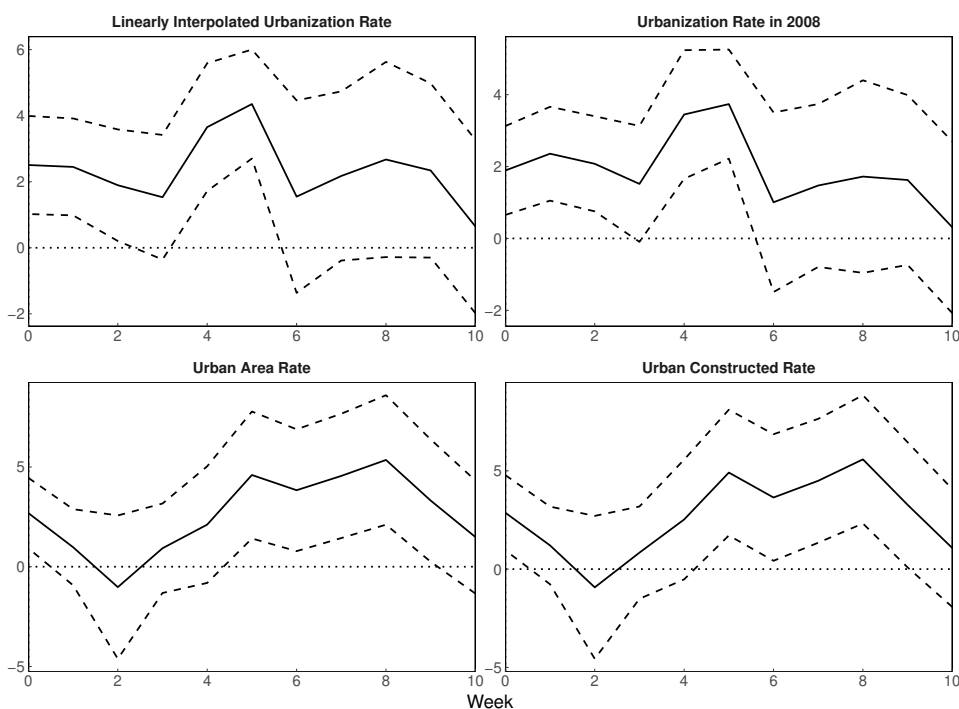


Figure 15: NTL Response to Interaction of US MPS and Urbanization, City level

Notes: The dashed ribbons are the 90 percent confidence intervals generated based on standard errors clustered to city and week.

<sup>24</sup>For each city, the urban area rate is defined as the percentage of the administrative area that is built up. The urban constructed rate is defined as the percentage of the administrative area that is used for building human facilities.

<sup>25</sup>Our results are robust to weather controls, which are omitted for space saving and are available upon request.



Consistently, we find that cities that experience higher growth in recent land transactions are also more affected by the US tightening because construction-related activities are more intensively involved in these cities. The same logic, cities with a bigger fixed asset investment to GDP ratio, and with more projects under construction, are more affected. The results are shown in Figure 16.

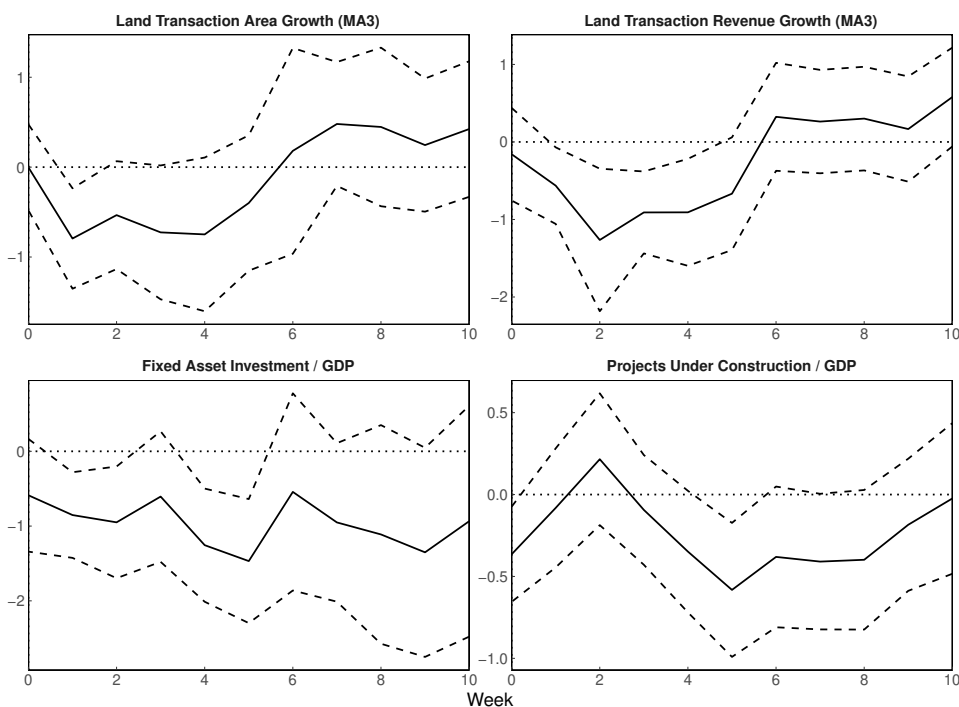


Figure 16: NTL Response to Interaction of US MPS and Land Transaction or Related Investment, City level

Notes: For each city, the growth rate is calculated as the moving average of the annualized growth rates of aggregated values in the last three years (inclusive). The dashed ribbons are the 90 percent confidence intervals generated based on standard errors clustered to city and week.

## 6.2 Financial Market Conditions

As we have shown in previous sections, the US tightening deteriorates China's financial market, which worsens firms' operations and then causes a decline in construction related activities. Consequently, cities with more fragile financial conditions should experience a larger adverse impact. In light of this, we first look at the role of financial market

development, which is proxied by the number of bank subsidiaries per capita.<sup>26</sup> The identification strategy is the same as the urbanization rate regression (Equation 3), except for replacing the urbanization rate indicator with the financial market development indicator. The result is in the first panel of Figure 17. It is seen that the adverse effects are more pronounced for cities with less developed financial environments. This is plausible as in those places, the financing conditions are fragile and are more likely to be aggravated facing the US tightening, which then causes a larger decline in construction-related activity as is reflected in the NTL of non-built-up areas. The results using alternative indicators of financial market development, such as the ratio of loan and deposit to GDP, are in the middle panel of Figure 17, which are qualitatively consistent with the baseline indicator. What's more, we also find that cities with more floor space waiting to sell suffer larger drops in NTL because these cities usually have worse liquidity and more vulnerable financial conditions.<sup>27</sup>

---

<sup>26</sup>In advanced countries, people usually use the ratio of equity value over GDP to measure the financial development of a region. By comparison, in emerging markets, indirect financing like bank loans is more pervasive than direct financing such as equity and bond, thus using the intensity of bank subsidiaries is more suitable. This is especially relevant for the construction sector, where most of the firms are not listed.

<sup>27</sup>The map plot of bank subsidiaries per capita and floor space waiting to sell are in Figure D.9 and Figure D.10.

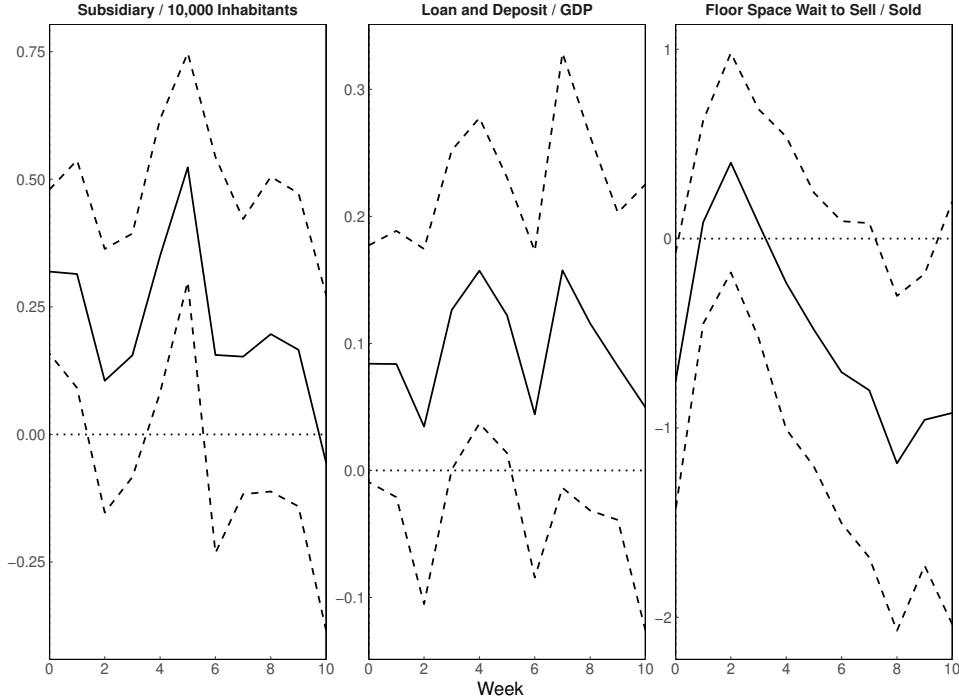


Figure 17: NTL Response to Interaction of US MPS and Financial Market Development, City level

Notes: The dashed ribbons are the 90 percent confidence intervals generated based on standard errors clustered to city and week.

Moreover, we predict that in a place, where the firms in the construction sector have worse financial conditions, the NTL response should be more negative. To verify this prediction, for each city, we look at the average financial-expense-to-revenue ratio, average liability-to-asset ratio, and average accounts-receivable-to-revenue ratio. Higher values mean tighter financial conditions. We use a similar specification as Equation 3 and replace the urbanization variable with firms' financial conditions. The coefficients of the interaction term are displayed in Figure 18. All the indicators negatively impact the response to MPS, implying cities, where construction firms have worse financial conditions, are more negatively impacted by a US tightening. Similarly, the financial conditions of real estate firms, which are supposed to be at downstream of the construction sector, also affect the degree of responses. We show that cities where real estate firms have higher financial-expense-revenue ratio and liability-to-asset ratio are also more harmed by the

US tightening, as shown in Figure D.11.

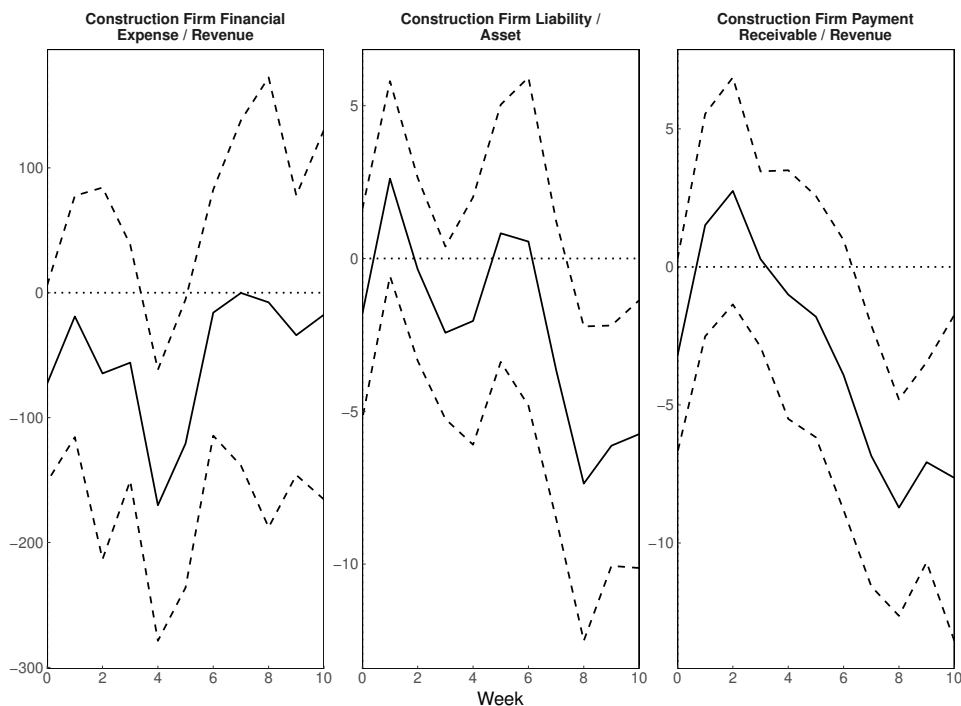


Figure 18: NTL Response to Interaction of US MPS and Construction Firms' Financial Condition, City level

Notes: The aggregated firm data are at the province level. For each city in each year, I assign the corresponding indicators of the province to which the city belongs. The dashed ribbons are the 90 percent confidence intervals generated based on standard errors clustered to city and week.

## 7 Extension

We discuss four extensions in this section. Firstly, we show that trade exposure could partially offset the adverse impacts. Secondly, we investigate the different NTL responses to conventional and unconventional monetary policy. Thirdly, we study the responses of NTL to monetary shocks in the European Central Bank and the Bank of Japan. Finally, we apply the same identification to other countries.

## 7.1 Trade Exposure

Although the overall negative responses are driven by construction investment, we find that trade exposure could mitigate these adverse impacts. This has already been verified in the previous low-frequency results where the net export of China increases after a tightening US shock. Consistently, we have also looked at the exchange rate responses (Chinese Yuan versus US Dollar) to the US MPS. Intuitively, a positive US MPS will depreciate the Chinese Yuan against the US Dollar (see Figure E.1), which will potentially boost the export.

Besides, we also provide some cross-sectional evidence. To start with, we show the ratio of net exports to GDP for each city with available data in 2020. The map plot is in Figure E.2. The trade balance is vastly uneven across China. The eastern coastal cities, notably cities in southern Guangdong, Zhejiang, and eastern Shandong, have a relatively high net export exposure. In contrast, cities in the northeast and the west have a relatively lower and even negative exposure. We predict that cities with more trade exposure are less negatively impacted by a positive US MPS.

The identification strategy is the same as the urbanization rate regression (Equation 3), except for replacing the urbanization rate indicator with the net export share. In the baseline, we use net export share in the last year as the proxy for net export share to preclude endogeneity issues. The key coefficient estimate is  $\beta_2$ . The IRF of  $\beta_2$  obtained from varying  $h$  from 0 to 10 is in Figure 19. Consistent with our prediction, the interaction term is overall positive, which suggests that cities with higher net export share have a smaller adverse impact from the US MPS.

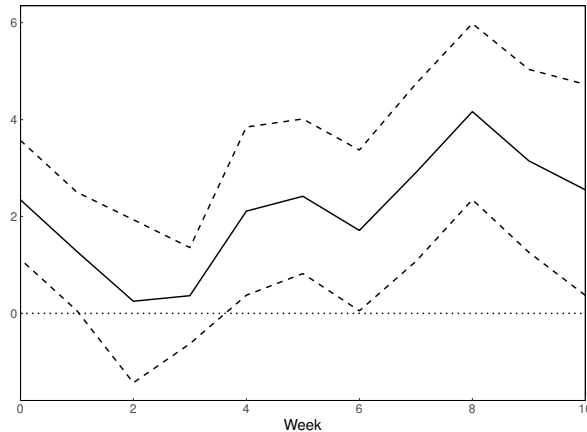


Figure 19: NTL Response to Interaction of US MPS and Trade Exposure, City level

Notes: The dashed ribbons are the 90 percent confidence intervals generated based on standard errors clustered to city and week.

This conclusion is robust to several additional checks. (1) As the trade exposure level substantially differs across regions, we look at the spatial heterogeneity for different subsamples of Chinese cities. We divide the cities into the East (least negative responses overall), the Middle, and the West and Northeast (most negative responses overall).<sup>28</sup> The results shown in Figure E.3 suggest that the mitigation effect of trade is more prominent in the East, and the West and Northeast. (2) We control for the weather factor for NTL orthogonal to economic activities. We use the weather indicators at  $t - 1$  to exclude potential endogeneity issues. The result is in Figure E.4 and is qualitatively the same as the baseline.

## 7.2 Conventional versus Unconventional Monetary Policy

To compare the effects of conventional monetary policy (CMP) and unconventional monetary policy (UMP), we test the impacts of target shock (close to the federal fund rate shock in the baseline) and path shock (i.e. forward guidance).<sup>29</sup> The US MPS we use

<sup>28</sup>The East contains the seven provinces defined as the East by NBSC plus Guangdong. The Middle contains NBSC's North excluding Inner Mongolia and Central and South excluding Guangdong. The West and Northeast contain Inner Mongolia and NBSC's Southwest and Northwest.

<sup>29</sup>These shocks were identified by R. Gürkaynak and Sack (2005) and then updated by Acosta (2022). This data is on the personal website of Miguel Acosta.

other than our baseline are shown in Figure E.5. The comparison is displayed in Figure 20. It is found that only targeted FFR shock has a negative impact on NTL, but not forward guidance, which suggests that the conventional monetary policy is more effective in affecting real output. The results using other UMP proxies by Jarociński (2024), including Large-scale asset purchase shock (LSAP), forward guidance (or called Odyssean forward guidance, close to the path shock in R. Gürkaynak and Sack, 2005), and information shock (or called Delphic forward guidance) are not significant either as shown in Figure E.6.

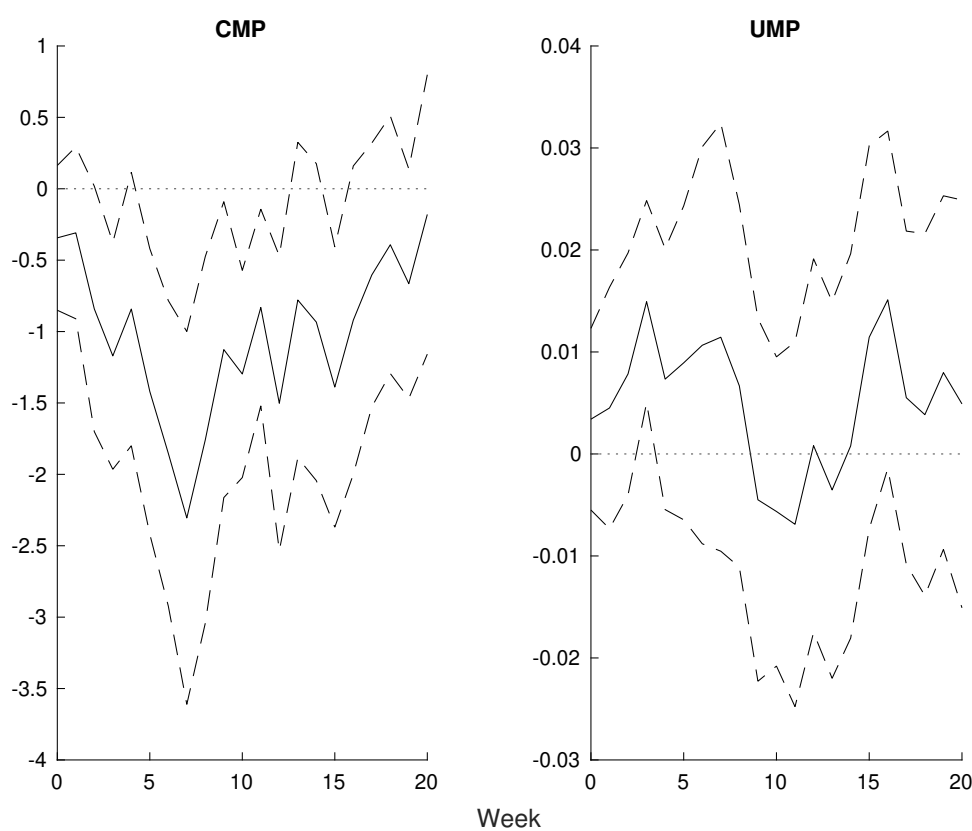


Figure 20: Local Projection of NTL on US MPS: CMP vs UMP

Notes: CMP and UMP denote the impact of target shock and path shock respectively. Shocks are aggregated to the weekly frequencies consistent with the dependent variable. The number of lags of the dependent variable ( $Q$ ) and the shock ( $M$ ) are selected by the AIC criteria for up to 4 periods. The dashed ribbons are the 90 percent confidence intervals generated based on the Newey-West standard errors.

In addition, to test the confounding effects of asset purchase, we define the Non-QE

period as from October 29th, 2014 to March 15th, 2020 and since March 9th, 2022. Correspondingly, the QE period is from early 2012 to October 29th, 2014, and from March 15th, 2020 to March 9th, 2022. We apply the baseline LP identification for the two subperiods and the results are in Figure E.7. It suggests that the impacts are negative in both periods implying that the use of asset purchase will not affect the effectiveness of policy rate change. The effectiveness of unconventional monetary policy in affecting the macro economy is still an open question (see Bhattarai and Neely, 2022 for more discussion).

### **7.3 MPS of Other Economies**

Apart from MPS by the Fed, we also study the impact of MPS by other major central banks, such as the European Central Bank (ECB) and the Bank of Japan (BOJ) on the real economy in China, as shown in Figure E.8. Specifically, we apply the baseline LP identification and replace US MPS with the shocks by ECB and BOJ. The IRFs are in Figure 21.



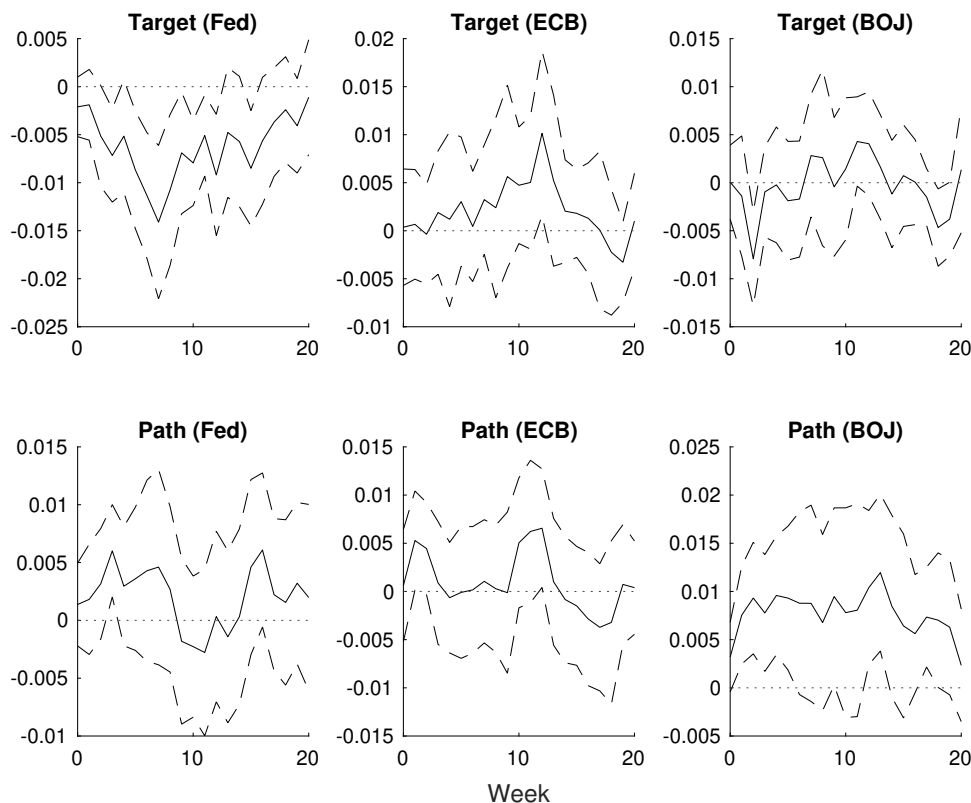


Figure 21: Local Projection of NTL on MPS by Different Central Banks

Notes: MPS is aggregated to the weekly frequencies consistent with the dependent variable. We normalize the standard deviation of all the shocks to be 1 for the full sample so that the impacts across the shocks are more comparable. The number of lags of the dependent variable ( $Q$ ) and the shock ( $M$ ) are selected by the AIC criteria for up to 4 periods. The dashed ribbons are the 90 percent confidence intervals generated based on the Newey-West standard errors.

Compared with the Fed, the MPS by ECB and BOJ have less impact on the Chinese economy and the coefficients are overall insignificant no matter for target shock or path shock. These results are consistent with previous literature such as Miranda-Agrippino and Nenova (2022) which documents that the US monetary policy is more effective in influencing other countries than ECB shocks. This makes sense as the US dollar constitutes a dominant role in international trade and financial transactions (Gopinath et al., 2020) and the US monetary policy is a key driver of the global finance cycle (Miranda-Agrippino and Rey, 2020). Moreover, China's exchange rate is partially pegged to the US dollar, which may enhance the spillover effects from the US monetary policy.

## 7.4 International Comparison

We extend our results to all economies in the world using monthly NTL data pre-processed by Earth Observation Group (Colorado School of Mines, n.d.-a).<sup>30</sup> The results are in Figure 22. It is seen that the US tightening has almost negative effects throughout the world with a bigger impact on emerging economies than on advanced economies, which is in line with previous literature (e.g. Bräuning and Ivashina, 2020, Dedola et al., 2017). Moreover, among emerging markets, the effects are more prominent for those economies with rapid urbanization in Asia and Africa, which is consistent with our construction channel. Admittedly, the detailed reasons for country heterogeneity are mixed and the impacts depend on the receiving countries' characteristics such as trade and financial integration, exchange rate regime, financial market development, labor market rigidity, industry structure, and participation in global value chains (Georgiadis, 2016). This is beyond the scope of our paper and may be interesting for future study.

Apart from using monthly data for all the economies, we also selected several of mainland China's neighbors employing weekly NTL, which is more similar to our baseline analysis on China.<sup>31</sup> The results are in Figure E.9. The conclusion is consistent that emerging markets are usually more sensitive than advanced economies. However, we should be cautious to interpret this difference between EM and AE as the real activities featured in these two types of economies are different. For example, urbanization and night shifts, two important sources of NTL in EM, are not pervasive in AE. By comparison, in advanced countries, NTL is more reflected in service activities at night, such as the operation of entertainment venues. Consequently, the transmission channel may differ from the one we proposed, which calls for future exploration.

---

<sup>30</sup>The VIIRS data covering all the world area starts from 2014. Therefore, we use the VIIRS instrument data since 2014. For months before 2014, we use the DMSP instrument data and match the trends with a conversion DMSP-to-VIIRS factor. The conversion factor is based on annual VIIRS and DMSP instrument data in 2012.

<sup>31</sup>The processing of weekly data is very time-consuming, so we only chose several countries for illustration. Emerging market economies include China, Mongolia, North Korea, Vietnam, Bangladesh, and India while advanced economies incorporate Hong Kong, Macau, Taiwan, South Korea, and Japan.

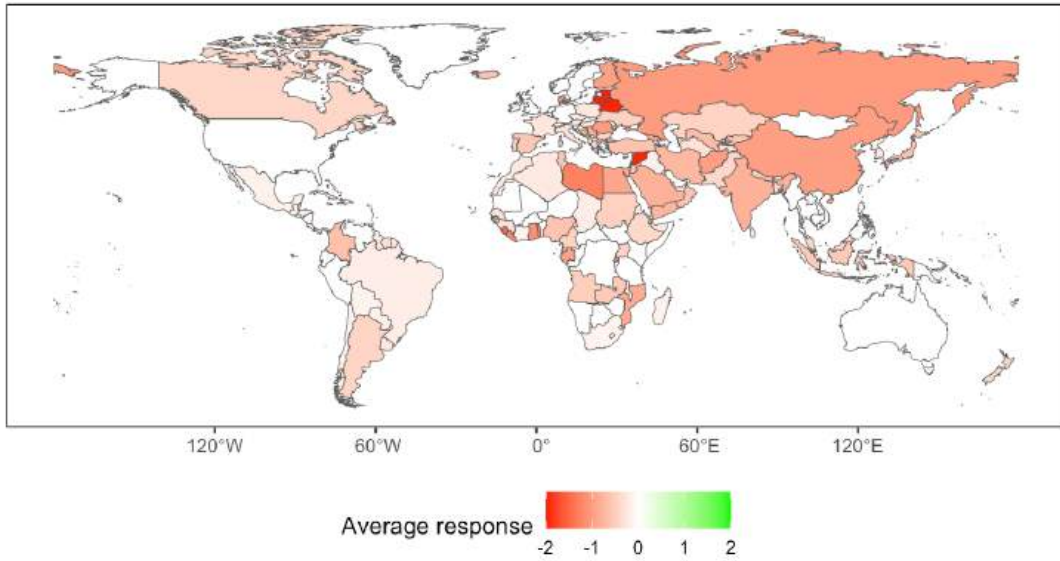


Figure 22: Average Response of NTL on US MPS by Economy

Notes: MPS is aggregated to the monthly frequencies consistent with the dependent variable. The number of lags of the dependent variable ( $Q$ ) and the shock ( $M$ ) are selected by the AIC criteria for up to 4 periods. When taking the average across the time horizon from the month the MPS is realized to 20 months later, insignificant values at a 90 percent confidence level are treated as zero. If the region has both significantly positive and significantly negative responses, the average response by the region is interpreted as zero. Extreme values with absolute values greater than 2 are winsorized on the map.

## 8 Conclusion

In this study, we use a new data source, the weekly or daily nighttime light (NTL), to capture changes in real economic activities in China after a US monetary policy shock (MPS). We find that the unexpected US monetary tightening has an overall negative effect on China's real economy. Benefiting from this high-frequency data, we could achieve a sharper identification of the policy effect using an event-study approach and it is revealed that the spillover is much quicker than traditional expectations. Besides, with this

new measurement in hand, we are allowed to explore finer spatial heterogeneity, such as the different impacts on city centers, suburbs, and non-built-up areas. This also helps us to reveal a new channel where the US tightening could affect China's output through construction-related activities in non-built-up areas. Moreover, consistent with the construction channel, we show that cities with lower urbanization rates and tighter financial conditions are more adversely affected by a US tightening shock. Without concerns for the quality of official data and different statistical standards, it is easy to compare the US spillover effects across countries.

Our paper is the first attempt to introduce high-frequency NTL data into the study of monetary economics and revisit several classical questions in this area. We believe in the future this data could also be employed in other research where a high frequency of real economic activity measurement is needed, especially for emerging markets where the NTL is closely related to output. Admittedly, we only use NTL data to explore one of the mechanisms and some other channels like consumption are not well reflected in NTL data, which calls for future investigation.

## References

- Aastveit, K. A., & Anundsen, A. K. (2022). Asymmetric Effects of Monetary Policy in Regional Housing Markets. *American Economic Journal: Macroeconomics*, 14(4), 499–529. <https://doi.org/10.1257/mac.20190011>
- Acosta, M. (2022). The perceived causes of monetary policy surprises. *Published manuscript*.
- Akinci, Ö., & Queralto, A. (2024). Exchange Rate Dynamics and Monetary Spillovers with Imperfect Financial Markets (S. Giglio, Ed.). *The Review of Financial Studies*, 37(2), 309–355. <https://doi.org/10.1093/rfs/hhad078>
- Bhattarai, S., & Neely, C. J. (2022). An Analysis of the Literature on International Unconventional Monetary Policy. *Journal of Economic Literature*, 60(2), 527–597. <https://doi.org/10.1257/jel.20201493>
- Bickenbach, F., Bode, E., Nunnenkamp, P., & Söder, M. (2016). Night lights and regional GDP. *Review of World Economics*, 152(2), 425–447. <https://doi.org/10.1007/s10290-016-0246-0>
- Bluedorn, J. C., & Bowdler, C. (2011). The open economy consequences of U.S. monetary policy. *Journal of International Money and Finance*, 30(2), 309–336. <https://doi.org/10.1016/j.jimonfin.2010.11.001>

- Bluhm, R., & Krause, M. (2022). Top lights: Bright cities and their contribution to economic development. *Journal of Development Economics*, 157, 102880. <https://doi.org/10.1016/j.jdeveco.2022.102880>
- Bräuning, F., & Ivashina, V. (2020). U.S. monetary policy and emerging market credit cycles. *Journal of Monetary Economics*, 112, 57–76. <https://doi.org/10.1016/j.jmoneco.2019.02.005>
- Bustamante-Calabria, M., Sánchez De Miguel, A., Martín-Ruiz, S., Ortiz, J.-L., Vílchez, J. M., Pelegrina, A., García, A., Zamorano, J., Bennie, J., & Gaston, K. J. (2021). Effects of the COVID-19 Lockdown on Urban Light Emissions: Ground and Satellite Comparison. *Remote Sensing*, 13(2), 258. <https://doi.org/10.3390/rs13020258>
- Chari, A., Dilts Stedman, K., & Lundblad, C. (2021). Taper Tantrums: Quantitative Easing, Its Aftermath, and Emerging Market Capital Flows (A. Karolyi, Ed.). *The Review of Financial Studies*, 34(3), 1445–1508. <https://doi.org/10.1093/rfs/hhaa044>
- Chen, K., Higgins, P., & Zha, T. (2024). Constructing quarterly Chinese time series usable for macroeconomic analysis. *Journal of International Money and Finance*, 143, 103052. <https://doi.org/10.1016/j.jimonfin.2024.103052>
- Chen, X., & Nordhaus, W. D. (2011). Using luminosity data as a proxy for economic statistics. *Proceedings of the National Academy of Sciences*, 108(21), 8589–8594. <https://doi.org/10.1073/pnas.1017031108>
- Chor, D., & Li, B. (2024). Illuminating the effects of the US-China tariff war on China's economy. *Journal of International Economics*, 150, 103926. <https://doi.org/10.1016/j.jinteco.2024.103926>
- Clark, H., Pinkovskiy, M., & Sala-i-Martin, X. (2020). China's GDP growth may be understated. *China Economic Review*, 62, 101243. <https://doi.org/10.1016/j.chieco.2018.10.010>
- Cohen, F., & Gonzalez, F. (2024). Understanding the Link between Temperature and Crime. *American Economic Journal: Economic Policy*, 16(2), 480–514. <https://doi.org/10.1257/pol.20220118>
- Colorado School of Mines. (n.d.-a). Earth Observation Group - Payne Institute for Public Policy. <https://payneinstitute.mines.edu/eog/>
- Colorado School of Mines. (n.d.-b). Earth Observation Group - Payne Institute for Public Policy. <https://payneinstitute.mines.edu/eog/>
- Dedola, L., Karadi, P., & Lombardo, G. (2013). Global implications of national unconventional policies. *Journal of Monetary Economics*, 60(1), 66–85. <https://doi.org/10.1016/j.jmoneco.2012.12.001>
- Dedola, L., Rivolta, G., & Stracca, L. (2017). If the Fed sneezes, who catches a cold? *Journal of International Economics*, 108, S23–S41. <https://doi.org/10.1016/j.jinteco.2017.01.002>
- Di Giovanni, J., & Rogers, J. (2024). The Impact of U.S. Monetary Policy on Foreign Firms. *IMF Economic Review*, 72(1), 58–115. <https://doi.org/10.1057/s41308-023-00218-7>
- Drechsler, I., Savov, A., & Schnabl, P. (2022). How monetary policy shaped the housing boom. *Journal of Financial Economics*, 144(3), 992–1021. <https://doi.org/10.1016/j.jfineco.2021.06.039>
- Fratzscher, M., Lo Duca, M., & Straub, R. (2018). On the International Spillovers of US Quantitative Easing. *The Economic Journal*, 128(608), 330–377. <https://doi.org/10.1111/eoj.12435>

- Georgiadis, G. (2016). Determinants of global spillovers from US monetary policy. *Journal of International Money and Finance*, 67, 41–61. <https://doi.org/10.1016/j.jimonfin.2015.06.010>
- Gibson, J., Olivia, S., Boe-Gibson, G., & Li, C. (2021). Which night lights data should we use in economics, and where? *Journal of Development Economics*, 149, 102602. <https://doi.org/10.1016/j.jdeveco.2020.102602>
- Gopinath, G., Boz, E., Casas, C., Díez, F. J., Gourinchas, P.-O., & Plagborg-Møller, M. (2020). Dominant Currency Paradigm. *American Economic Review*, 110(3), 677–719. <https://doi.org/10.1257/aer.20171201>
- Gürkaynak, R., Karasoy-Can, H. G., & Lee, S. S. (2022). Stock Market’s Assessment of Monetary Policy Transmission: The Cash Flow Effect. *The Journal of Finance*, 77(4), 2375–2421. <https://doi.org/10.1111/jofi.13163>
- Gürkaynak, R., & Sack, B. (2005, November). *Do Actions Speak Louder Than Words? The Response of Asset Prices to Monetary Policy Actions and Statements* (Computing in Economics and Finance 2005 No. 323). Society for Computational Economics. Retrieved August 9, 2024, from <https://econpapers.repec.org/paper/scsescecf5/323.htm>
- Gürkaynak, R. S., & Wright, J. H. (2013). Identification and Inference Using Event Studies. *The Manchester School*, 81(S1), 48–65. <https://doi.org/10.1111/manc.12020>
- Henderson, J. V., Storeygard, A., & Weil, D. N. (2012). Measuring Economic Growth from Outer Space. *American Economic Review*, 102(2), 994–1028. <https://doi.org/10.1257/aer.102.2.994>
- Ho, S. W., Zhang, J., & Zhou, H. (2018). Hot Money and Quantitative Easing: The Spillover Effects of U.S. Monetary Policy on the Chinese Economy. *Journal of Money, Credit and Banking*, 50(7), 1543–1569. <https://doi.org/10.1111/jmcb.12501>
- Iacoviello, M. (2005). House Prices, Borrowing Constraints, and Monetary Policy in the Business Cycle. *American Economic Review*, 95(3), 739–764. <https://doi.org/10.1257/0002828054201477>
- Jarociński, M. (2024). Estimating the Fed’s unconventional policy shocks. *Journal of Monetary Economics*, 144, 103548. <https://doi.org/10.1016/j.jmoneco.2024.01.001>
- Jiang, H., Sun, Z., Guo, H., Xing, Q., Du, W., & Cai, G. (2022). A standardized dataset of built-up areas of China’s cities with populations over 300,000 for the period 1990–2015. *Big Earth Data*, 6(1), 103–126. <https://doi.org/10.1080/20964471.2021.1950351>
- Jiang, L., & Liu, Y. (2023). China’s Largest City-Wide Lockdown: How Extensively Did Shanghai COVID-19 Affect Intensity of Human Activities in the Yangtze River Delta? *Remote Sensing*, 15(8), 1989. <https://doi.org/10.3390/rs15081989>
- Jordà, Ò. (2005). Estimation and Inference of Impulse Responses by Local Projections. *American Economic Review*, 95(1), 161–182. <https://doi.org/10.1257/0002828053828518>
- Jordà, Ò., Schularick, M., & Taylor, A. M. (2015). Betting the house. *Journal of International Economics*, 96, S2–S18. <https://doi.org/10.1016/j.jinteco.2014.12.011>
- Kim, D. (2022). Assessing regional economy in North Korea using nighttime light. *Asia and the Global Economy*, 2(3), 100046. <https://doi.org/10.1016/j.aglobe.2022.100046>

- Kim, J., Kim, K., Park, S., & Sun, C. (2022). The Economic Costs of Trade Sanctions: Evidence from North Korea. *SSRN Electronic Journal*. <https://doi.org/10.2139/ssrn.4032573>
- Kim, S. (2001). International transmission of U.S. monetary policy shocks: Evidence from VAR's. *Journal of Monetary Economics*, *48*(2), 339–372. [https://doi.org/10.1016/S0304-3932\(01\)00080-0](https://doi.org/10.1016/S0304-3932(01)00080-0)
- Kolasa, M., & Wesołowski, G. (2020). International spillovers of quantitative easing. *Journal of International Economics*, *126*, 103330. <https://doi.org/10.1016/j.jinteco.2020.103330>
- Lakdawala, A., Moreland, T., & Schaffer, M. (2021). The international spillover effects of US monetary policy uncertainty. *Journal of International Economics*, *133*, 103525. <https://doi.org/10.1016/j.jinteco.2021.103525>
- Lee, S., & Cao, C. (2016). Soumi NPP VIIRS Day/Night Band Stray Light Characterization and Correction Using Calibration View Data. *Remote Sensing*, *8*(2), 138. <https://doi.org/10.3390/rs8020138>
- Li, X., Zhou, Y., Zhao, M., & Zhao, X. (2020). A harmonized global nighttime light dataset 1992–2018. *Scientific Data*, *7*(1), 168. <https://doi.org/10.1038/s41597-020-0510-y>
- Maćkowiak, B. (2007). External shocks, U.S. monetary policy and macroeconomic fluctuations in emerging markets. *Journal of Monetary Economics*, *54*(8), 2512–2520. <https://doi.org/10.1016/j.jmoneco.2007.06.021>
- Martínez, L. R. (2022). How Much Should We Trust the Dictator's GDP Growth Estimates? *Journal of Political Economy*, *130*(10), 2731–2769. <https://doi.org/10.1086/720458>
- Michalopoulos, S., & Papaioannou, E. (2018). Spatial Patterns of Development: A Meso Approach. *Annual Review of Economics*, *10*(1), 383–410. <https://doi.org/10.1146/annurev-economics-080217-053355>
- Miranda-Agrippino, S., & Nenova, T. (2022). A tale of two global monetary policies. *Journal of International Economics*, *136*, 103606. <https://doi.org/10.1016/j.jinteco.2022.103606>
- Miranda-Agrippino, S., & Rey, H. (2020). U.S. Monetary Policy and the Global Financial Cycle. *The Review of Economic Studies*, *87*(6), 2754–2776. <https://doi.org/10.1093/restud/rdaa019>
- Miranda-Agrippino, S., & Ricco, G. (2021). The Transmission of Monetary Policy Shocks. *American Economic Journal: Macroeconomics*, *13*(3), 74–107. <https://doi.org/10.1257/mac.20180124>
- Nakamura, E., & Steinsson, J. (2018). High-Frequency Identification of Monetary Non-Neutrality: The Information Effect\*. *The Quarterly Journal of Economics*, *133*(3), 1283–1330. <https://doi.org/10.1093/qje/qjy004>
- NASA. (2020, July). NASA's Black Marble. <https://blackmarble.gsfc.nasa.gov>
- National Institute for Environmental Studies. (2023). ODIAC Fossil Fuel Emission Dataset. Retrieved December 29, 2023, from <https://db.cger.nies.go.jp/dataset/ODIAC/>
- NewHorizon. (2022). NewHorizon. <http://horizon2021.xyz>
- NOAA National Centers of Environmental Information. (1999). Global Surface Summary of the Day - GSOD. 1.0. <https://www.ncei.noaa.gov/metadata/geoportal/rest/metadata/item/gov.noaa.ncdc:C00516/html>

- Pinkovskiy, M., & Sala-i-Martin, X. (2016). Lights, Camera ... Income! Illuminating the National Accounts-Household Surveys Debate. *Quarterly Journal of Economics*, 131(2), 579–631. <https://doi.org/10.1093/qje/qjw003>
- Rogers, J. H., Sun, B., & Sun, T. (2024). U.S.-China Tension. *SSRN Electronic Journal*. <https://doi.org/10.2139/ssrn.4815838>
- Rudebusch, G. D. (1998). Do Measures of Monetary Policy in a Var Make Sense? *International Economic Review*, 39(4), 907. <https://doi.org/10.2307/2527344>
- Sherman, L., Proctor, J., Druckenmiller, H., Tapia, H., & Hsiang, S. (2023, March). *Global High-Resolution Estimates of the United Nations Human Development Index Using Satellite Imagery and Machine-learning* (tech. rep. No. w31044). National Bureau of Economic Research. Cambridge, MA. <https://doi.org/10.3386/w31044>
- Swanson, E. T. (2021). Measuring the effects of federal reserve forward guidance and asset purchases on financial markets. *Journal of Monetary Economics*, 118, 32–53. <https://doi.org/10.1016/j.jmoneco.2020.09.003>
- Team, S. D. C. (2020). Metadata record for: A harmonized global nighttime light dataset 1992-2018 [Artwork Size: 4268 Bytes Pages: 4268 Bytes]. <https://doi.org/10.6084/M9.FIGSHARE.12312125>
- Uribe, M., & Yue, V. Z. (2006). Country spreads and emerging countries: Who drives whom? *Journal of International Economics*, 69(1), 6–36. <https://doi.org/10.1016/j.jinteco.2005.04.003>
- Wang, X. (n.d.). Historical data of air quality and weather in China. <https://quotsoft.net/air/>
- Xu, G., Xiu, T., Li, X., Liang, X., & Jiao, L. (2021). Lockdown induced night-time light dynamics during the COVID-19 epidemic in global megacities. *International Journal of Applied Earth Observation and Geoinformation*, 102, 102421. <https://doi.org/10.1016/j.jag.2021.102421>
- Yang, P., & Pan, J. (2022). Estimating Housing Vacancy Rate Using Nightlight and POI: A Case Study of Main Urban Area of Xi'an City, China. *Applied Sciences*, 12(23), 12328. <https://doi.org/10.3390/app122312328>



# Appendix A Data Appendix

## A.1 Baseline Panel Summary Statistics

Table A.1: Summary Statistics: Weekly NTL and Shocks

	N	Mean	SD	Min	Max
Year	624	2017.51	3.45	2012.00	2024.00
Log NTL	624	0.00	0.17	-0.46	0.50
MPS: FFR	624	0.00	0.01	-0.06	0.06
MPS: FFR (Alternative 1)	624	0.01	0.15	-1.48	1.22
MPS: Target	624	0.01	0.29	-2.61	3.39
MPS: Path	624	0.00	0.01	-0.06	0.06
MPS: Forward Guidance	624	-0.01	0.40	-3.04	3.35
MPS: LSAP	624	-0.01	0.28	-4.13	1.74
MPS: Information	624	0.02	0.24	-1.84	1.92
News: GDP	624	-0.01	0.13	-1.40	1.00
News: CPI	624	0.00	0.03	-0.29	0.25
News: PPI	624	-0.01	0.15	-1.63	1.06
News: EMP	624	-0.01	0.04	-0.40	0.15
News: Asset Return	624	-0.01	0.11	-0.98	0.56

Notes: Date ranges from 2012-01-16 to 2024-01-01. The last week with non-zero baseline MPS: FFR is on 2023-05-01. MPS and News shocks are aggregated to week level. For MPS, a week includes at most one shock, so the value for the week is either zero or the shock in that week.

## A.2 Details of NTL Data

### A.2.1 Data Availability

Partially-corrected raw daily data (Black Marble) are available on the official website of NASA at: <https://ladsweb.modaps.eosdis.nasa.gov/missions-and-measurements/products/VNP46A2>, and Google Earth Engine (GEE) at: [https://developers.google.com/earth-engine/datasets/catalog/NOAA\\_VIIRS\\_001\\_VNP46A2](https://developers.google.com/earth-engine/datasets/catalog/NOAA_VIIRS_001_VNP46A2).

As an illustration, the map of NTL in the East Asia and Pacific region released by NASA in 2016 is as follows.<sup>32</sup>

<sup>32</sup>The original file is publicly available at: <https://www.nasa.gov/specials/blackmarble/media/BlackMarble20161km.jpg>.



Figure A.1: Nighttime Luminosity Captured by NASA Satellite in 2016

The shape files used to crop the GeoTiff files of NTL are from NewHorizon, most recently updated in 2022: <http://horizon2021.xyz>. Using the official shape files published by the National Bureau of Statistics of China (NBSC) in 2020 does not substantially change the results of the study.

## A.2.2 Daily NTL Data Processing

**Data Source** The daily NTL data is derived from NASA’s Black Marble product using the VIIRS instrument (NASA 2020). The product code of the stray light-corrected daily NTL series is VNP46A2. It corrects for stray light, such as wildfire and moonlight. It also adjusts for the satellite angle that varies each day when the satellite captures the image of the same place. The public access is available from NASA and GEE.

To smooth the cloud computing process on the Google Cloud Platform (GCP), we use the GEE repository to capture the daily NTL geospatial data. Firstly, we extract the map using a rectangle with longitudes from 75 to 135 degrees and latitudes from 18 to 53 degrees. The rectangle contains the whole land area of mainland China.<sup>33</sup> For each day’s map, we save four layers to the corresponding TIFF file: daily NTL (DNB\_BRDF\_Corrected\_NTL), NASA-filled daily NTL (Gap\_Filled\_DNB\_BRDF\_Corrected\_NTL), quality flag (Mandatory\_Quality\_Flag), and snow flag (Snow\_Flag). We do this for each day from 1 January 2018 to 31 December 2023 with 2,174 files.<sup>34</sup>

**Panel Construction** For each city, we use the GIS shape file as introduced in the data section. We crop from the daily rectangles using the shape file and only include cells where the center falls within the shape file. For the cropped dataset, we filter out observations without NASA-filled daily NTL, as the value is supposed to be available for

<sup>33</sup>For Hainan province, we use another rectangle with longitudes from 108 to 112 degrees and latitudes from 17 to 21 degrees. We omit Sansha, a remote city with a small area far from the main body of Hainan Island.

<sup>34</sup>The maps are unavailable for late July 2022 due to the satellite issue. However, the missing data in the period do not interfere with the study.

every legible cell in the map. The cropped dataset includes longitude, latitude, and the values of the four layers for each cell. For computational efficiency, we exclude cities with more than 500,000 cells. The coverage of city-level daily NTL is shown below.

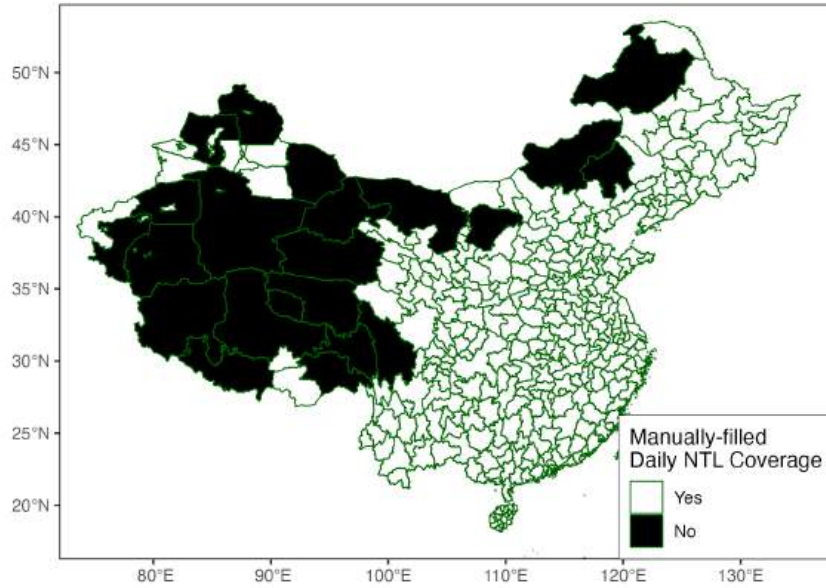


Figure A.2: Coverage of City-level Daily NTL

Notes: When processing the NTL geospatial data using GIS shape files, we exclude cities with more than 500,000 pixels.

We filter out cells with contaminated daily NTL and fill them with previous values. For each cell (defined by longitude and latitude), we keep the daily NTL value only if both the quality flag and the snow flag are zero, indicating no quality (e.g., cloud coverage) issue or snow-coverage issue in the cell. Then, we concatenate the dataset to a cell-level daily panel. For each cell, we obtain a time series with several missing values for the daily NTL. We fill the NA values with the latest valid value from the beginning to the end. Then, we fill the starting NA values using the earliest valid value, so the time series cell is fully filled as long as one valid value exists. We call the filled daily NTL series the manually-filled NTL series. Then, we aggregate the panel into a daily NTL series. For each day, we record the number of valid cells. In the aggregated daily NTL series, we drop the dates where the valid cell numbers are less than 90 percent of the maximum cell number for either the NASA-filled NTL or the manually-filled NTL. Finally, we concatenate the time series for each city, and the merged dataset is a city-level daily panel. The key variables in the panel include the city code and the date.

**Built-up Area and Other Economies** We also apply the GIS shape file for the built-up area to crop from the daily rectangles. Different from the process above for cities, we include a cell as long as it touches the shape file. We implement the adjustment as the built-up areas can be discretionary, and excluding potential light sources adds to the measurement error. Similar to the city-level daily panel of NTL, we generate a city-level daily panel of NTL for each definition of built-up area. The key variables in the panel

include the city code, the definition year of the built-up area (each five years from 1990 to 2015), and the date.

We apply the same method to crop regions in other economies, including Hong Kong, Macau, Taiwan, Mongolia, North Korea, South Korea, Japan, Vietnam, Bangladesh, and India. Like the balance we keep for computation power-saving and population coverage, we exclude some regions with relatively large area and small population. For Mongolia, we select 10 out of 21 regions, which represents over 70 percent of the national population. For Japan, we exclude Hokkaido. For Vietnam, we only include the 25 out of 63 regions, which are in the northern part and represent about 40 percent of the national population. For India, we include 498 out of 676 secondary regions, excluding the southern, western, and Jammu and Kashmir regions. For Mexico, we include the states of Baja California, Sonora, Chihuahua, Coahuila, Nuevo Leon, Tamaulipas, Chiapas, Quintana Roo, covering about 60 percent of the national population. For the United States, we include the states of Texas and Louisiana. For Australia, we include Australian Capital Territory, Victoria, New South Wales (coastal), Queensland (greater Brisbane area), and South Australia (Adelaide metropolitan area), which cover more than 80 percent of the national population.

**Mountain Areas** To remove mountain areas and other inhabitable areas in China, we use the land cover map from CLCD.<sup>35</sup> The geospatial map is derived from the Landsat satellite images on the Google Earth Engine. We use the version with 30 meter resolution identified for the year 2022. For each original cell, we identify it as inhabitable if it is not cropland or impervious, which consequently includes all forest, shrub, grassland, water, snow and ice, barren, and wetland cells. The cells are converted to 500-meter cells used in the NTL geospatial data. For each converted cell, we identify it as inhabitable if all associated original cells are inhabitable.

## A.3 Other Data

### A.3.1 National Accounts

To associate variations in NTL with changes in economic activities, we need to obtain GDP and other national account indicators and adjust the NTL data to the same frequency. Two datasets are used for this purpose. The first is the city-level annual panel in China, which corresponds to our baseline spatial heterogeneity analysis at city level. The second is the country-level annual panel, which supports our cross-country comparison. We obtain the city-level national accounts of China from statistical yearbooks, which are published annually by the NBSC, and use data from 2012 to 2021. Indicators we use include total GDP, GDP in the primary, secondary, and tertiary sectors, import, and export. The summary statistics of the city-level national accounts are in Table A.2. Then, we get country-level national accounts from the World Development Indicator (WDI) of the World Bank and associate them with country-level NTL series from the Light pollution statistics.<sup>36</sup> <sup>37</sup> We use data from 2012 to 2023 in line with the main panel. The

---

<sup>35</sup>The tif file is publicly available at: <https://zenodo.org/records/8176941>.

<sup>36</sup>The national accounts of the Republic of China (conventionally acknowledged as Taiwan) are from the IMF, as the WDI does not include the data.

<sup>37</sup>The country-level NTL data here are from the Light pollution map, but they are derived from the same source as our main NTL series.

summary statistics of the country-level national accounts are in Table A.3.

Table A.2: Summary Statistics: National Accounts, Annual series, City

	N	Mean	SD	Min	Max
Year	6798	2009.84	6.83	1998.00	2021.00
GDP	6466	1603.15	2878.95	5.30	43215.00
Primary sector GDP share	6395	15.09	9.63	0.03	53.20
Secondary sector GDP share	6395	46.18	11.40	2.66	90.97
Tertiary sector GDP share	6392	38.73	9.64	8.50	85.34
Import	1449	424.75	1943.09	0.00	24891.68
Export	1456	512.92	1668.20	0.00	19263.41
Population	6483	429.56	307.58	0.00	3416.00
Nonrural population	3235	133.97	133.98	6.00	1693.00
Number of bank subsidiaries	4359	840.46	733.57	1.00	7518.00

Notes: The unit of GDP, import, and export is 100 million Yuan. The unit of GDP share is percent.

Table A.3: Summary Statistics: National Accounts, Annual series, Country

	N	Mean	SD	Min	Max
Year	2321	2017.00	3.16	2012.00	2022.00
GDP	2209	393083.69	1688939.02	31.95	20926835.05
Import share in GDP	1908	48.93	29.10	1.13	221.01
Export share in GDP	1908	43.30	32.77	1.57	221.61
Population	2321	35815141.62	138030915.26	10444.00	1417173173.00
NTL	2321	860425.20	2874406.73	0.00	34976796.00

Notes: The unit of GDP is one million constant 2015 US Dollar (World Bank API indicator code: NY.GDP.MKTP.KD). The unit of GDP share is percent. The unit of NTL is the sum of  $nW/cm^2/sr$  across cells.

### A.3.2 Weather

Like the NTL data, weather data are also available daily. Weather potentially impacts NTL through channels irrelevant to productivity. Therefore, we control for daily weather conditions as a robustness check. The weather series can also be used as a placebo test, as their changes are supposed to be relatively irrelevant to the MPS. The data source is the Global Surface Summary of the Day (GSOD) from the National Oceanic and Atmospheric Administration (NOAA).<sup>38</sup> We use the average daily temperature, precipitation, visibility, and wind speed data since 2014 in the study. The summary statistics of the weather data are in Table A.4.

<sup>38</sup>The data are publicly accessible at: <https://www.ncei.noaa.gov/access/metadata/landing-page/bin/iso?id=gov.noaa.ncdc:C00516>.

Table A.4: Summary Statistics: Weather Data, Daily Series, City

	N	Mean	SD	Min	Max
Year	881043	2018.47	2.86	2014.00	2023.00
Average temperature	881043	14.15	11.63	-45.39	42.67
Precipitation	873000	0.03	0.10	0.00	4.80
Visibility	867629	1.65	0.84	0.00	7.00
Wind speed	877511	0.91	0.48	0.00	14.63

Notes: Date ranges from 2014-01-01 to 2023-12-31. Each observation is a city (average across weather stations) in a day. Temperature is in degrees Celsius. Precipitation is in millimeter. Visibility is in kilometer. Wind speed is in kilometer per hour.

### A.3.3 Time Series Data of China at Different Regional Levels

Most of the time series data we use are from CEIC, a comprehensive database for aggregated economic indicators, including the China Premium Database. We use national, province-level, and city-level indicators at annual, quarterly, and monthly frequencies. We use the full sample starting from as early as 1990s. We also use some data from NBSC.

**National Data** Quarterly series we use include real GDP growth (YoY) (overall, consumption, investment, and net export). Monthly series we use include real estate investment growth (YoY, YTD) (overall, construction, residential building, land purchase), fixed asset investment (number of projects under construction), building sold growth (YoY, YTD), industrial production growth (YoY, YTD), and land transaction data from CREI (China Real Estate Information) (number of cases, land area, land sold, all in YoY growth YTD).

**Province-level Data** Annual series we use include construction firm data (number of enterprises, number of loss-making enterprises, total asset, project payment receivable, total liability, revenue, financial expense) and real estate firm data (total asset, total liability, financial expense, sales revenue). We also use GDP data from NBSC. Monthly series we use include fixed asset investment (number of projects under construction).

**City-level Data** Annual series we use include loan and deposit in financial institutions, urbanization indicators (population urbanization percentage, urban area percentage, percent of construction field across area), and financial development indicators (number of bank subsidiaries) from NBSC. From CEIC, we use investment-related indicators (real estate, fixed asset, floor space sold and waiting for sale, fixed asset investment in real estate).

### A.3.4 Time Series Data of the US

Data of the US economy are from the FRED database provided by the Federal Reserve Bank (Fed) of St. Louis. We use GDP data at quarterly frequency (GDPC1) and Industrial Production data at monthly frequency (INDPRO).

### A.3.5 Financial Data of China

We use China’s financial market data, including interest rates, stock market indices, and exchange rates. They are at daily frequency, and we use full sample starting from 1990s. Interest rates we use include DR007 (7-day interbank repo rate with collaterals) and SHIBOR (Shanghai Interbank Offering Rate) (from overnight to 9 months). Stock market indices we use include SSE (Shanghai Stock Exchange) indices (Composite, Industrial, Real Estate, Infrastructure, Financial, SSE 180). Exchange rates we use include the exchange rate of USD to CNY.

### A.3.6 Firm Data of China

The operation information of listed firms in China is from China Stock Market Accounting Research (CSMAR). It contains the quarterly financial reporting information of all listed firms in China’s equity market from 2007 to 2023. Each listed firm is identified by the stock quote code. Key information we use includes the industry of the firm as classified by CSRC, balance sheet indicators (bill and accounts receivable, bill and accounts payable), earning indicators (revenue, cost, profit, net profit, total comprehensive income) and cashflow indicators (total cashflow, and cashflow from operation, investment, and financing activities).

### A.3.7 Land Transaction Data of China

China’s land transaction data are processed from Land China ([www.landchina.com](http://www.landchina.com)).<sup>39</sup> Each land transaction is identified by an Electronic Identification number (EID). The sample period ranges from 2000 to 2020. For each land transaction, the data records the city, the address, the source of the land, the area, the financial amount of the transaction, the upper and lower bounds of the contracted floor-area ratio, the signing date of the contract, and the transacted party (usually a person or a firm).

To match each land transaction with a listed firm, we identify the best match from the name of the transacted party, searching for the name of the potential parent firm of the transacted party. Additionally, we expand the scope to subsidiaries of each listed firm, including those not directly identified from their names. If the name of a transacted party matches a subsidiary firm, we match the transaction with the parent firm corresponding to the subsidiary firm. Currently, matches are available for all transactions from 2007 to 2015 and from 2017 to 2019.

To aggregate the data to city level, we add the total area or revenue of all the transactions occurred within each city. We also aggregate the transactions by category of land transaction purpose. For both area and revenue, we classify all transactions into four categories: commercial, industrial, residential, and public.

---

<sup>39</sup>We thank Xiaoyu Zhang for sharing the processed data, including matching transactions to list firms and aggregating them to city level.

## Appendix B More Results on NTL and Output

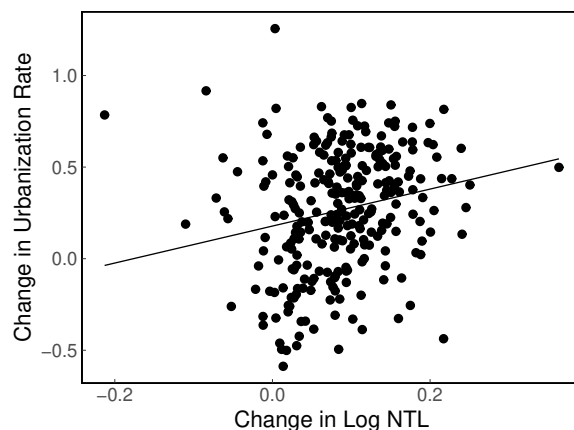


Figure B.1: NTL and Urbanization Rate by City

Notes: Log NTL is converted to the corresponding frequency of the national account indicator. Log NTL shown is the logged value of the average NTL across every day in the converted periods. For each day, NTL is the average value of all cells in each city. The graph shows the changes from 2012 to 2021.

Table B.1: Regression of GDP on NTL: Periods

Dependent Variable:		Log GDP	
Period:	All	2012-2016	2017-2021
Model:	(1)	(2)	(3)
<i>Variables (Second stage)</i>			
Log NTL	0.3958*** (0.0648)	1.1839*** (0.1447)	0.1298* (0.0695)
<i>Variables (First stage)</i>			
Log NTL (Lag 1)	0.8403*** (0.0138)	0.4440*** (0.0380)	0.6928*** (0.0195)
<i>Fixed-effects</i>			
City	Yes	Yes	Yes
Year	Yes	Yes	Yes
<i>Fit statistics</i>			
N	2,569	1,136	1,433
R <sup>2</sup>	0.9830	0.9935	0.9918
F-test	1,868.8	14,349.0	6,881.5

Notes: Significance levels are based on Clustered (Region) standard-errors. Significance Codes: \*\*\*: 0.01, \*\*: 0.05, \*: 0.1.



Table B.2: Regression of GDP on NTL: Trade and Construction Indicators

Dependent Variables: Urbanization rate	Net export	Export	Import	
Model:	(1)	(2)	(3)	(4)
<i>Variables (Second stage)</i>				
Log NTL	0.0433*** (0.0121)	700.1340*** (134.5621)	1,400.0952*** (243.8391)	705.3521*** (200.2484)
<i>Variables (First stage)</i>				
Log NTL (Lag 1)	0.8419*** (0.0141)	0.6942*** (0.0197)	0.6927*** (0.0193)	0.6959*** (0.0199)
<i>Fixed-effects</i>				
City	Yes	Yes	Yes	Yes
Year	Yes	Yes	Yes	Yes
<i>Fit statistics</i>				
N	2,484	1,414	1,421	1,415
R <sup>2</sup>	0.9876	0.8246	0.8472	0.8443
F-test	2,441.4	270.2	317.0	309.6

Notes: Significance levels are based on Clustered (Region) standard-errors. Significance Codes: \*\*\*: 0.01, \*\*: 0.05, \*: 0.1.

Table B.3: Regression of GDP on NTL: Countries by Income Group

Dependent Variable: Group:	Log GDP		
	All	Higher income	Lower income
Model:	(1)	(2)	(3)
<i>Variables (Second stage)</i>			
Log NTL	0.1420*** (0.0444)	0.0403 (0.0717)	0.1277** (0.0511)
<i>Variables (First stage)</i>			
Log NTL (Lag 1)	0.7791*** (0.0407)	0.6812*** (0.0460)	0.7687*** (0.0588)
<i>Fixed-effects</i>			
Country	Yes	Yes	Yes
Year	Yes	Yes	Yes
<i>Fit statistics</i>			
N	1,997	984	1,003
R <sup>2</sup>	0.9990	0.9992	0.9986
F-test	19,166.4	11,904.7	7,313.8

Notes: The economies are classified into higher income and lower income economics by comparing their GDP per capita in 2012 with the median of all the economies in the sample. GDP value used is the constant GDP in 2015 US dollars (World Bank API indicator code: NY.GDP.MKTP.KD). Significance levels are based on Clustered (Region) standard-errors. Significance Codes: \*\*\*: 0.01, \*\*: 0.05, \*: 0.1.

## Appendix C More Results on Spillover Effects

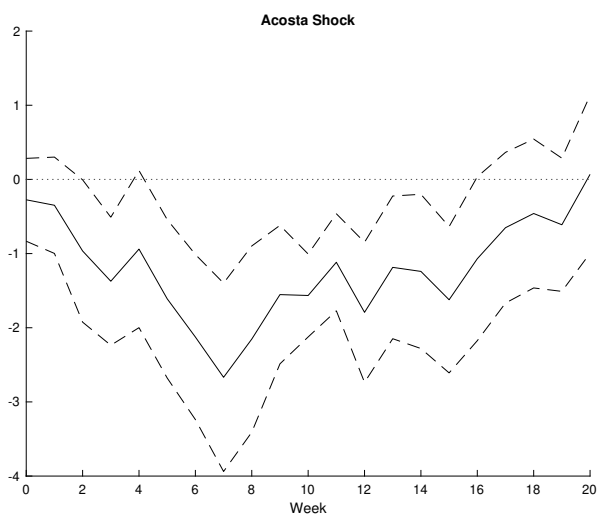


Figure C.1: Local Projection of NTL on US MPS: Acosta Shock

Notes: MPS is aggregated to the weekly frequencies consistent with the dependent variable. The number of lags of the dependent variable ( $Q$ ) and the shock ( $M$ ) are selected by the AIC criteria for up to 4 periods. The dashed ribbons are the 90 percent confidence intervals generated based on the Newey-West standard errors.

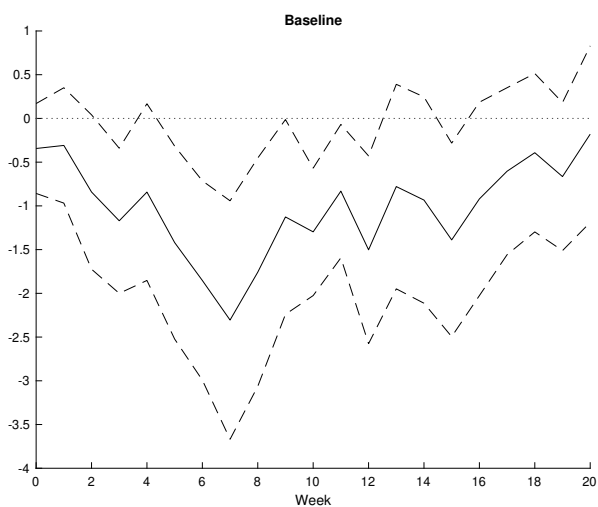


Figure C.2: Local Projection of NTL on US MPS: Baseline, Bootstrapped Standard Error

Notes: MPS is aggregated to the weekly frequencies consistent with the dependent variable. The number of lags of the dependent variable ( $Q$ ) and the shock ( $M$ ) are selected by the AIC criteria for up to 4 periods. The dashed ribbons are the 90 percent confidence intervals generated by bootstrapping with 1,000 draws.

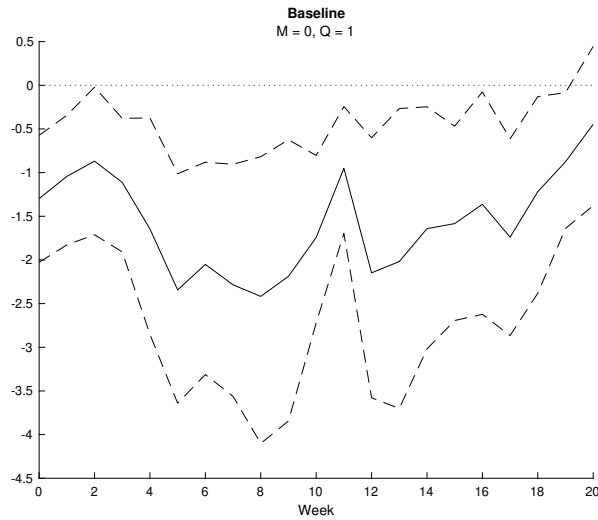


Figure C.3: Local Projection of NTL on US MPS:  $M = 0, Q = 1$

Notes: MPS is aggregated to the weekly frequencies consistent with the dependent variable. The dashed ribbons are the 90 percent confidence intervals generated based on the Newey-West standard errors.

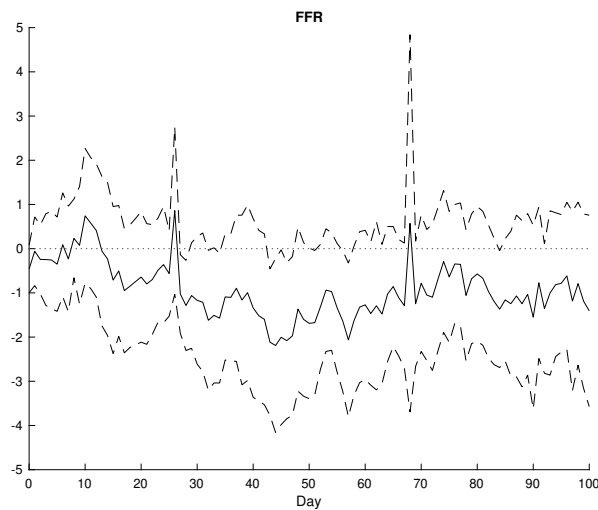


Figure C.4: Local Projection of NTL on US MPS: Daily

Notes: The number of lags of the dependent variable ( $Q$ ) and the shock ( $M$ ) are selected by the AIC criteria for up to 4 periods. The dashed ribbons are the 90 percent confidence intervals generated based on the Newey-West standard errors.

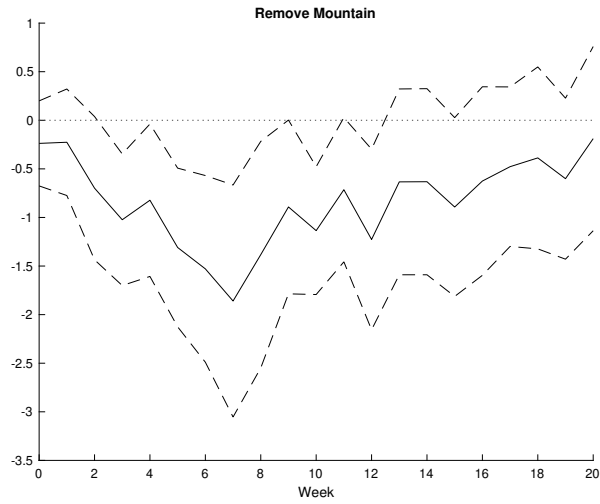


Figure C.5: Local Projection of NTL on US MPS: Remove Mountain Areas

Notes: MPS is aggregated to the weekly frequencies consistent with the dependent variable. The number of lags of the dependent variable ( $Q$ ) and the shock ( $M$ ) are selected by the AIC criteria for up to 4 periods. The dashed ribbons are the 90 percent confidence intervals generated based on the Newey-West standard errors.

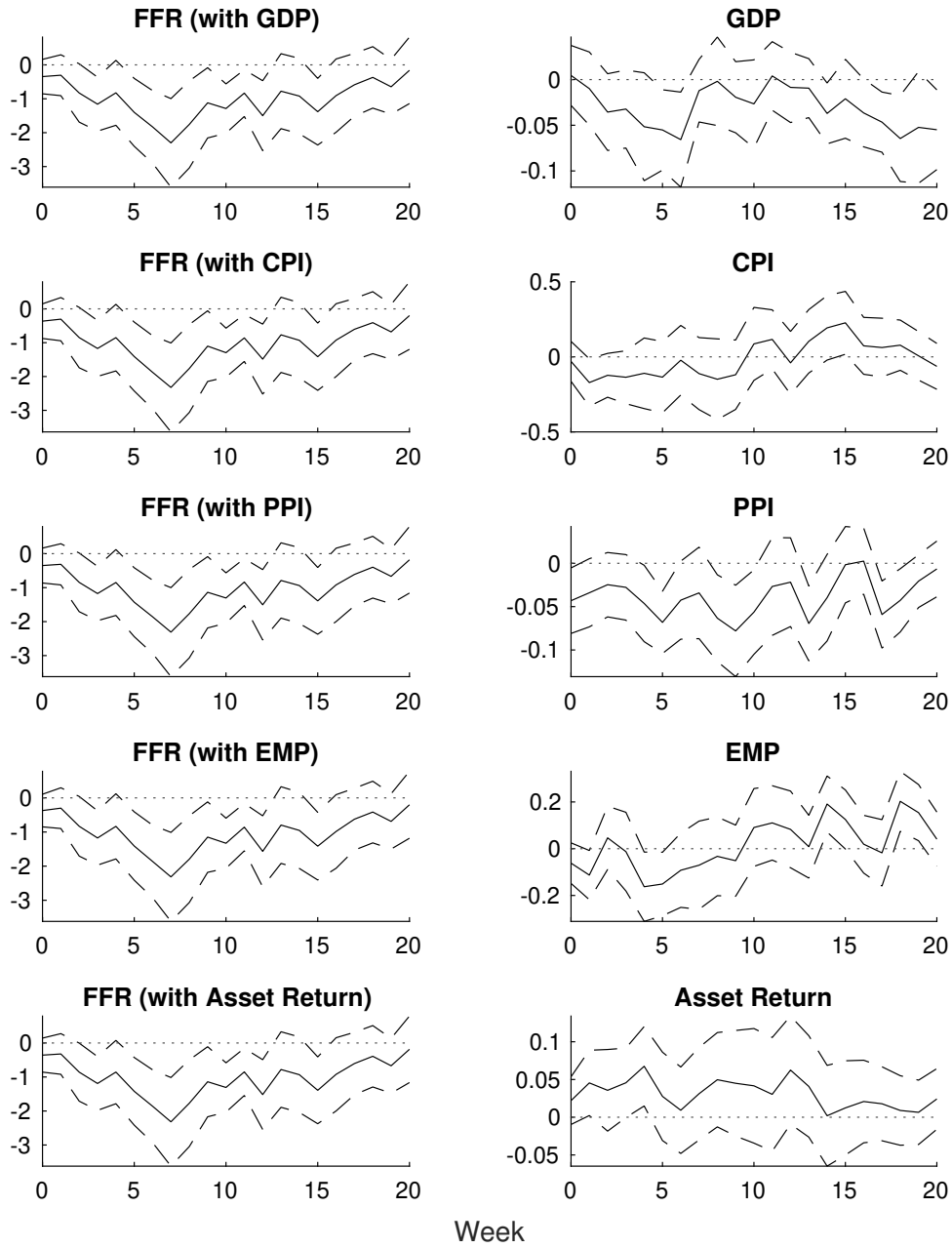


Figure C.6: Local Projection of NTL on US MPS and News Shock: News

Notes: Each row represents a LP regression, with the left column showing the NTL response to FFR, and the right column showing the NTL response to news shock. MPS is aggregated to the weekly frequencies consistent with the dependent variable. The number of lags of the dependent variable ( $Q$ ) and the shocks ( $M_1$  and  $M_2$ ) are selected by the AIC criteria for up to 4 periods. The dashed ribbons are the 90 percent confidence intervals generated based on the Newey-West standard errors.

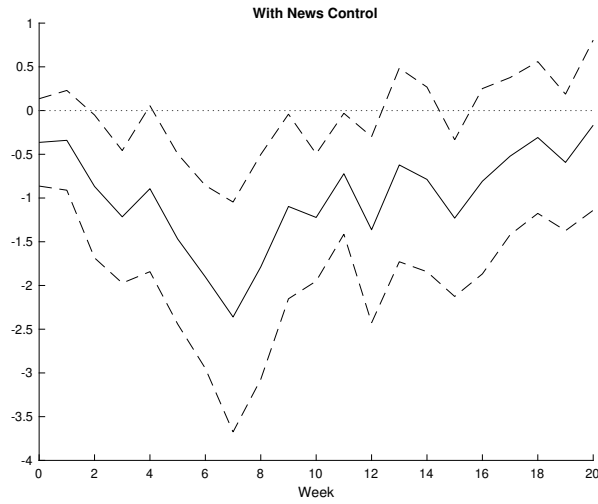


Figure C.7: Local Projection of NTL on US MPS and News Shock: Cumulative News

Notes: News shocks include GDP, CPI, PPI, employment, and asset return shocks. Each shock is cumulative with a 60-day window. MPS is aggregated to the weekly frequencies consistent with the dependent variable. The number of lags of the dependent variable ( $Q$ ) and the shocks ( $M_1$  and  $M_2$ ) are selected by the AIC criteria for up to 4 periods. The dashed ribbons are the 90 percent confidence intervals generated based on the Newey-West standard errors.

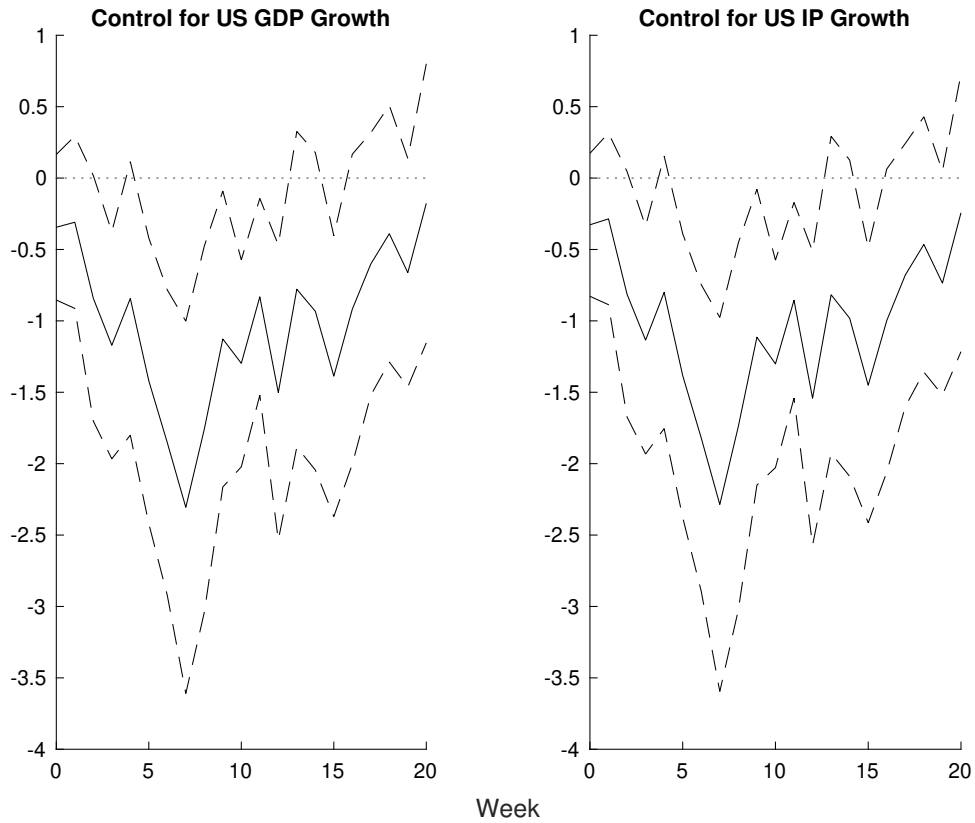


Figure C.8: Local Projection of NTL on US MPS: With US GDP or Industrial Production as Control

Notes: GDP is from quarterly series, and Industrial Production is from monthly series. Their values attached to each week are the period-to-period changes in the last period corresponding to the quarter or month of the week. MPS is aggregated to the weekly frequencies consistent with the dependent variable. The number of lags of the dependent variable ( $Q$ ) and the shock ( $M$ ) are selected by the AIC criteria for up to 4 periods. The dashed ribbons are the 90 percent confidence intervals generated based on the Newey-West standard errors.



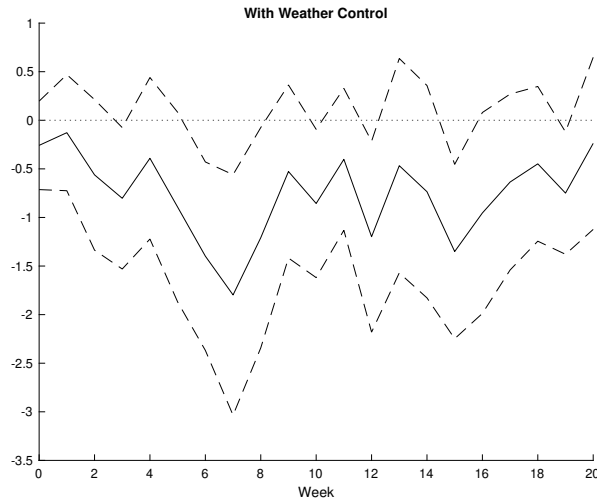


Figure C.9: Local Projection of NTL on US MPS: With Weather Control

Notes: MPS is aggregated to the weekly frequencies consistent with the dependent variable. The number of lags of the dependent variable ( $Q$ ) and the shock ( $M$ ) are selected by the AIC criteria for up to 4 periods. Weather control variables include average temperature, precipitation, visibility, and wind speed. The dashed ribbons are the 90 percent confidence intervals generated based on the Newey-West standard errors.

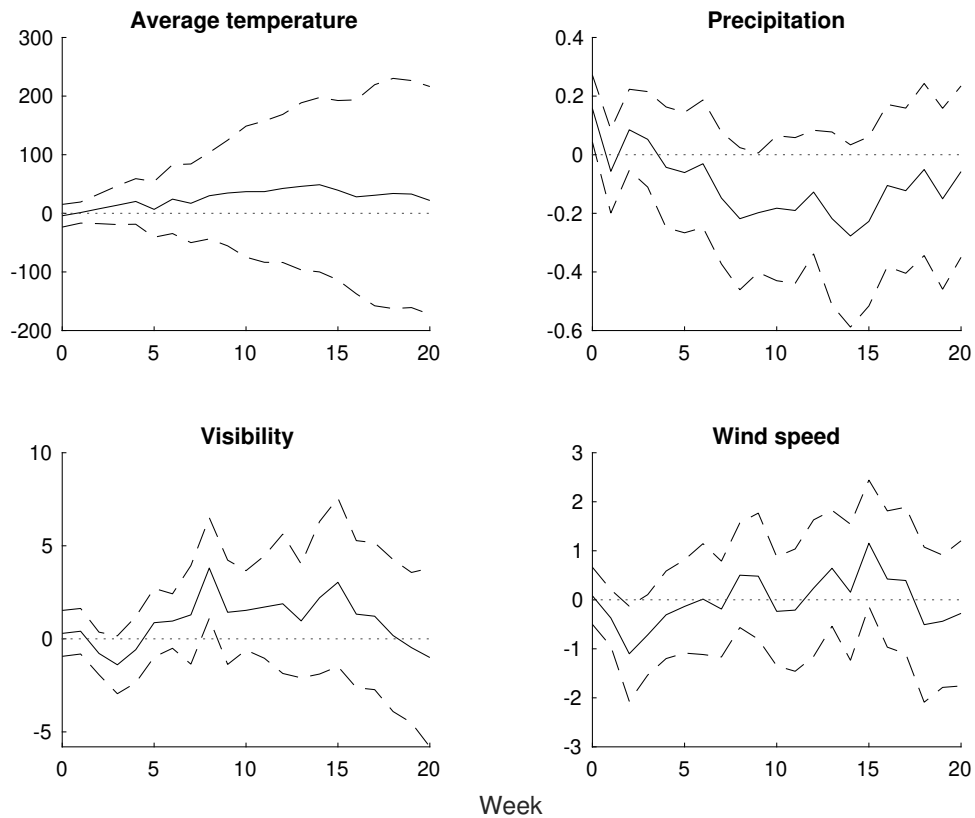


Figure C.10: Local Projection of Weather on US MPS

Notes: Weather indicators and MPS are aggregated to the weekly frequencies. The number of lags of the dependent variable ( $Q$ ) and the shock ( $M$ ) are selected by the AIC criteria for up to 4 periods. The dashed ribbons are the 90 percent confidence intervals generated based on the Newey-West standard errors.

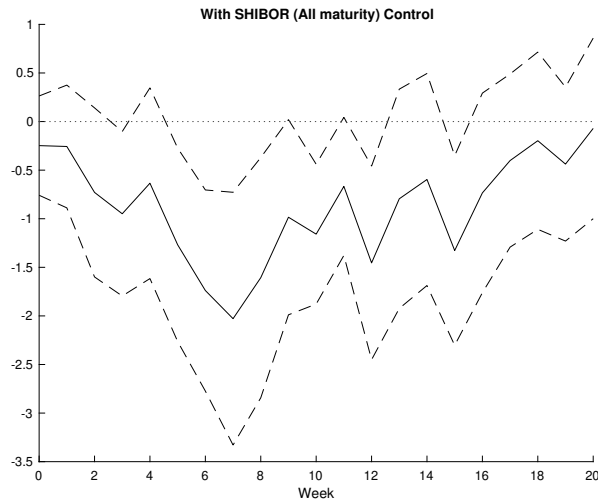


Figure C.11: Local Projection of NTL on US MPS: With SHIBOR (All maturity) Control

Notes: SHIBOR maturities include overnight, 1 week, 1 month, 3 months, 6 months, and 1 year. MPS is aggregated to the weekly frequencies consistent with the dependent variable. The number of lags of the dependent variable ( $Q$ ) and the shock ( $M$ ) are selected by the AIC criteria for up to 4 periods. Weather control variables include average temperature, precipitation, visibility, and wind speed. The dashed ribbons are the 90 percent confidence intervals generated based on the Newey-West standard errors.

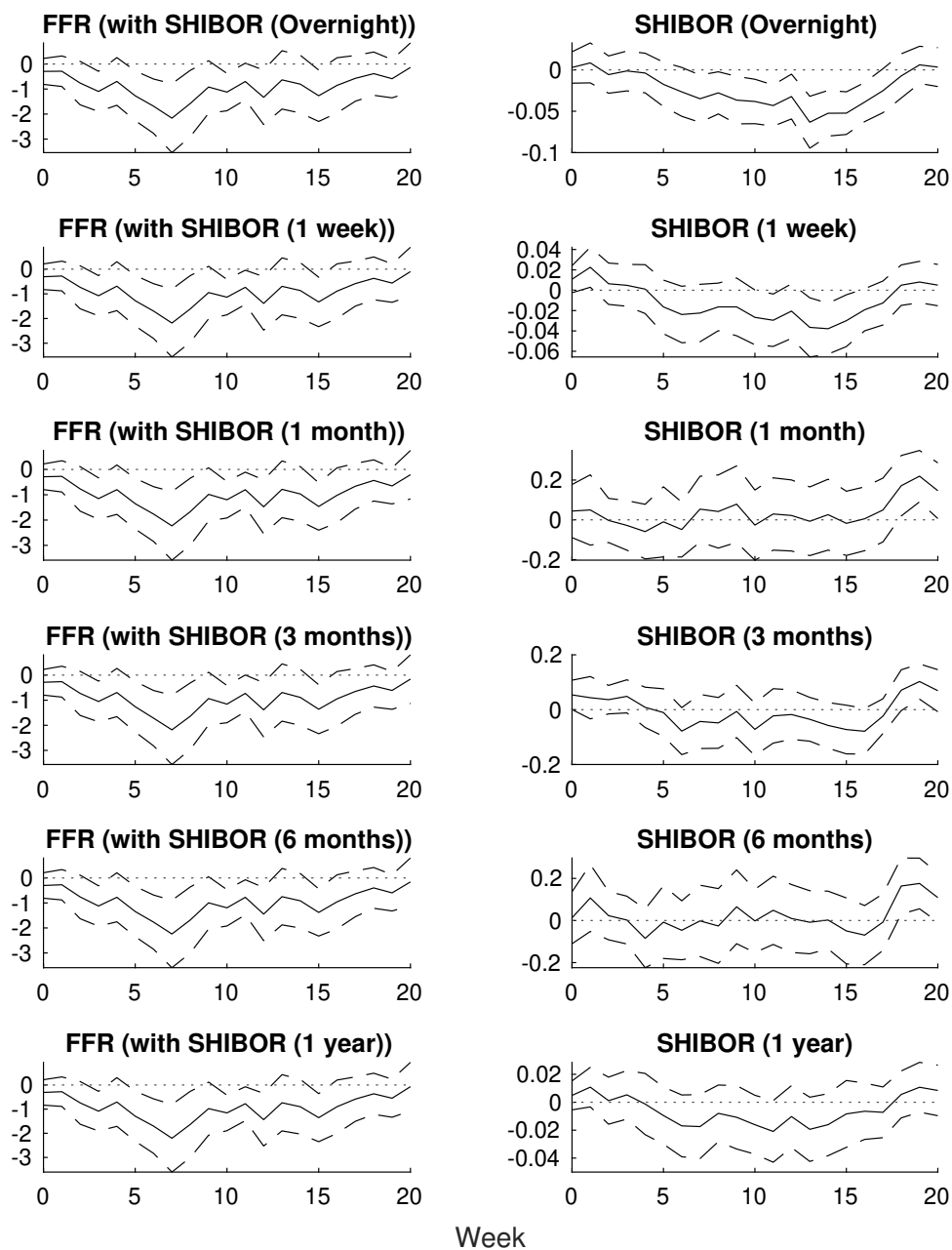


Figure C.12: Local Projection of NTL on US MPS and SHIBOR

Notes: MPS is aggregated to the weekly frequencies consistent with the dependent variable. The number of lags of the dependent variable ( $Q$ ) and the shocks ( $M_1$  and  $M_2$ ) are selected by the AIC criteria for up to 4 periods. The dashed ribbons are the 90 percent confidence intervals generated based on the Newey-West standard errors.

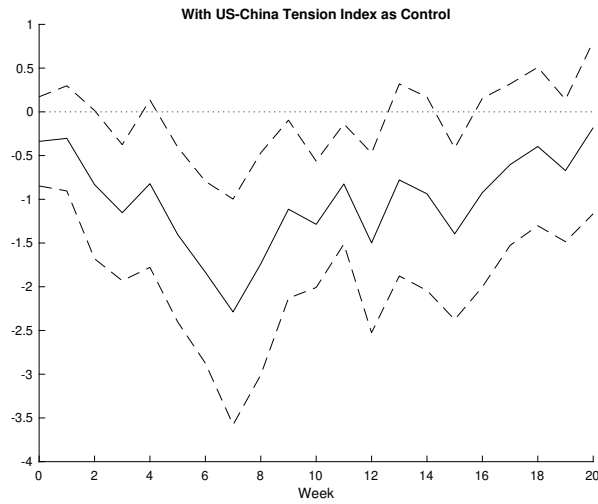


Figure C.13: Local Projection of NTL on US MPS: With US-China Tension Index as Control

Notes: MPS is aggregated to the weekly frequencies consistent with the dependent variable. The number of lags of the dependent variable ( $Q$ ) and the shock ( $M$ ) are selected by the AIC criteria for up to 4 periods. Weather control variables include average temperature, precipitation, visibility, and wind speed. The dashed ribbons are the 90 percent confidence intervals generated based on the Newey-West standard errors.

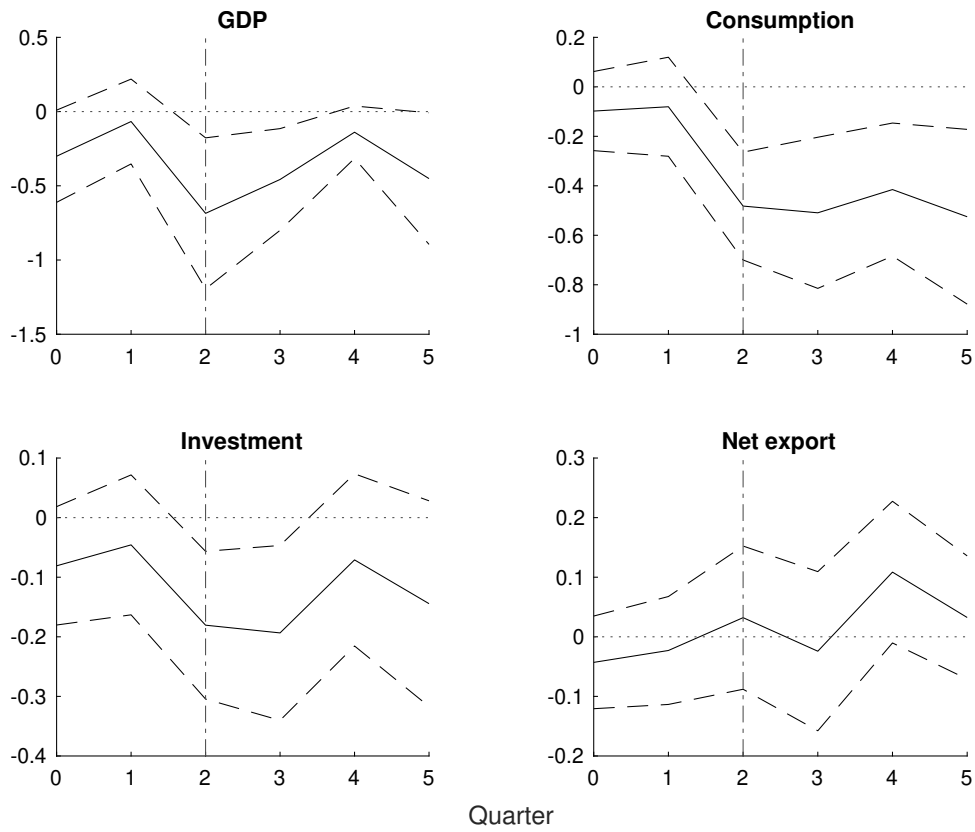


Figure C.14: IRF of China's Quarterly Consumption, Investment, and Net Export on US MPS

Notes: MPS is aggregated to the quarterly frequencies consistent with the dependent variable. The number of lags of the dependent variable ( $Q$ ) and the shock ( $M$ ) are selected by the AIC criteria for up to 4 periods. The dashed ribbons are the 90 percent confidence intervals generated based on the Newey-West standard errors.

## Appendix D More Results on Channel

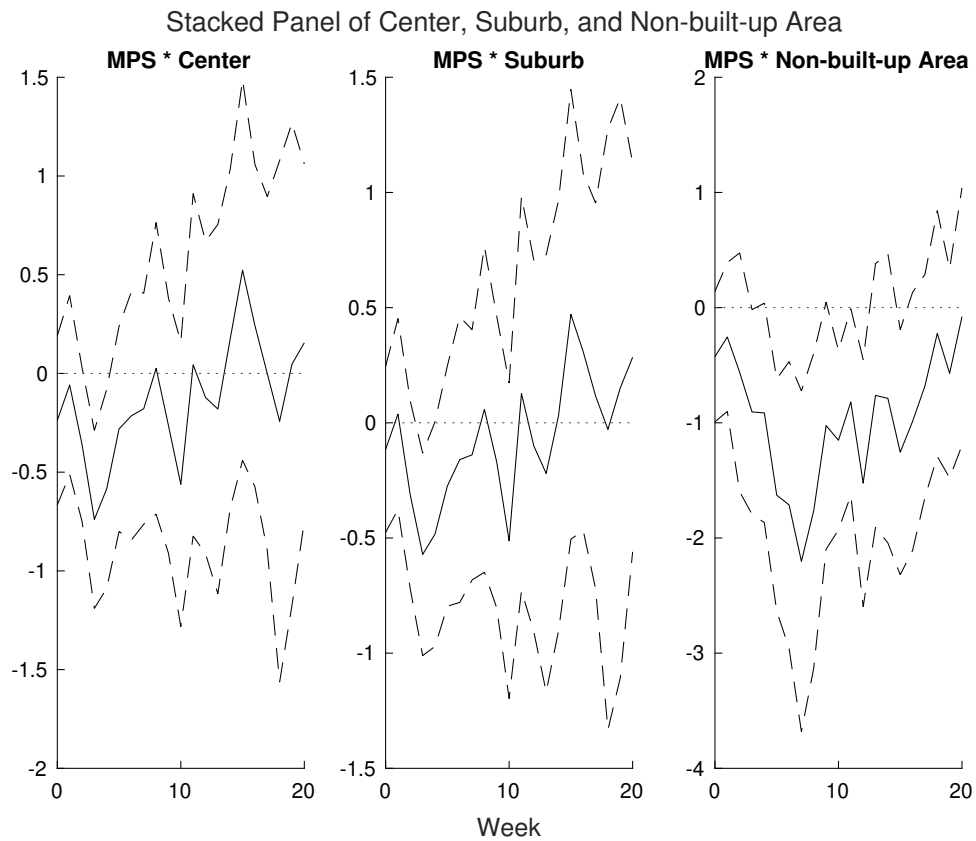


Figure D.1: Local Projection of NTL on US MPS: City Areas, Stacked Panel

Notes: MPS is aggregated to the weekly frequencies consistent with the dependent variable. The dashed ribbons are the 90 percent confidence intervals generated based on the Newey-West standard errors.

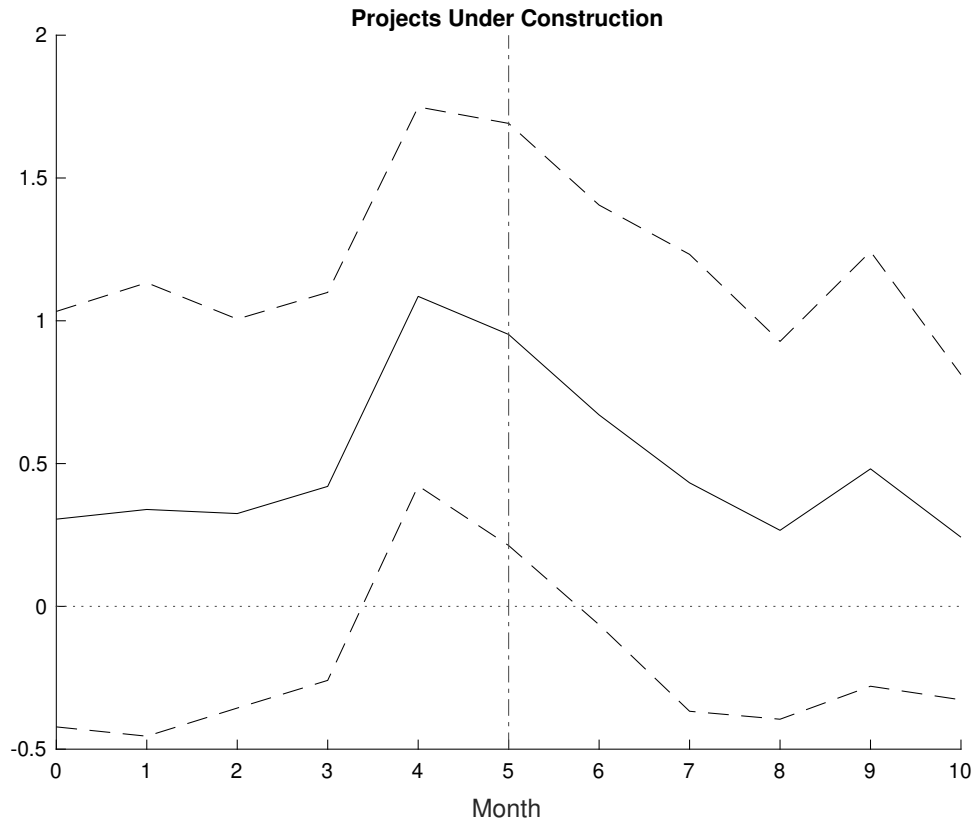


Figure D.2: IRF of NTL on China's Monthly Land Projects Under Construction (IV: US MPS)

Notes: MPS is aggregated to the monthly frequencies consistent with the dependent variable. In the first stage, the number of lags of the endogenous variable is selected by the AIC criteria for up to 4 periods. The number of lags of the shock is the IRF horizon (10 months). In the second stage, the number of lags of the dependent variable ( $Q$ ) and the endogenous variable ( $M$ ) are selected by the AIC criteria for up to 4 periods. The dashed ribbons are the 90 percent confidence intervals generated by bootstrapping with 1,000 draws.

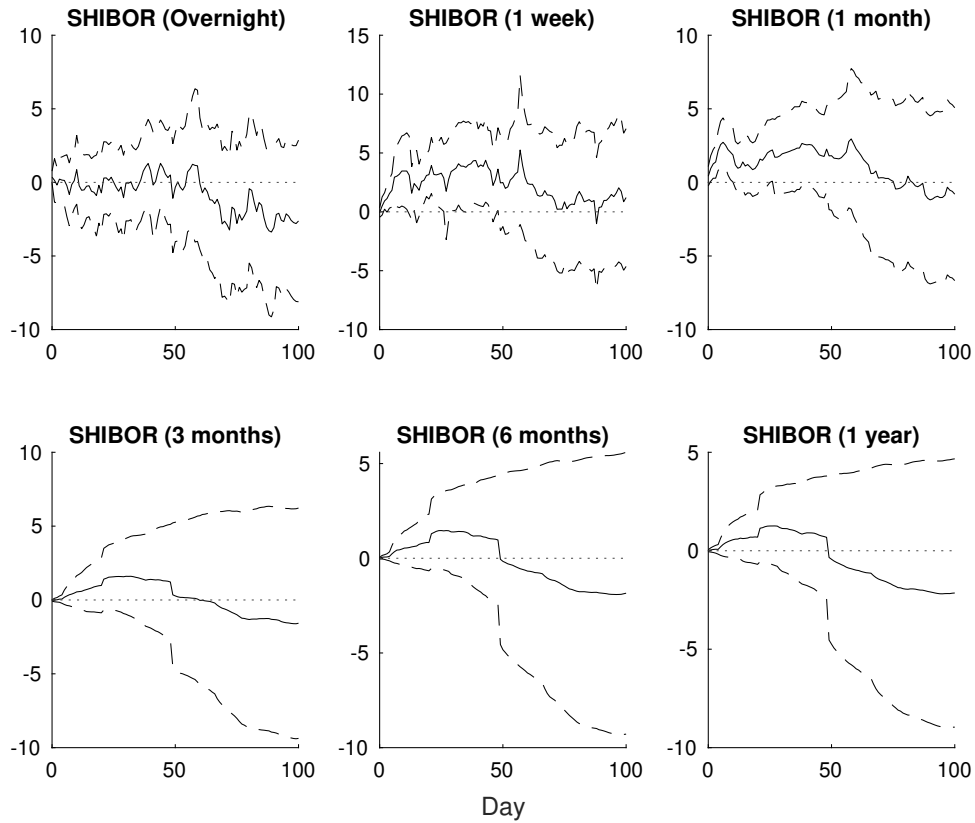


Figure D.3: IRF of SHIBOR on US MPS by Maturity

Notes: The number of lags of the dependent variable ( $Q$ ) and the shock ( $M$ ) are selected by the AIC criteria for up to 4 periods. The dashed ribbons are the 90 percent confidence intervals generated based on the Newey-West standard errors.

Table D.1: Firm Operation Condition Responses to MPS, by Firm Operation Indicator

	Revenue	Account Receiv- able	Account Payable	Profit
Real Estate	-0.0129 (0.0307)	-0.0123 (0.0172)	-0.0022 (0.0123)	-0.3389 <sup>+</sup> (0.2262)
MPS × Real Estate	-2.0428 <sup>+</sup> (1.3265)	-0.9729* (0.4499)	-1.0128** (0.3583)	-23.8807** (9.8719)
Firm FE	Yes	Yes	Yes	Yes
Year-Quarter FE	Yes	Yes	Yes	Yes
N	144,281	142,592	129,110	145,252
R <sup>2</sup>	0.1333	0.0362	0.0339	0.0240

Notes: Significance levels are based on Clustered (Year, Firm) standard-errors. Significance Codes: \*\*\*: 0.01, \*\*: 0.05, \*: 0.1, +: 0.2.



Table D.2: Real Estate Firm Operation Condition Responses to MPS, by Firm Operation Indicator

	Revenue	Account Receivable	Account Payable	Profit
MPS	-2.2486 <sup>+</sup> (1.5346)	-0.5504* (0.2558)	-1.0476** (0.3611)	-16.4012** (5.9230)
Firm FE	Yes	Yes	Yes	Yes
N	6,365	6,013	5,932	6,475
R <sup>2</sup>	0.0070	0.0146	0.0163	0.0029

Notes: Significance levels are based on Clustered (Year, Firm) standard-errors. Significance Codes: \*\*\*: 0.01, \*\*: 0.05, \*: 0.1, +: 0.2.

Table D.3: Land Transaction Impact on Real Estate Firm Operation Condition Responses to MPS, by Firm Operation Indicator

	Revenue	Account Receivable	Account Payable
Land transaction	0.0296 (0.0249)	0.0182 (0.0429)	0.0265 (0.0199)
MPS × Land transaction	-0.8812 <sup>+</sup> (0.5793)	-0.2758 (0.9244)	-0.5088* (0.2954)
Firm FE	Yes	Yes	Yes
Year-Quarter FE	Yes	Yes	Yes
N	5,361	5,043	4,927
R <sup>2</sup>	0.2548	0.0305	0.1174

Notes: Significance levels are based on Clustered (Year, Firm) standard-errors. Significance Codes: \*\*\*: 0.01, \*\*: 0.05, \*: 0.1, +: 0.2.

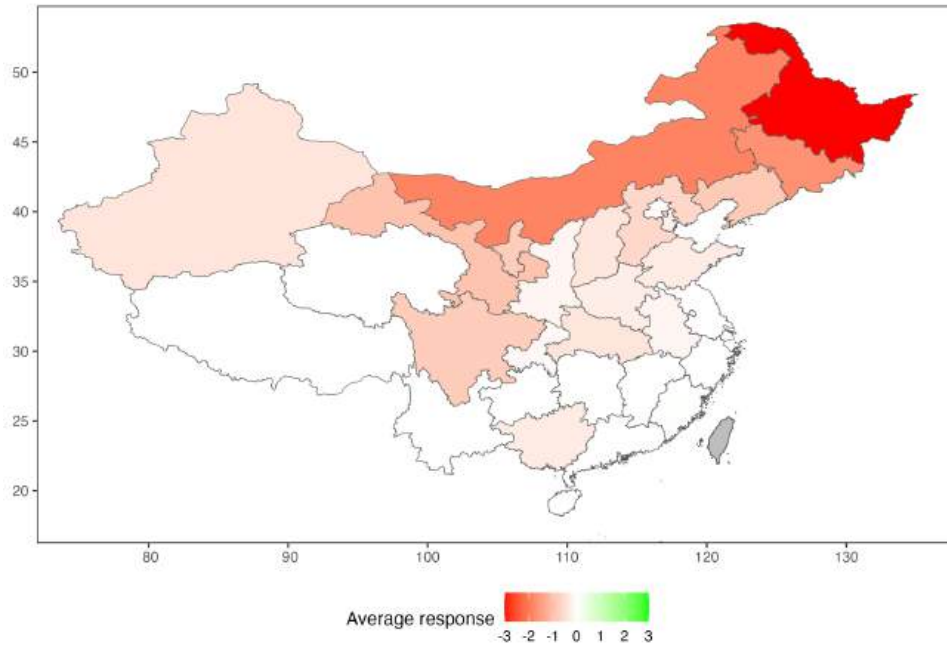


Figure D.4: Average Response of NTL on US MPS by Province

Notes: MPS is aggregated to the weekly frequencies consistent with the dependent variable. The number of lags of the dependent variable ( $Q$ ) and the shock ( $M$ ) are selected by the AIC criteria for up to 4 periods.

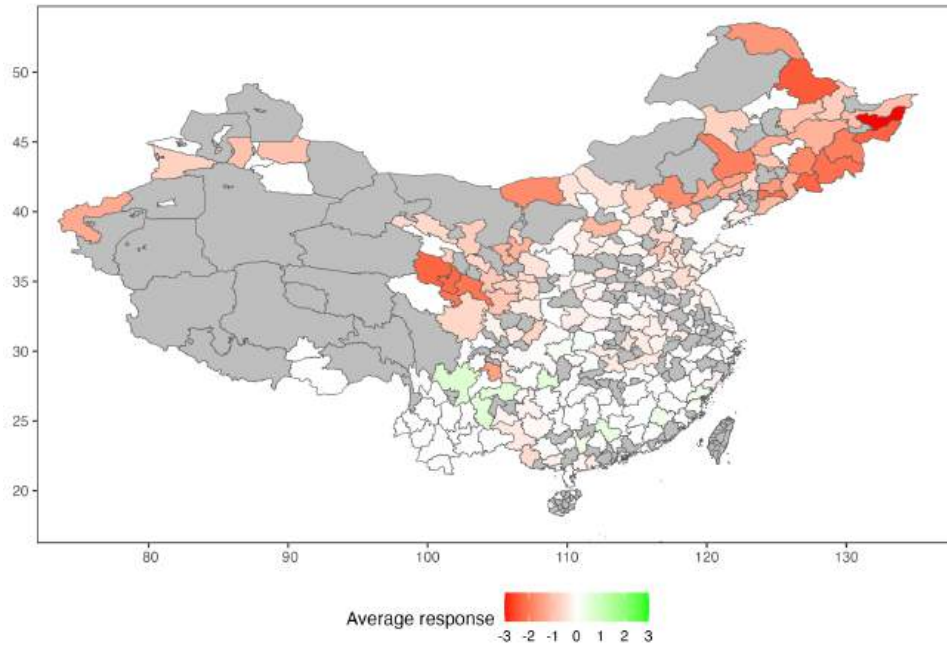


Figure D.5: Average Response of NTL on US MPS by City, With Weather Control

Notes: MPS is aggregated to the weekly frequencies consistent with the dependent variable. The number of lags of the dependent variable ( $Q$ ) and the shock ( $M$ ) are selected by the AIC criteria for up to 4 periods. Weather control variables include average temperature, precipitation, visibility, and wind speed.

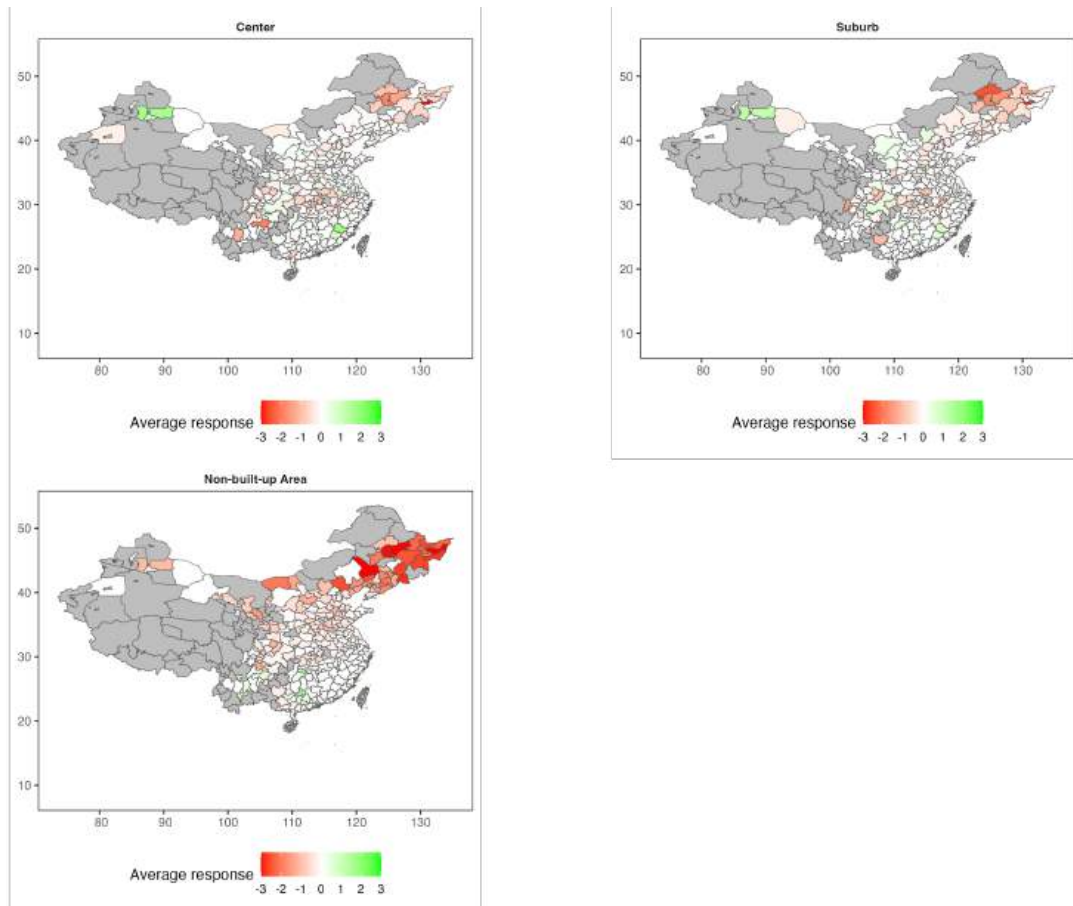


Figure D.6: Average Response of NTL on US MPS by City: City Areas

Notes: MPS is aggregated to the weekly frequencies consistent with the dependent variable. The number of lags of the dependent variable ( $Q$ ) and the shock ( $M$ ) are selected by the AIC criteria for up to 4 periods. When taking the average across the time horizon from the week the MPS is realized to 20 weeks later, insignificant values at a 90 percent confidence level are treated as zero. If the city has both significantly positive and significantly negative responses, the average response by the city is interpreted as zero. Extreme values with absolute values greater than 3 are winsorized on the map.

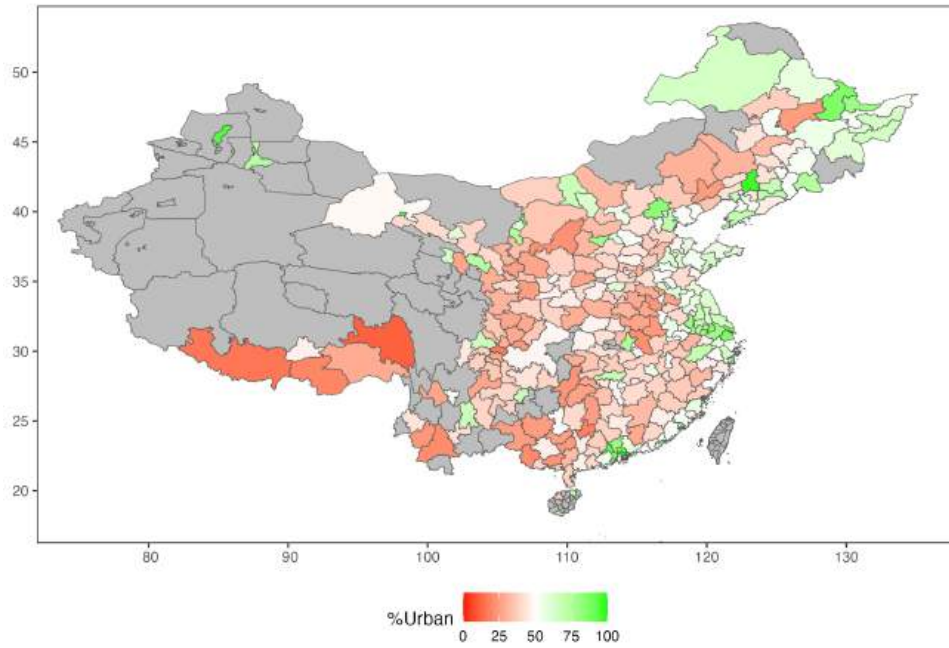


Figure D.7: Urbanization Rate in 2020 by City, Linearly Interpolated

Notes: The data are from the statistical yearbooks of each city published by NBSC.

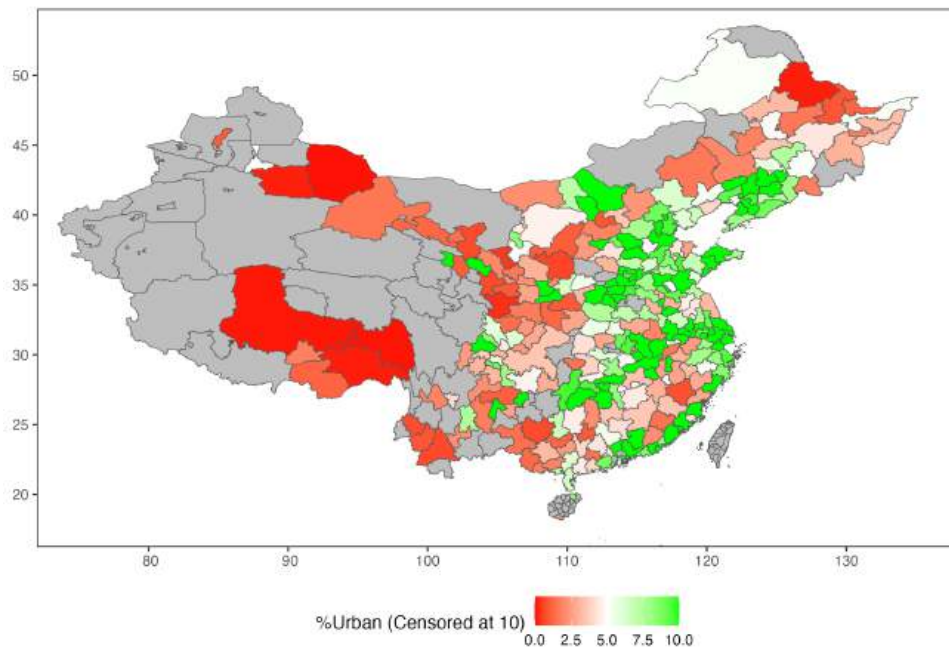


Figure D.8: Urbanization Area Rate in 2019 by City

Notes: The data are from the statistical yearbooks of each city published by NBSC. Extreme values greater than 10 are winsorized on the map.

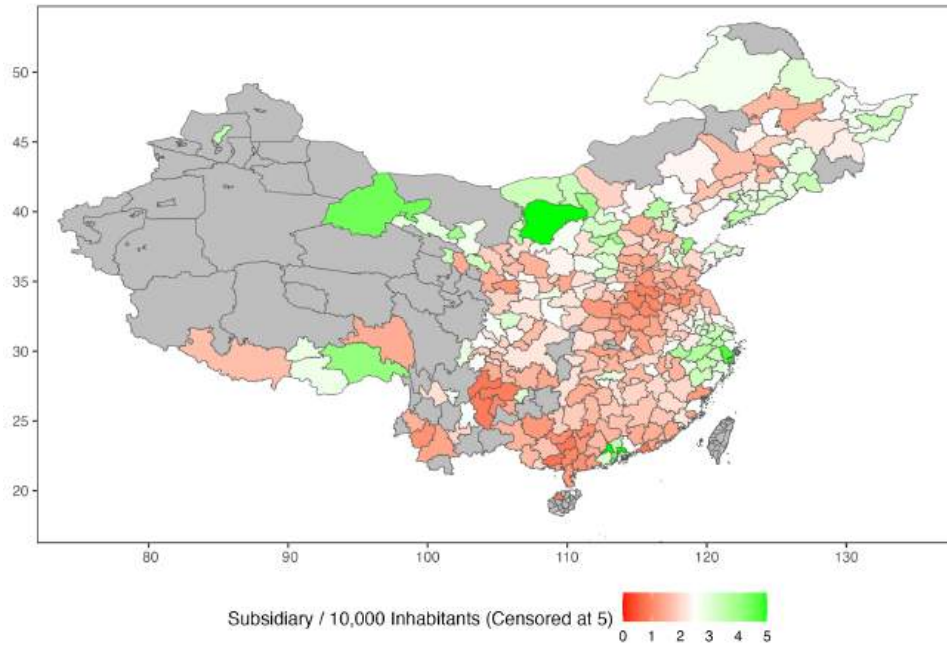


Figure D.9: Number of Bank Subsidiaries Per 10,000 Inhabitants in 2020 by City

Notes: The data are from the statistical yearbooks of each city published by NBSC. The population of each city is based on the household residency (hukou) status. Extreme values greater than 5 are winsorized on the map.

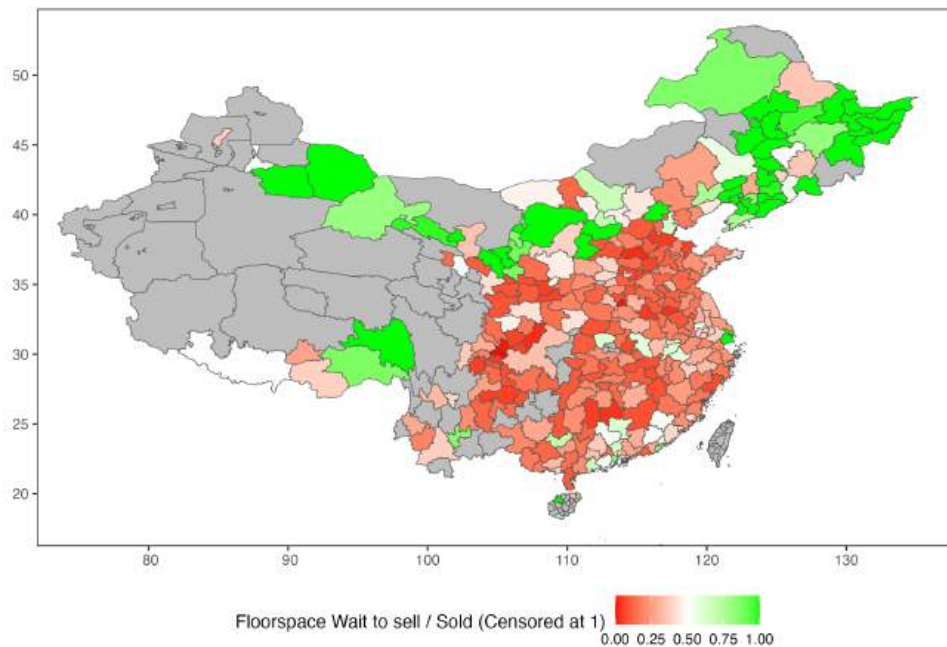


Figure D.10: Ratio of Floor Space Wait to Sell over Floor Space Sold in 2020 by City

Notes: The data are from CEIC China Premium Database. Extreme values greater than 1 are winsorized on the map.

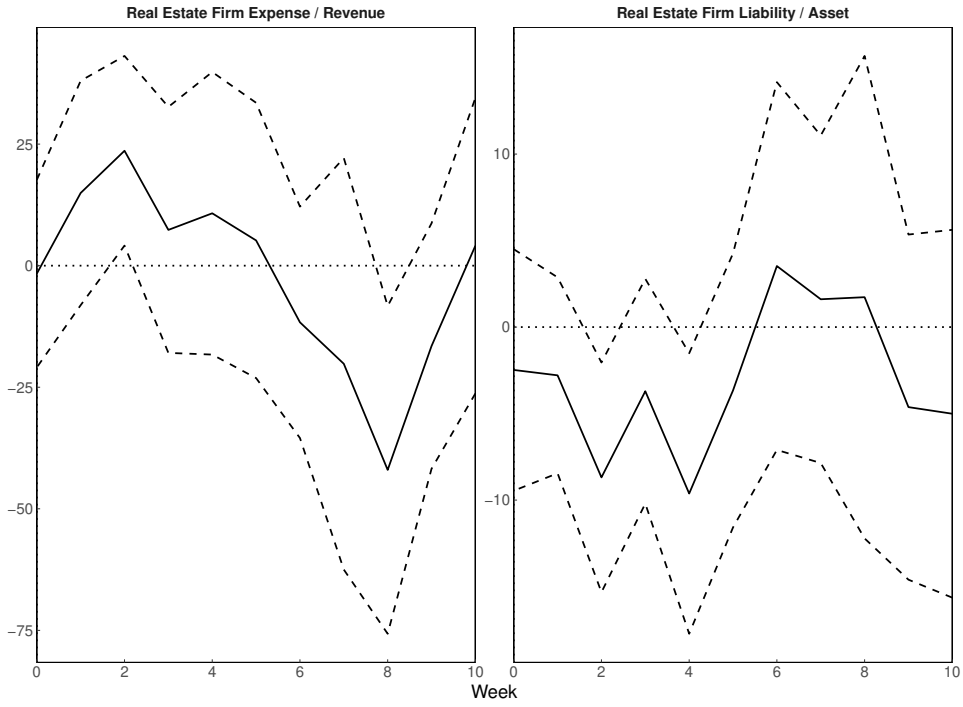


Figure D.11: NTL Response to Interaction of US MPS and Real Estate Firms' Financial Condition, City level

Notes: The aggregated firm data are at the province level. For each city in each year, I assign the corresponding indicators of the province the city belongs to. The dashed ribbons are the 90 percent confidence intervals generated based on standard errors clustered to city and week.

## Appendix E More Results on Extension

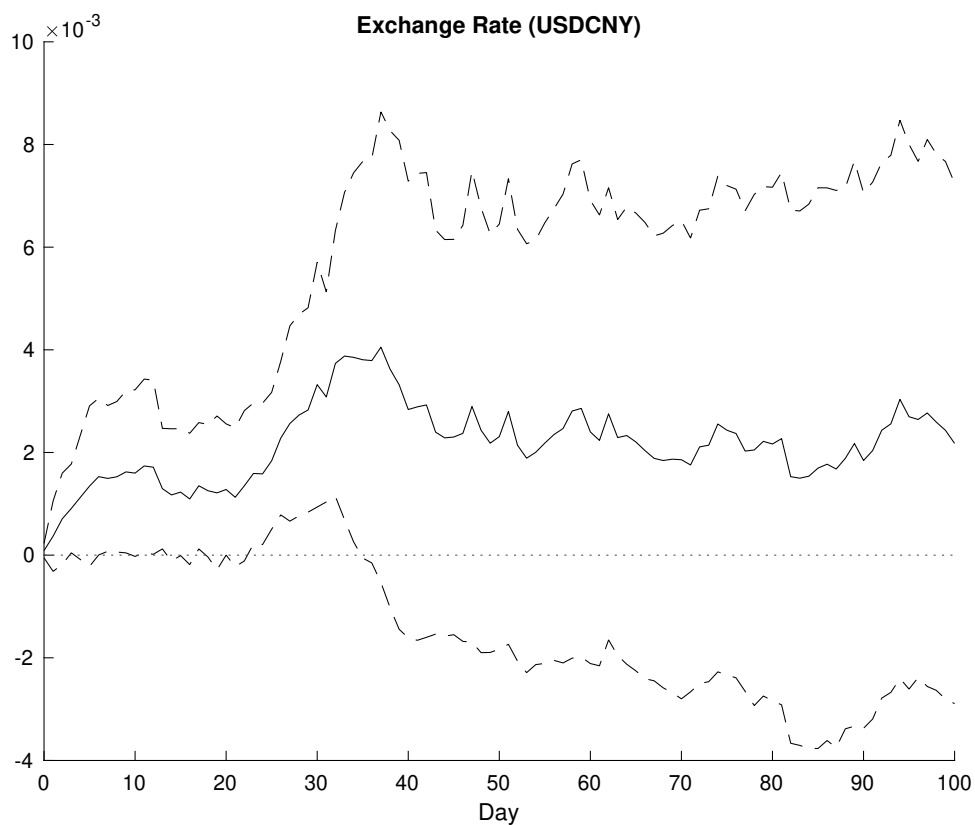


Figure E.1: IRF of Exchange Rate of USD/CNY on US MPS, by MPS Specification

Notes: The number of lags of the dependent variable ( $Q$ ) and the shock ( $M$ ) are selected by the AIC criteria for up to 4 periods. The dashed ribbons are the 90 percent confidence intervals generated based on the Newey-West standard errors.



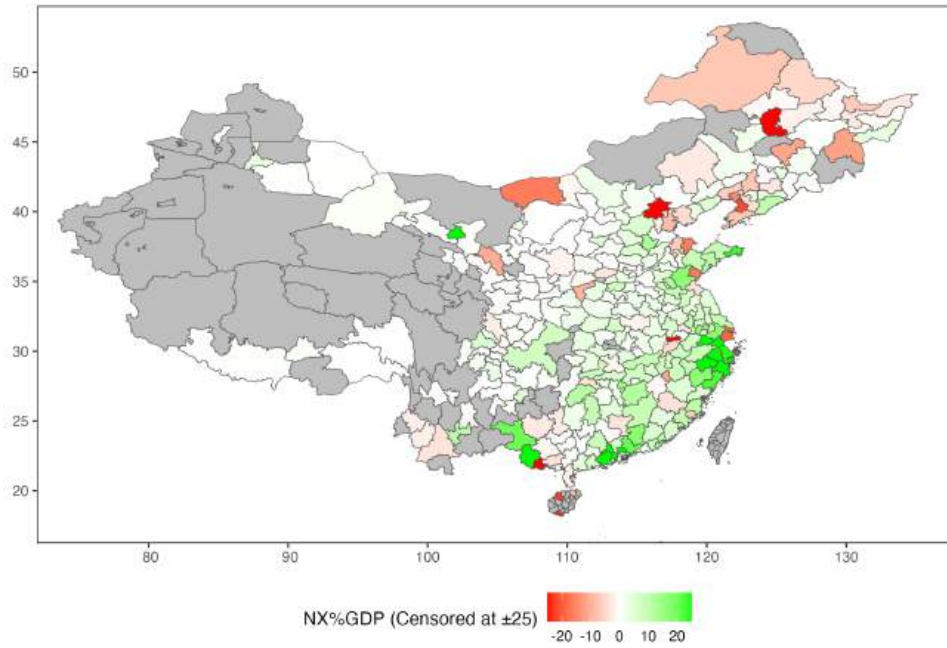


Figure E.2: Trade Exposure in 2020 by City

Notes: The data are from the statistical yearbooks of each city published by NBSC. Trade exposure is calculated as export value minus import value, then divided by GDP, all in current Chinese Yuan units. By comparison, the national overall ratio in 2020 was about 2.5 percent. Extreme values with absolute values greater than 25 are winsorized on the map.

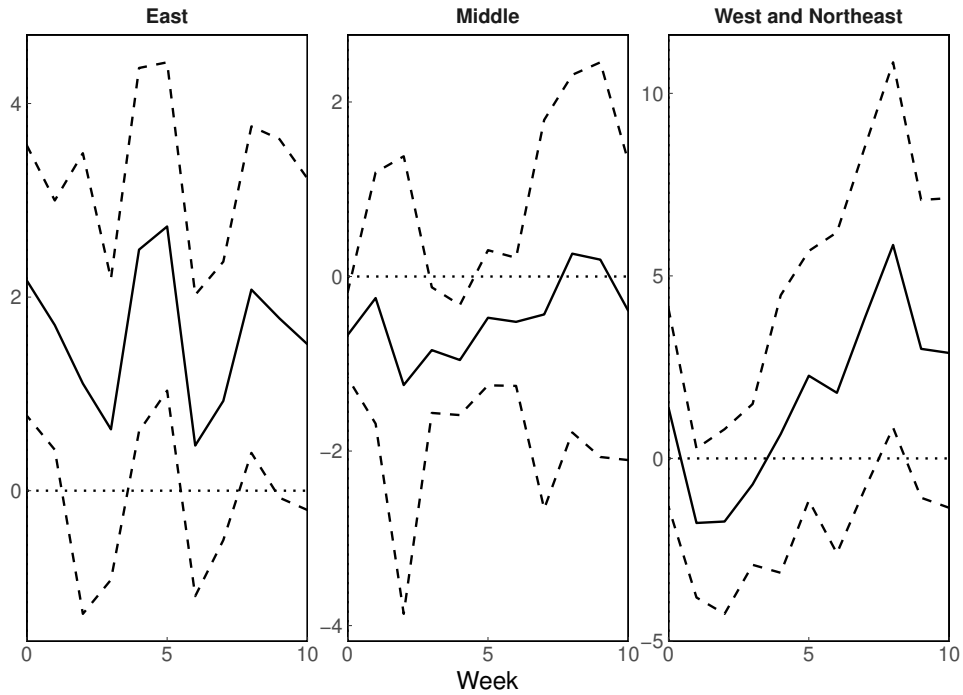


Figure E.3: NTL Response to Interaction of US MPS and Trade Exposure, City level, by Region

Notes: The dashed ribbons are the 90 percent confidence intervals generated based on standard errors clustered to city and week.

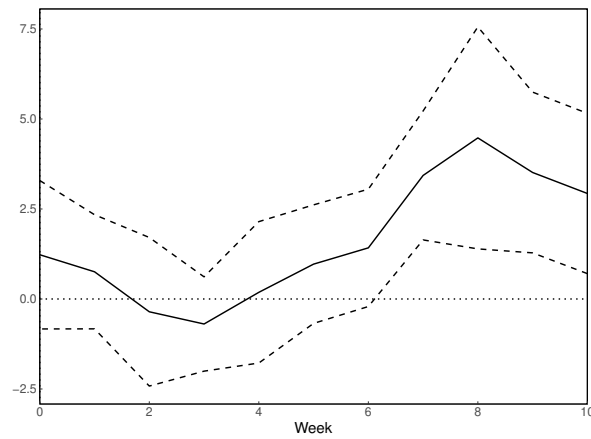


Figure E.4: NTL Response to Interaction of US MPS and Trade Exposure, City level, With Weather Control

Notes: Weather control variables include average temperature, precipitation, visibility, and wind speed. The dashed ribbons are the 90 percent confidence intervals generated based on standard errors clustered to city and week.

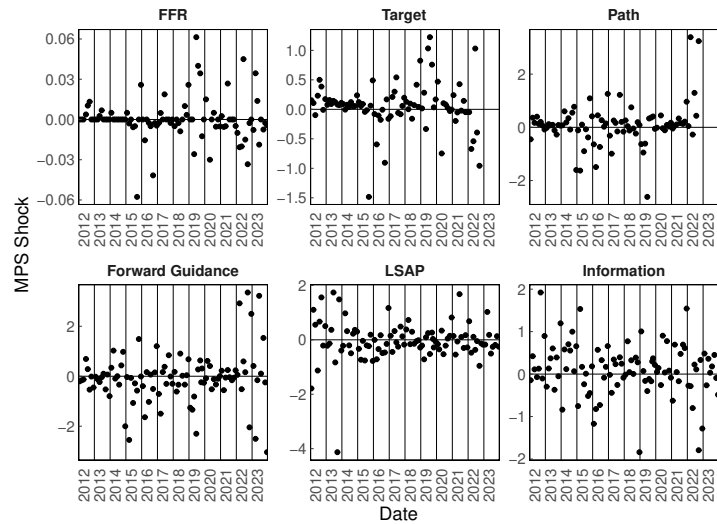


Figure E.5: Proxies of Monetary Policy Shock

Notes: For each MPS event, the corresponding date is the day when the FOMC is held.

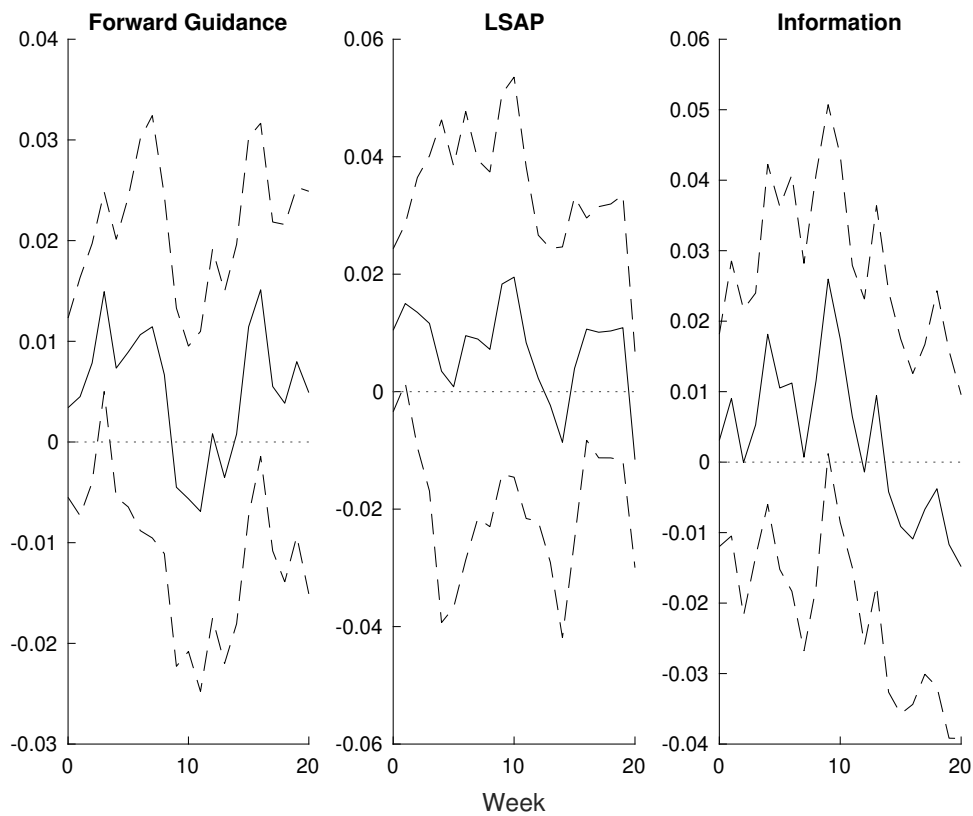


Figure E.6: Local Projection of NTL on US MPS: Alternative Unconventional MPS

Notes: MPS is aggregated to the weekly frequencies consistent with the dependent variable. The number of lags of the dependent variable ( $Q$ ) and the shock ( $M$ ) are selected by the AIC criteria for up to 4 periods. The dashed ribbons are the 90 percent confidence intervals generated based on the Newey-West standard errors.

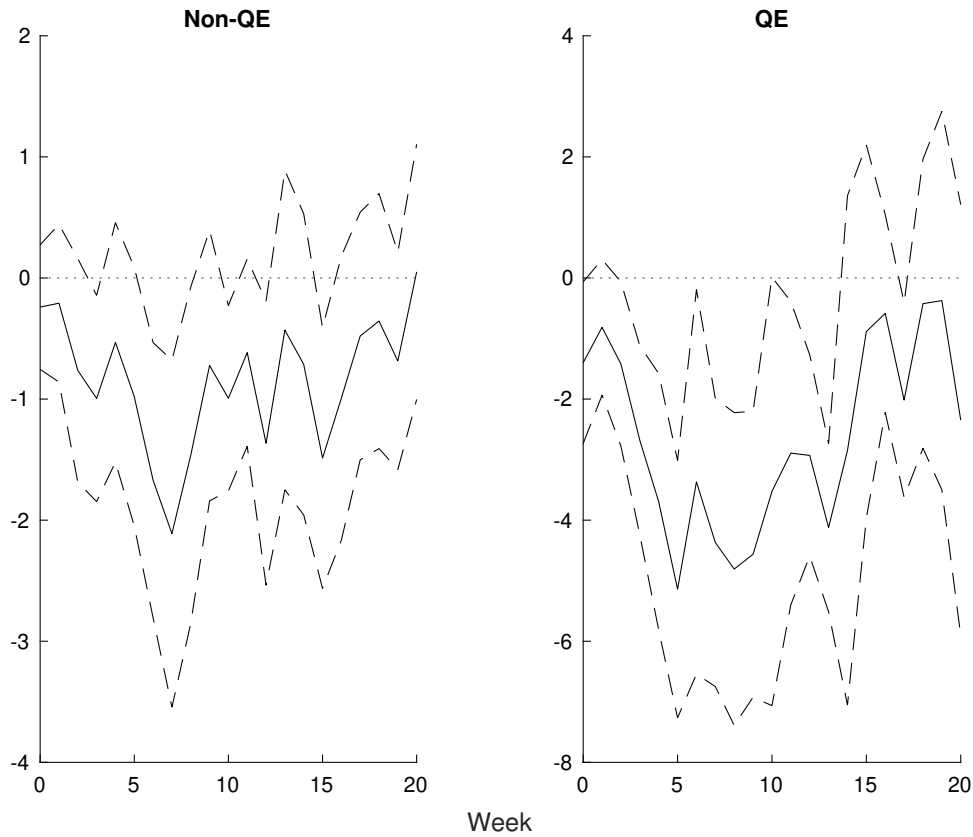


Figure E.7: Local Projection of NTL on US MPS: QE

Notes: The Non-QE period is from October 29th, 2014 to March 15th, 2020 and from March 9th, 2022 to late 2023. Correspondingly, the QE period is from early 2012 to October 29th, 2014 and from March 15th, 2020 to March 9th, 2022. MPS is aggregated to the weekly frequencies consistent with the dependent variable. The number of lags of the dependent variable ( $Q$ ) and the shock ( $M$ ) are selected by the AIC criteria for up to 4 periods. The dashed ribbons are the 90 percent confidence intervals generated based on the Newey-West standard errors.

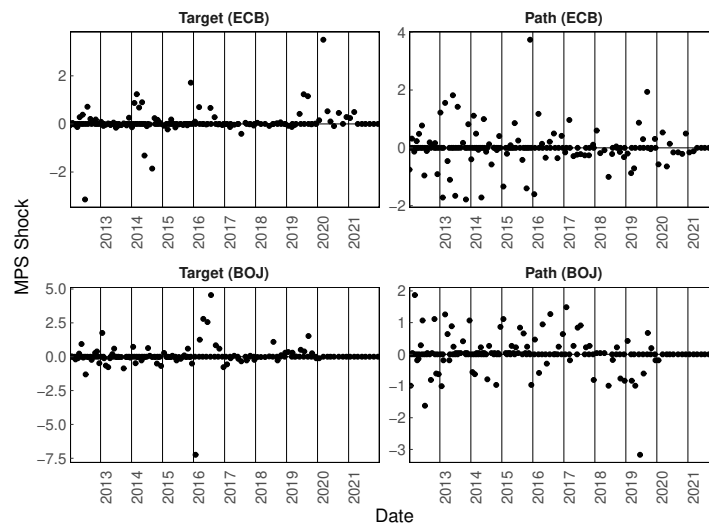


Figure E.8: Proxies of Monetary Policy Shock: Other Central Banks

Notes: For each MPS event, the corresponding date is the day when the FOMC is held.

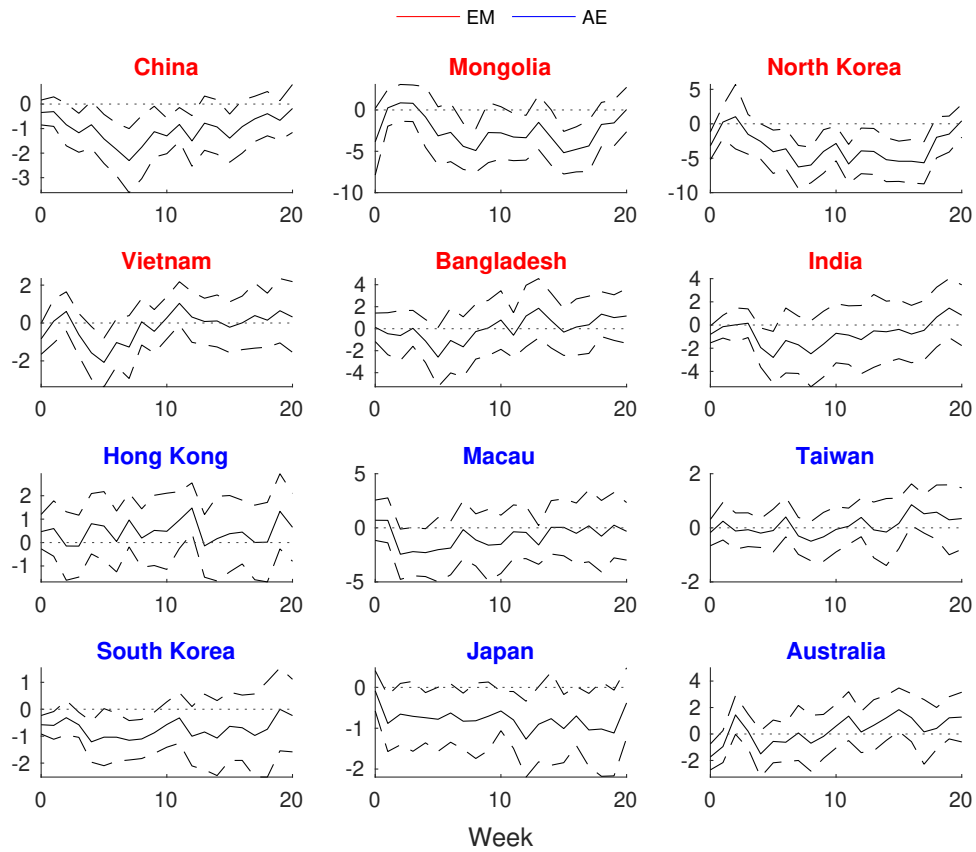


Figure E.9: Local Projection of NTL on US MPS: Other Economies

Notes: We apply the baseline specification on different economies respectively. MPS is aggregated to the weekly frequencies consistent with the dependent variable. The number of lags of the dependent variable ( $Q$ ) and the shock ( $M$ ) are selected by the AIC criteria for up to 4 periods. The dashed ribbons are the 90 percent confidence intervals generated based on the Newey-West standard errors.